CFD MODELING AND SIMULATIONS OF CATALYTIC HYDROTREATMENT OF BIO-OIL

Submitted in partial fulfillment of the

requirements for the degree of

DOCTOR OF PHILOSOPHY

by

Mr. Gollakota Anjani Ravi Kiran

DEPARTMENT OF CHEMICAL ENGINEERING

INDIAN INSTITUTE OF TECHNOLOGY GUWAHATI

GUWAHATI, ASSAM – 781039, INDIA

OCTOBER 2015

Department of Chemical Engineering
Indian Institute of Technology Guwahati
Guwahati - 781039, India

CERTIFICATE

This is to certify that the thesis entitled **"CFD Modeling and Simulations of Catalytic Hydrotreatment of Bio-oil"** being submitted by ***Gollakota Anjani Ravi Kiran*** (Roll No. 11610707) for the award of PhD degree has been carried out under our guidance and supervision. The work documented in this thesis has not been submitted to any other University or Institute for the award of any degree or diploma.

(Dr. Nanda Kishore)
Associate Professor
Department of Chemical Engineering,
Indian Institute of Technology Guwahati
Guwahati - 781039, India.

Dedicated to

beloved parents and my Wife

Mr. Gollakota Achuta Rama Sreenivas & Mrs. Gollakota Anjani Rani

Mrs. Dr. Saileela

Acknowledgements

Words fail me when i yearn to depict my profoundest feelings of gratitude for the people who have rendered invaluable help during the course of my dissertation. Yet, I intend to make a sincere effort in portraying my deepest sense of gratitude and respect in the form of words.

I would like to express my deepest gratitude to my advisor, Dr. Nanda Kishore, whose expertise, understanding, guidance, caring, patience added considerably to my research. I admire his vast knowledge and skills in many areas (e.g. Bubbles & Drops, Slip flows, Upgradation of bio-fuels, Molecular dynamics, Fluid mechanics, Thermodynamics), and his assistance in writing reports, project proposals and this thesis which have on occasion made me GREEN with envy. I am highly grateful to the Doctoral committee headed by Dr. Pugazhenthi, Dr. T.K. Mandal and Dr. A.Dalal for their assistance and continual suggestions they provided at all levels of the research. I sincerely thank all the other faculty members of their concern and motivation towards my endeavor.

A very special and sincere thanks to Prof. Sai Gu, research collaborator United Kingdom, for his thoughts, kindness, research support and working environment during the course of research at Cranfield University, UK. A very special acknowledgement to Dr. Pannerselvam Ranganathan for his assistance and brain storming sessions related to CFD models at the initial level of this research.

I would like to thank Department of Chemical Engineering, Indian Institute of Technology Guwahati, for proving excellent facilities and environment for the research. My sincere thanks to my lab mates Subramanyam, Rahul Ramteke, Rajasekhar Reddy, Vasu Kiran, Harsharaj and others for their support throughout my research.

I have been fortunate to have friend's Vikranth, Anjali, Anil, Rajeev Parmar, Satyanarayana, for listening to me, offering me advice; cherish me despite of my eccentricities and supporting me through this entire process. Thanks to my UK friends Yashwanth, Daniel, Ali, Marion, Elisa, Jelila for their suggestions and help during my course of research at Cranfield University, United Kingdom. Also to my friends scattered around the globe, thank you for the thoughts, well wishes/ prayers, phone-calls, e-mails, texts, visits, editing advice, and being there whenever i needed a friend. If i miss someone who really cared for my wellbeing, please excuse me it's not intentional but plead paucity of space.

Last but not the least, this journey would not have been possible without the support of my family members. I am especially grateful to my parents and this word ***grateful*** will not suffice the love, caring, support, advice, sharing emotions towards me. Thank you mom, dad, sister and my wife for showing faith in me and giving me liberty to choose what i desired. I consider myself the luckiest in the world to have such a supportive family, standing behind me with their love and support. I extend my respect to my parents, my in-laws and all elders to me in the family.

Gollakota Anjani Ravi Kiran

Research Output

Anjani R.K. Gollakota, Malladi D.Subramanyam, Nanda Kishore, Sai Gu, "CFD simulations on effects of catalysts on hydrodeoxygenation of bio-oil", *RSC Advances*, 5, 2015**,** 41855-41866.

Malladi D. Subramanyam, Anjani R.K. Gollakota, Nanda Kishore, "CFD simulations of catalytic hydrodeoxygenation of bio-oil using Pt/Al_2O_3 in a fixed bed reactor", *RSC Advances*, 2015, 90354-90366.

Anjani R.K. Gollakota, M.D. Subramanyam, Nanda Kishore, Sai Gu. Upgradation of bio-oil derived from lignocellulose biomass – A Numerical approach. Accepted in the inaugural issue of Journal of Biofuels and Bioenergy (Springer)

Anjani R.K Gollakota, P. Ranganathan, Sai Gu, "CFD Modeling of an ebullated bed reactor for the upgradation of Bio-oil derived from Lignocellulose Biomass", PYRO conference 2014, Birmingham, United Kingdom, May 19-23. (Poster)

Anjani R.K. Gollakota, M.D. Subramanyam, Nanda Kishore, Sai Gu. A Review on the upgradation techniques of bio-oil. Manuscript under review.

Malladi D. Subramanyam, Anjani R.K. Gollakota, Nanda Kishore. Effect of catalyst load on hydrodeoxygenation of bio-oil in an up flow packed bed reactor". Manuscript under preparation.

Table of Contents

Table Captions

Figure Captions

Nomenclature

2D = two dimensional

A = arrhenius constant , min^{-1}

AHM = ammonium hepta molybdate

Al_2O_3 = aluminum Oxide

API = American petroleum institute

B = boron

b = buoyancy force, N

C = Carbon

C_d = drag coefficient

CFD = computational fluid dynamics

CO = Carbon-monoxide

CO_2 = Carbon-dioxide

Co-Mo = Cobalt-Molybdenum oxide

C_p = specific heat, J kg^{-1} K^{-1}

CUS = coordinated unsaturated sites

D = diffusion coefficient of species, m^2 s^{-1}

DMS = distributed matrix structure

d_p = solid catalyst particle diameter, m

E = activation energy, kJ mol^{-1}

EBR = ebullated bed reactor

EIA = Energy information agency

f = drag force, N

FBR = fixed bed reactor

FCCU = fluid catalytic cracking unit

Fe = Ferrous

FMOx/Zeol = Flouro-molybdenum oxalate zeolite support catalyst

$\overrightarrow{F_q}$ = external forces, N

$\vec{g}$ = acceleration due to gravity, $m^2\ s^{-1}$

G_b = generation of turbulent kinetic energy due to buoyancy, kJ

G_k = generation of turbulent kinetic energy, kJ

H = specific enthalpy, kJ

H/C = Hydrogen to carbon ratio

H+ = Hydrogen ion

H_2 = Hydrogen

H_2O = Water

HBEA = Hydrogen ion exchanged Beta polymorph A catalyst

HCl = Hydrochloric acid

HDM = Hydrodemethylization

HDO = Hydrodeoxygenation

HDS = Hydrodesulphurization

HNV = Heavy non volatiles

HYD = Hydrogenation

i,j = components

IEA = International energy agency

k = thermal conductivity, $W\ m^{-1}\ K^{-1}$

k = turbulent kinetic energy, J

k = rate constant

K = interface exchange coefficient, dimensionless

KOH = Potassium hydroxide

l = liquid phase

LNV = Light non-volatile

LTH = low thermal hydrogenation

$\dot{m}$ = mass flow rate, kg s^{-1}

MBR = moving bed reactor

MgO = Magnesium oxide

Mo = Molybdenum

MO_2N = amorphous molybdenum nitride

MoNaph = Molybdenum napthenate

MSW = municipal solid waste

n = number of phases

N = Nitrogen

Nb = Niobium

Ni-Cu = Nickel Copper

Ni-Mo = Nickel molybdenum oxide

Norit = type of activated carbon

NOx = Nitrogen oxides

Nu = Nusselt number (dimensionless)

O = oxygen

P = pressure, Pa

p = fluid phase (secondary phase)

Pd = Palladium

Pr = Prandtl number, dimensionless

Pt = Platinum

q = fluid phase (primary phase)

Q = intensity of heat exchange, J

q_h = heat transfer coefficient, $Wm^{-2} K^{-1}$

$\overrightarrow{q_q}$ = heat flux, $J s^{-1}$

r = rate of a reaction

r = mixture phase

Re = Reynolds number, dimensionless

Rh = Rhenium

Ru = Ruthenium

S = Sulfur

S = source term

s = solid phase

SBA = mesoporous silica

SBR = slurry bed reactor

SH- = Bisulfide ion

SiO_2 = Silicon oxide

SRGO = straight run gas oil

T = temperature, K

t = time, s

TDM = MoS_2 exfoliations

Ti = Titanium

V = Vanadium

v = velocity, m s^{-1}

V = volume, m^3

W = Tungsten

WHSV = weightily hour space velocity, h^{-1}

WOx = tungsten oxalate

WP = tungsten oxalate

Y = local mass fraction of species (dimensionless)

Y_M = fluctuation dilation

ZrO_2 = Zirconium oxide

ZSM = Zeolite

ϵ = rate of dissipation

ρ = density, kg m^{-3}

ε_g = volume fraction of gas phase

ε_l = volume fraction of bio-oil phase

ε_s = volume fraction of solid catalyst phase

μ = shear viscosity, Pa.s

Greek Symbols

$\overline{\overline{\tau_q}}$ = stress-strain tensor, Pa

$\left(-p_s\bar{\bar{I}} + \bar{\bar{T}}\right): \nabla\overrightarrow{v_s}$ = generation of energy by solid tensor

$\emptyset_{ls}$ = exchange between fluid and solid phase, J

ε_{mf} = minimum fluidization velocity, m s^{-1}

Θ_s = granular temperature, K

σ_k = turbulent Prandtl numbers

C_ϵ = constant

$\bar{\bar{I}}$ = second order invariant

K_{Θ_s} = diffusion coefficient

S_k = kinetic energy source term

S_ϵ = dissipation energy source term

e_{ss} = coefficient of restitution for particle collisions

$g_{0,ss}$ = radial distribution function

r' = rate of reaction, mol l^{-1} s^{-1}

ε_g = Volume fraction of gas phase

ε_l = Volume fraction of bio-oil phase

ε_s = Volume fraction of solid catalyst phase

τ_p = particle relaxation time

α = volume fraction

λ = bulk viscosity, Pa.s

μ = shear viscosity, Pa.s

ρ = density, kg m^{-3}

S= modulus of the mean rate-of-strain tensor

$\gamma\Theta_s$ = collisional dissipation energy, kg m^{-1} s^{-3}

ϵ = Turbulent dissipation, J

Abstract

The term biofuel is referred to liquid, gas, and solid fuels produced from biomass. Biofuels include energy security reasons, environmental concerns, foreign exchange savings, and socioeconomic issues related to rural sector. Biofuels include bioethanol, bio-methanol, vegetable oils, biodiesel, biogas, bio synthesis gas, bio-oil, bio-char, and bio hydrogen etc. Whereas, bio-oil refers to the synthetic fuel produced from the seeds like jatropha, karanja, corn etc., by destructive distillation or pyrolysis process at a temperature of 500^{o}C produces both liquids and gases. Further cooling this mixture leads to a liquid form termed as bio-oil. They are also known as second generation bio fuels. These second generation bio-fuels from pyrolysis process are incompatible with the conventional fuels mainly due to the higher oxygen content, high solids, content, high viscosity, high moisture content and chemically unstable, along with higher contents of char formation. Hence upgradation of the bio-oil from the pyrolysis process is highly advisable. Among the various upgradation processes hydrodeoxygenation (HDO) process appears to be the promising technique carried in the presence of a conventional catalysts using H_2 gas that is also termed as catalytic upgradation of pyrolytic oil. This Ph.D. dissertation entitled "CFD Modeling and Simulation of Catalytic Hydrotreatment of Bio-oil" deals with the modeling and simulation of lumped kinetics of the HDO process in the presence of three different catalysts, namely Pt/Al_2O_3, Ni-Mo/Al_2O_3, and Co-Mo/Al_2O_3. The simulations are performed using commercial computational fluid dynamics (CFD) based software, Ansys Fluent 14.5, for a wide range of pertinent conditions i.e., weight hourly space velocity ranging between $2 \leq WHSV\ (h^{-1}) \leq 4$, temperature ranging between $623 \leq T\ (K) \leq \mathbf{673}$ and pressure values between $6996 \leq P\ (kPa) \leq 10443$. The numerical methodology implemented for the present simulation studies comprising Ranz –marshall, and Gunn for heat interaction, Gidaspow

and Schillar Naumann for drag interaction between solid and fluid phases; kinetic theory of granular flow for solid catalyst, $k-\epsilon$ turbulence model for flow characteristics, and finite rate/ eddy dissipation method to study the chemical reaction kinetics are implemented and thoroughly validated with the experimental literature and good agreement is observed between two results. From the simulation studies a wide range of results in terms of volume fractions of three phases with respect to the pertinent conditions are presented. Similarly, the lumped reaction kinetics mechanism has been included in order to characterize the mass fraction of the species after the HDO process to estimate the performance of the process. Some of the key findings include that Co-Mo/Al_2O_3 produces the major desired species of alkanes and aromatics, phenols are higher with the Ni-Mo/Al_2O_3 catalyst and gaseous streams are dominating with Pt/Al_2O_3 catalyst. It is also observed that the hydrodeoxygenation of unprocessed bio-oil in the presence of Co-Mo/Al_2O_3 catalyst yields higher amounts of alkane and aromatics. The amount of LNV is found to be significant during the HDO process of bio-oil compared to HNV in the presence of three catalysts. Finally, the yields of alkanes and aromatics varying with respect to the operating parameters in the presence of catalysts follows the order Co-Mo/Al_2O_3 > Pt/Al_2O_3 > Ni-Mo/Al_2O_3.

1.1. Present global scenario of energy and fuel

The increment in the worldwide economy is relied upon to be four fold (between 2005 – 2050) for the developed nations and for developing nations it is required to be ten folds (Miguel Mercader, 2010). The increment in the economy is accompanied by the increment in the energy demand. The fundamental cause for the rapid development in twentieth century is without a doubt because of this baffling energy treasure, petroleum. This abstruse fortune called petroleum has changed the geopolitical circle of the world, making some desolate area forsakes as the wealthiest places on the planet. As shown in Figure 1.1, as per the statistics of the International Energy Agency (IEA) on the aggregate word energy supply by 2011 fossil fuels still leads the table with 32% as the major contributor for the energy era emulated by the others.

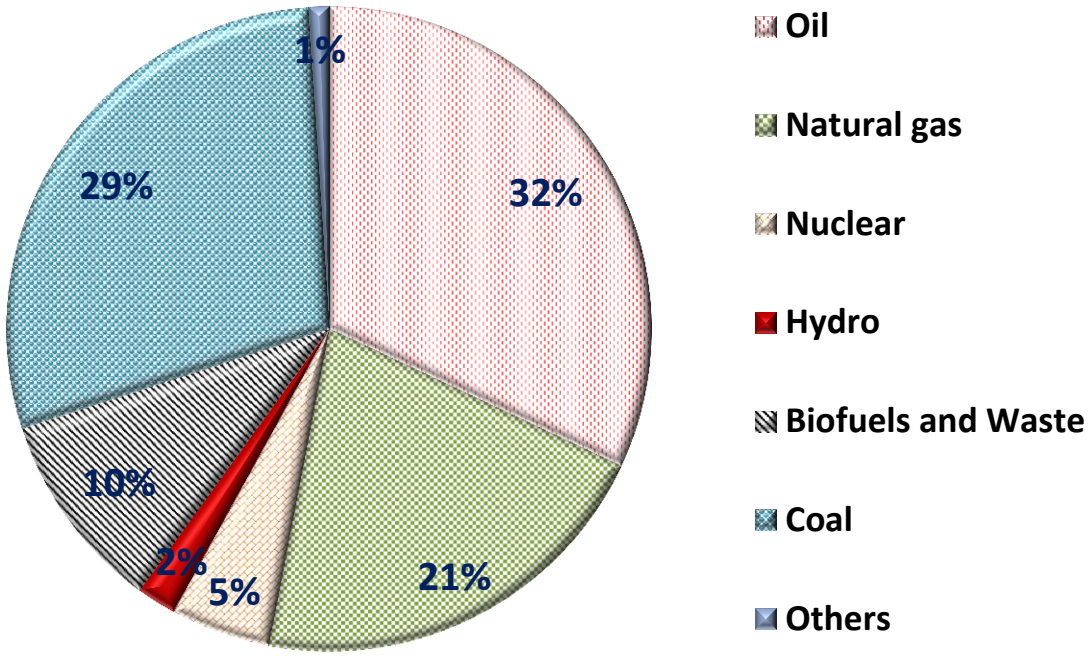

Figure 1.1. Total world energy supply by source 2011 statistics taken from key world energy IEA. (Source: http://www.iea.org/publications/freepublications/)

In the recent couple of decades, there is paradigm shift observed gradually to an all-electric society through which electrons are delivered from renewable sources like wind and sun based, though the utilization of oil stays same for particular instants. Furthermore, without any doubt, the petroleum oil is found to be a superior alternative than other sources because of the following primary reasons Groeneveld (2008).

- Energy stockpiling is simple and easy transportation is possible.
- The oil loses at the maximum 1% of its energy content while transportation; on the other hand, other energy sources lose 21% for their energy content.
- Oil is still column for the petrochemical business, and utilized for the generation of carbon based chemicals.

Figure 1.2 shows the statistics of top-10 and least-10 energy consuming countries. It can be seen from this figure that India position at no.3 in the top-10 energy consuming countries. This indicate the current and future energy demand of India are very high and the nation has to find more sources (possibly renewable sources because of the non-renewable energy sources depleting rapidly) to meet its energy requirements in the future. These benefits of the petroleum oil and the moderate progressions in the new advances for the option wellsprings of energy infer that the interest for oil will be expanded in the impending decades. The exceptional use of these customary fuels prompts discharge of greenhouse gasses and the CO_2 outflow is expected to be expanded by 130% as presented by the Intergovernmental Plan on Climate Change (2008) amid the period (2005-2050).

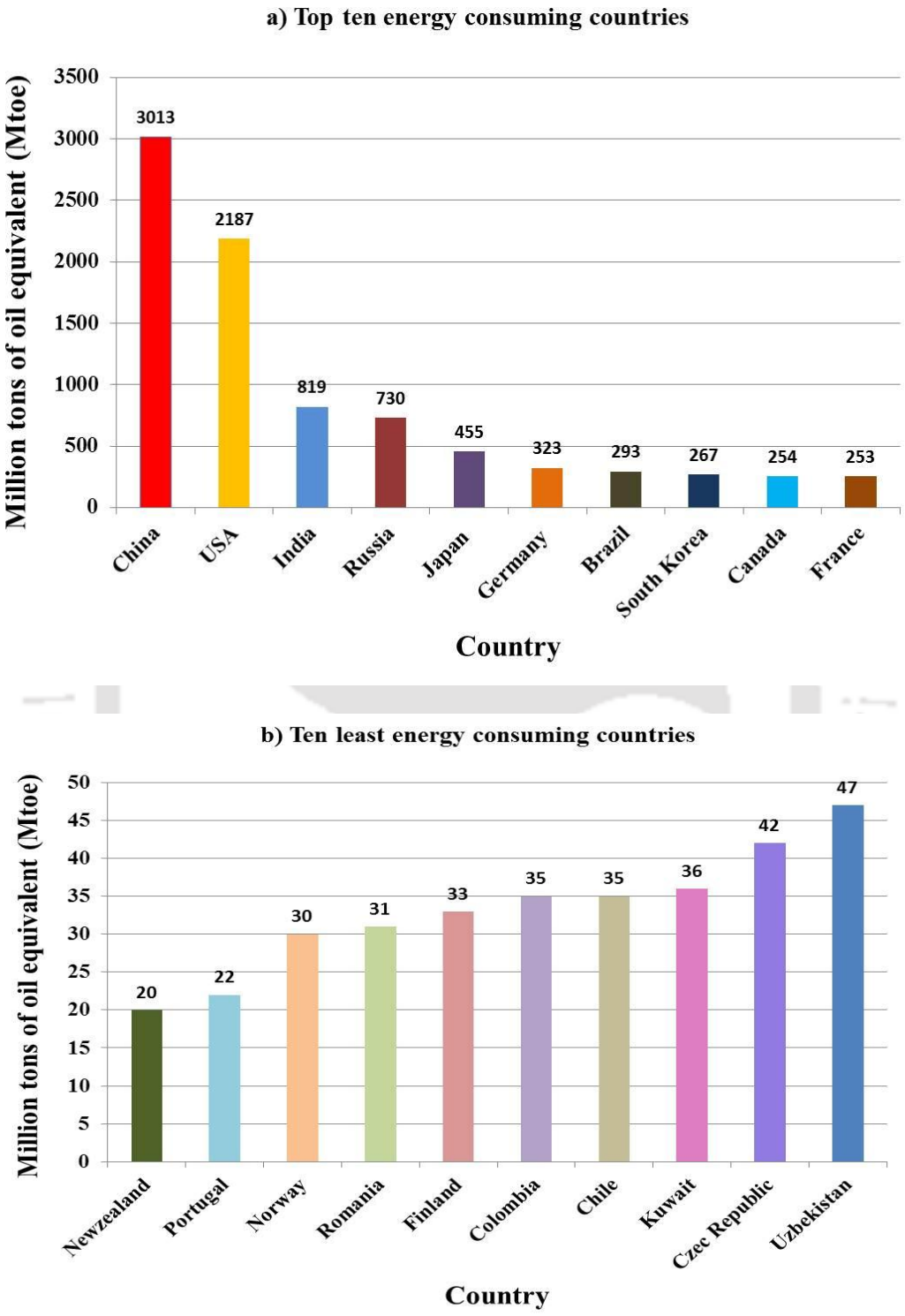

Figure 1.2: Top 10 and least 10 energy consuming countries.

(**Source:**https://yearbook.enerdata.net/crude-oil-production.html#energy-consumption-data.html)

1.2. Demerits of conventional fuels

1.2.1. Petroleum

Petroleum oil is thought to be the most astounding energy generator among all the accessible sources while the issue lies in scarcity. It has taken about 50-300 million years to structure oil reserves, but the globe has figured out how to smolder a large portion of all worldwide oil reserves in simply 125 years. The world now expends 85 million barrels of oil every day, or 40,000 gallons every second more or less and the interest is developing exponentially. Oil generation in 33 out of 48 nations has now crested, including oil rich nations like Kuwait, Russia, and Mexico. Thus the worldwide oil generation is currently anticipated to be approaching a record-breaking crest and can conceivably end the mechanical development. After a substantial research on the petroleum reserves for more than fifty years, it is understood that the petroleum reserves are depleting at a faster rate. Hence, the global oil producing nations are facing the difficulties in meeting the demands of the energy requirements globally. So there is an exigency need of examining the possibilities of covering part of energy demand through other sources.

1.2.2. Natural Gas

Natural gas is considered to have the least greenhouse emanation impact of all fossil fuels as reported by the ecological assurance organization (Environmental and Energy study institute). **Though the natural gas produced by various methods**, the extraction of characteristic natural gas through hydraulic driven cracking (fracking) constitutes risky chemicals mixed in substantial amounts with water and sand and infused at high pressures prompting the water contamination.

1.2.3. Nuclear Energy

Nuclear energy is one of the most clean energy which does not utilize fossil fuels and thus do not add greenhouse gases to the environment. Because of these reasons, **30%** or more of energy requirements of the developed nations like USA are met from nuclear power plants. However, the major demerits of nuclear energy are proper radio activity disposal; precise technology to handle radioactive materials and safety issues such as terror attack, etc. Another major hindrance of utilizing atomic energy is that it involves huge financial commitments to set a nuclear power plant. This energy utilizes uranium as source which is rare in numerous nations; and the uranium which India has, is not suitable for energy production.

1.2.4. Biomass

To numerous individuals, the most natural wellspring of renewable energy is the wind and the sun; while, biomass (plant material and creature animal waste) is the most seasoned manifestation of renewable energy. As per the measurements of Energy Information Administration (EIA-2007) biomass supplied significantly more renewable energy or bio-energy than the combination of wind and sun based sources. It is a renewable energy source not just on the grounds that the energy it originates from the sun, additionally it grows over a moderately shorter periods of time. The term biomass refers to the organic matter that has stored energy through the process of photosynthesis that takes place in the plant cells called chlorophyll. This chlorophyll captures the sun's energy by converting CO_2 from air and water from ground into carbohydrates, complex compounds of carbon, hydrogen and oxygen. When these carbs are burned, they transform into carbon dioxide and water and discharge the energy they captured from sun. Along these lines biomass works as a kind of natural battery for storing the sun

oriented energy called the solar energy. This natural battery (solar energy) lasts long and provide low carbon energy until the biomass is produced sustainably, to meet the current demands, without diminishing resources or the lands capacity to regrow biomass and recapture carbon. The use of biomass can help to differentiate and secure the energy supply. In addition the CO_2 produced amid the usage of biomass can be reabsorbed by the new developing era and henceforth shutting the CO_2 cycle. This is conceivable just the usage and developing rates are adjusted well. Besides the use of fossil fuels to deliver bio fuels ought to be lower than the energy substance of the final product. Alongside unfriendly impacts of biodiversity, water use, land, and soil exhaustion ought to be assessed when picking biofuel as the mode of renewable energy. Also growing crops for bio fuels is often criticized because of its direct competition for land for food production. If consumption of bio fuel are scaled up enough to significantly reduce the need for fossil fuel, enormous land areas will be required with serious impacts on the environment and food security. Even if does not cause an acute shortage of food, it will definitely put pressure on the current growth of crops. One major worry being faced by farmers is that the growing use of biofuels may just mean a rise in food prices as well.

1.3. Merits of renewable energy not counted in standard monetary records

Renewable energy provides sustainable benefits to the climate, and economy. The generation of the renewable energy can improve the financial stature in rural areas and avoids the urban relocations. Secondly, growing biomass on degraded and barren lands can provide financial incentives, support rural development, prevent erosion and provide better habitat to the wildlife. Further, these renewable energy innovations like methanol and hydrogen for fuel cells

doesn't release greenhouse emissions into atmosphere; reduces the acid deposition, global warming and the air pollution. The carbon dioxide released through the burning of biofuels is equally balanced by the adsorption of the biomass plantations. Furthermore, the renewable energy sources reduce the monopoly by many (fossil fuel) oil industries due to the fuel supply diversity through these alternative sources of energy. This would stabilize and reduce the energy prices and also creates new opportunities for energy suppliers. Finally, the competitive renewable energy resources could reduce the infrastructure for the production, storage and transportation for the nuclear power plants. This will avoid the dependency on the costly energy source and nuclear war proliferation.

1.4. Sources of Biomass

Figure 1.3 show different sources of biomass which can be used for bio-oil production. Figure 1.4 shows the different class of sources of biomass along with some examples. The details of each of these categories are discussed in details here.

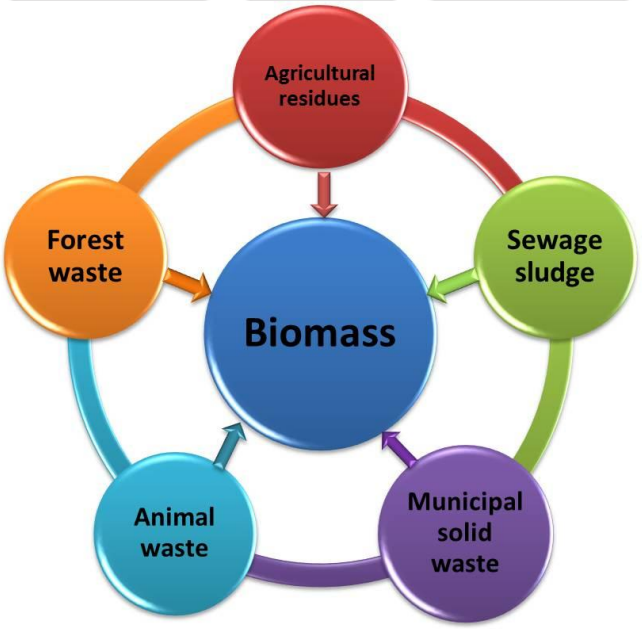

Figure 1.3: Different sources of Biomass

1.4.1. Agricultural Residues

Agricultural residues incorporate all the horticultural squanders, for example, bagasse, straw, stem, stalk, husk, shell peel, mash, stubble and so forth. Huge amounts of harvest residues are delivered yearly and endlessly underutilized. Some of them are mentioned here. Rice produces both rice straw and husks at the transforming plant which can be helpfully and effectively changed over into energy. Critical amounts of biomass stay in the fields as cob when maize is collected and can be converted into energy. Sugarcane collecting prompts harvest deposits in the fields while transforming produces stringy bagasse both of which are great sources of energy. Notwithstanding the reaped harvest, vast amounts of deposits are produced in agrarian creation frameworks/ agricultural productions. These residues constitute significant piece of the aggregate yearly generation of biomass deposits and are an imperative source of energy for both household and modern purposes. Numerous agricultural products and procedures yield buildups that can conceivably be utilized for the energy applications in various ways. Figure 1.4 shows the different class of sources of biomass along with some examples**.**

Sources incorporate

- Arable harvest deposits, for example, straw and husk
- Animal fertilizers and slurries
- Animal bedclothes, for example, poultry litter
- Most natural material from overabundance creation or lacking business sector, for example, grass silage

Current cultivating practice is normally to furrow these deposits go into the dirt, or they are burnt, left to deteriorate, or munched by dairy cattle. These residues could be prepared

into liquid fuels or thermo chemical transformed to deliver heat, electricity and power. Agricultural residues are described by the occasional accessibility and have the qualities that vary from other solid fuels, for example, wood, charcoal, burn briquette. The primary contrasts are the high substance of unpredictable volatile matter, lower density and burning time. Agricultural residues can be grouped as dry residues and wet residues. The dry residues include those parts of arable products not to be utilized for the main role of delivering nourishment, food or fiber, used animal sleeping beeding and quills. A few samples are straw, corn stover, and poultry litter.

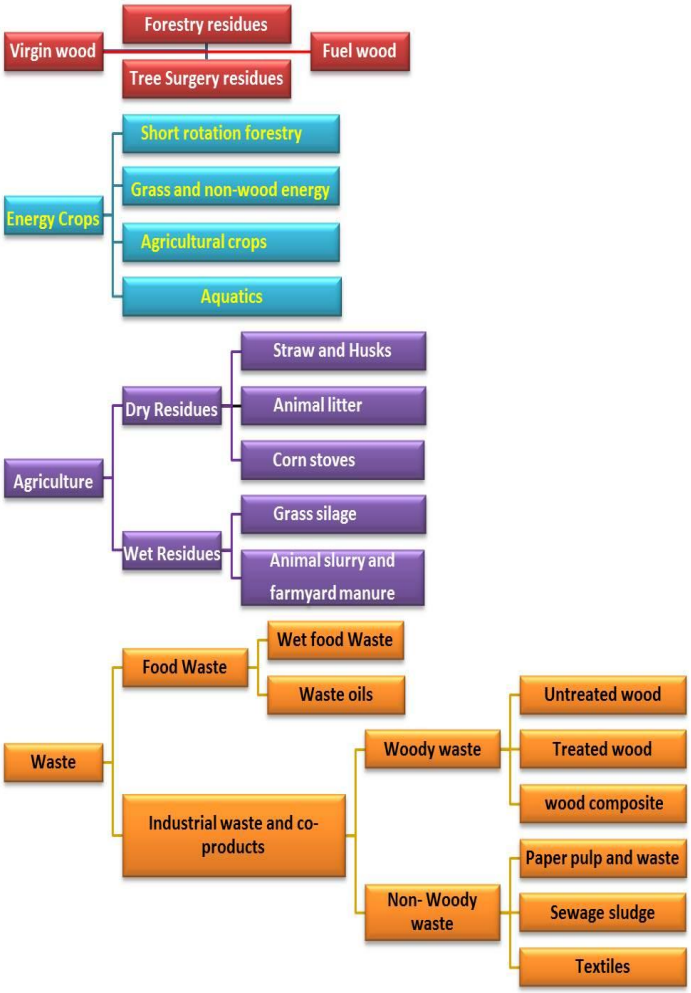

Figure 1.4: Agricultural and crop residues of biomass

The wet residues have high water content as gathered. This makes them vivaciously wasteful to use for ignition or gasification, fiscally and enthusiastically immoderate to transport. Run of the mill wet deposits incorporate creature slurry and farmstead compost, grass silage, etc.

1.4.2. Animal Waste

There are an extensive variety of animal squanders/wastes that can be utilized as a source of biomass energy. The most widely recognized sources are animal and poultry composts. In the past this waste was recouped and sold as compost or just spread onto rural areas. But, the stern ecological regulations by waste management administration on odor, water contamination; further motivating to convert these wastes to energy. The most appealing system for changing over these waste materials to helpful structure is anaerobic absorption which gives biogas that can be utilized as a fuel for internal combustion engines, to create electricity for small turbines, smoldered specifically for coking, or for water heating.

1.4.3. Municipal Solid Waste (MSW)

Millions of tons of household waste are gathered every year with the dominant part discarded in open fields. The biomass asset in municipal solid waste includes the putrescible, paper and plastic which midpoints the 80% of aggregate MSW gathered. These squanders can be converted into energies by immediate ignition, or by common anaerobic assimilation/digestion in the engineered landfill. At the land fill destinations the gas created by the deterioration of MSW gives half methane and half carbon dioxide. This must be gathered, scoured and cleaned with the goal that it serves as a feed to the internal combustion engines or gas turbines to create heat and power. The organic fraction of MSW can be anaerobically settled in a high rate digester for power or steam era. The normal sources of municipal solid waste squanders which are utilized as

biomass are paper, cardboards, folded boxes, nourishment fats, junk, glass flasks, oils, paints, plastics, polyethylene, clothes, etc.

1.4.4. Industrial Waste

The nourishment business delivers a substantial number of buildups and by-items which can be used as the biomass for the generation of renewable energy. These waste materials are created from all divisions of the nourishment business of meat generation, candy parlor creation and so on so forth. Strong squanders incorporate peelings and scraps from leafy foods, nourishment that do not meet quality control principles, mash and fiber from sugar, starch extraction, channel sludge, etc. Liquid squanders are produced by washing meat, foods grown from the ground, whitening products of the soil, precooking meats, poultry and fish, cleaning and handling operations and in addition wine making. These washed waters comprise of sugars, starches and disintegrated solid natural matters. The potential exists for these modern squanders to be anaerobically processed to deliver biogas, or matured to create ethanol, and a few other business illustrations of waste to energy transformation as of now exists. Mash and paper industry is a standout amongst the most contaminating commercial ventures which devour a lot of energy and water in different unit operations. The waste water released by this industry is profoundly heterogeneous as it comprises of mixes embodying wood, other crude materials, transformed chemicals, etc.

1.4.5. Wood Waste

Wood transforming businesses essentially incorporate sawmilling, plywood, wood board, furniture, building part, flooring, molecule board, trim, jointing and specialty commercial ventures. Wood squanders by and large are aggregated at the handling production lines, e.g.

plywood plants and sawmills. The measure of waste created from wood preparing commercial ventures fluctuates starting with one sort industry then onto the next relying upon the manifestation of crude material and completed item. By and large, the waste from wood commercial enterprises, for example, saw millings and plywood, lacquer and others are sawdust, off-cuts, trims and shavings. Sawdust emerge from cutting, estimating, re-sawing, edging, while trims and shaving are the outcome of trimming and smoothing of wood. By and large, preparing of 1,000 kg of wood in the furniture commercial ventures will prompt waste era of practically a large portion of (45 %), i.e. 450 kg of wood. Correspondingly, when handling 1,000 kg of wood in sawmill, the waste will sum to a larger portion of (52 %), i.e. 520 kg wood. So this wood which is the deposit from the business can be transformed and utilized as sources of biomass.

1.4.6. Sewage Sludge Waste

Sewage slime is a carbon-unbiased biomass and a viable asset for counteractive action of biomass, sewage muck/sludge has favorable element that the generated sum and quality is just about steady as the year progressed, so in business field which heaps of fossil fuel is utilized, sewage ooze has been considered as a successful new energy asset for aversion of a dangerous atmospheric deviation. The conversion of sewage slop biomass to fuel venture have some major advantages in terms of decreased sewage slop, diminishes the emission of greenhouse gases. This is achieved by increasing the recycling rate of sewage slimes rather than the direct incineration. Additionally, for thermal power plant, CO_2 emanation and fossil fuel utilization can be lessened and the use of new energy utilizing biomass can be advanced. Particularly, as of late, the cost of fossil fuel has been expanding. Sewage is a source of biomass energy that is very much alike to the next animal squanders. Energy can be removed from sewage utilizing

anaerobic digestion to deliver biogas. The sewage slop that remaining parts can be burned or experience pyrolysis to deliver more biogas. Around 20% of created slop in 2002 was used for construction work. In Japan, dewatered slop is burned to diminish its volume, and ash is utilized as soil adjustment added substance, roadbed material, and so forth. Additionally, incinerations fiery debris is blended with other material, and tile, block, dirt pipe, etc, which contain incineration cinder, is made. As of late, new engineering making block just from incineration fiery debris was created.

Further it is also required to understand the elemental composition along with ash and moisture contents in the sources of biomass to have a technical understanding of the process to be selected for the production of bio-oil or bioenergy. Thus Table 1.1 presents the elemental (CHNS-O) analysis along with ash and moisture percentage in various sources of biomass.

Table 1.1: Elemental analysis of biomass from various sources

Feed stock	C	H	N	O	S	Ash	Moisture	Reference
Agricultural Residues	-	-	-	-	-	7.71	5.79	Zanzi et al. (1996)
Algae	28.9	2.8	5	-	-	26.5		Bird et al. (2010)
Almond shell	50.5	6.6	0.3	44.5	0.006	3.3	0.6	Cabellaro et al. (1997)
Bamboo	45.66	4.32	0.24	49.78	-	5.55	5.73	Wang (2006)
Banana waste	43.28	6.23	0.98		0.49	6.23	7.91	McKendry (2002)
Barley straw	45.7	6.1	0.4	38.3	-	6	30	McKendry (2002)
Beech wood	50.4	7.2	0.3	41	0	1	-	Blasi et al. (2000)
Birch	44	6.9	0.1	49	-	0.004	18.9	Oasmaa and Czernik (1999)
Bituminous coal	73.1	5.5	1.4	8.7	1.7	9	8-12	McKendry (2002)
Hardwood liquor	30.8	3.6	0.01	-	-	-	-	Demirbas (2002)
Cardboard	45.5	6.1	44.5	0.2	0.1	3.6	-	Tchibanoglaus (1977)
Corn Stover	47.28	5.06	0.8	40.63	0.22	4.5	25	Agblevor et al. (1996)
Corncob	43.04	6.32	1.02	49.26	-	2.41	8.64	Mullen et al. (2010)
Corrugated box	43.8	5.7	45.1	0.1	0.2	5.1	-	McKendry (2002)
Cypress	55	6.5	-	38.1	-	0.4	-	McKendry (2002)
Dactylis lomarata	42.96	5.7	1.9	49.44	-	7.5	-	Fahmi et al. (2008)
Danish Pine	-	-	-	-	-	1.6	8	McKendry (2002)
Dry sewage	20.5	3.2	17.5	2.3	0.6	56	-	Dominguez et al. (2008)

Feed stock	C	H	N	O	S	Ash	Moisture	Reference
Electronic	38.85	3.56	7.46	0.03	-	-	-	Wess et al. (2004)
Festuca arundinacea	42.22	5.64	1.5	50.65	-	7.3	-	Fahmi et al. (2008)
Fire wood	50	6	-	44	-	1.98	7.74	Reina et al. (1998)
Food fats	76.7	12.1	11.2	0	0	0	-	Raymundo et al. (2005)
Food waste	50	6	3	38	0.4	2.6	-	Lucie et al. (2013)
Gadren Trimmings	47.8	6.0	38.0	3.4	0.3	-	30-80	Othman (2008)
Garbage	45	6.4	28.8	3.3	0.5	16	-	Shan and Zhang (2005)
Hard wood	49.9	6	0.3	43.8	-	1.47	2.56	Sipila et al. (1998)
Hazlenut shell	50.08	5.13	1.38	41.99	-	1.4	-	Putun et al. (2001)
Hazle nut	46.76	5.76	45.83	0.22	0.67	0.77	-	Guney (2013)
Hybrid poplar	-	-	-	-	-	0.5-2	45	Agblevor et al. (1996)
Leather waste	43.59	6.95	32.28	10.84	1.45	4.89	8-12	Mohan et al. (2006)
Leaves	50	5.7	0.82	0.1	36	44	7.3	Mullen et al. (2010)
Lolium perenne	43.12	5.8	1.28	49.8		6.2	-	Fahmi et al. (2008)
Metal cans (Labels)	4.5	0.6	4.3	0.1	0	90.5	-	Tchobanoglaus (1977)
Miscanthus	48.1	5.4	42.2	0.01	0.5	1.5-4.5	11.5	McKendry (2002)
Oat straw	-	-	-	-	-	17.3	6.7	Jahirul et al. (2012)
Olive baggage	66.9	9.2	2	21.9	-	-	-	Encinar et al. (1996)
Olive husk	52.8	6.7	0.5	36.7	0.05	3.3	-	Demirbas et al. (2000)
Paper	43.5	6	44	0.3	0.2	-	4-10	Tchnobenoglaus (1977)

Feed stock	C	H	N	O	S	Ash	Moisture	Reference
Industrial Paper	44.9	6.1	47.8	0	0.1	1.1	-	Tchnobenoglaus (1977)
Peat	51.2	5.7	33.2	1.4	0.3	8.2	-	Oasmaa and Boocock (1992)
Pecan nut shell	47.3	6.4	0.7	45.5	-	0.93	10.28	Soltes et al. (1977)
Pine	45.7	7	0.1	47	-	0.03	17	Oasmaa and Czernik (1999)
Plastics	60	7.2	22.6	0	0	10.2	-	Scheirs and Kaminsky (2006)
Polar	48.1	5.3	0.14	46.1	-	0.007	16.8	Scott and Piskorz (1982)
Polyethylene	85.6	14.4	-	-	-	-	-	Li et al. (2013)
Reed canary grass	45.36	5.81	0.34	48.49	-	5.1	-	Fahmi et al. (2008)
Rice husk	47.4	6.7	0.8	45.1	0.25	20.26	7.66	Zheng Ji-lu (2007)
Rice straw	41.4	5	39.9	0.1	0.7	15.25	8.11	McKendry (2002)
Rubber	77.7	10.3	0	0	2	10	-	Ramadhas et al. (2005)
Sawdust	49.0	6.0	-	-	0.10	-	1-4	Chen et al. (2007)
Scots	56.4	6.3	0.1	-	-	0.09	-	Jahirul et al. (2012)
Sewage sludge	39.48	6.19	25.46	3.93	1.45	23.51	76.7	Dominguez et al. (2008)
Soft wood	53.2	6	0.4	40.4	-	0.3	2.7	Boucher et al. (2000)
Sugarcane bagasse	46.27	6.55	46.9	0.15	0.11	3.2-5.5	-	Islam et al. (2001)
Sunflower shell	47.4	1.4	5.8	41.4	0.05	4	-	Demirbas (2006)
Switch grass	47.45	5.75	42.37	0.74	0.08	3.61	-	Agblevor et al. (1996),
Tea waste	48.6	5.43	3.8	42.17	-	3.88	7.26	Demirbas (2001)
Textile	55	6.6	31.2	4.6	0.15	-	6-15	Tchnobenoglaus (1977)

Feed stock	C	H	N	O	S	Ash	Moisture	Reference
Walnut shell	50.8	6.41	0.39	41.21	-	2.8	-	Demirbas (2006)
Wheat straw	45.5	5.1	1.8	34.9	0.06	13.4	-	McKendry (2002)
Willow	47.78	5.9	0.31	46.1	-	1.3	-	Fahmi et al. (2008)
Wood	51.6	6.3	0.1	41.5	-	0.4-1	20	Tchnobenoglaus (1977)
Wool	50	7	22-25	16-17	3-4	-	30	Zoccola et al. (2009)
Wood waste chips	43.43	6.08	46.29	0.67	0.43	3.11	-	Wang et al. (1995)

1.5. Methods of Processing Biomass

There may be several methods to convert biomass into bio-oil; and some of the extensively used methods are

a) Physio-chemical conversion process

b) Bio-chemical conversion process

c) Thermo-chemical conversion process

Figure 1.5 pictorially represents the processes and sub processes of conversion of biomass into bio-oil that are currently available in the present literature. Details of each of these processes are presented as follows.

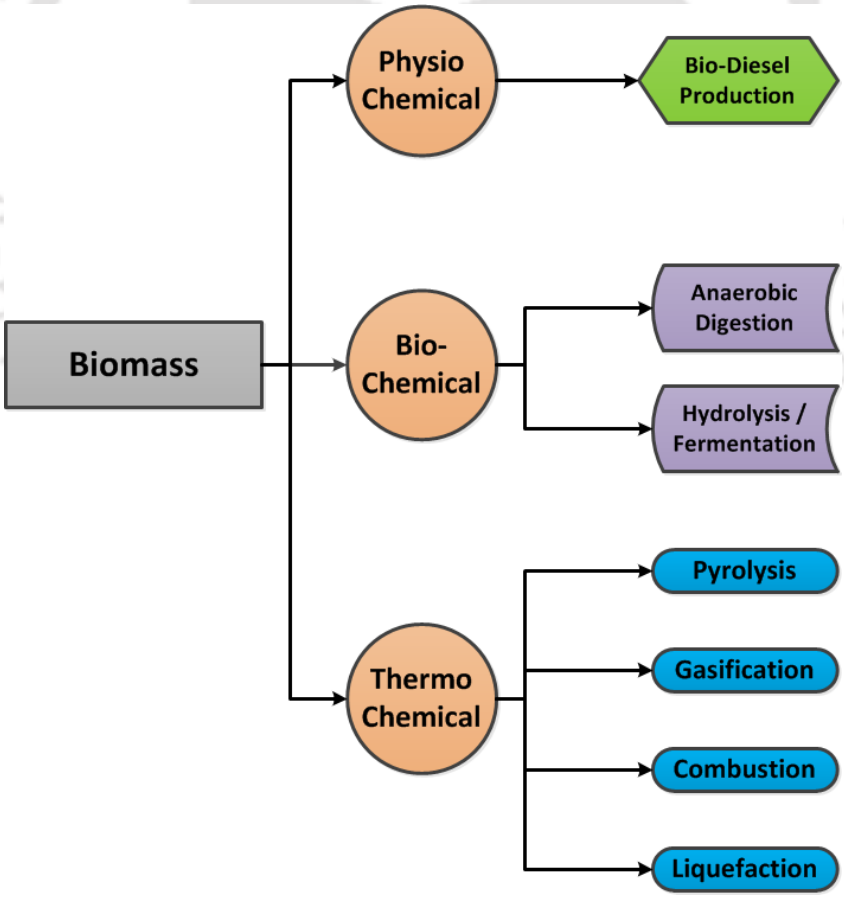

Figure 1.5: Methods of converting biomass feedstock into bio-oil

1.5.1. Physio-chemical conversion technologies

Physio-chemical conversion involves the synthesis of products using a physical and chemical processing at near ambient temperature and pressure. **These temperature and pressure conditions** are primarily associated with the transformation of fresh or used vegetable oils, animal fats, greases, tallow, and other suitable feedstocks into usable liquid fuels and chemicals such as biodiesel. To achieve the most promising and the available conversion methodology is transesterification. This is carried out by blending refined, dyed, and aerated vegetable oil or animal fat with a liquor (methanol by and large) in the presence of base or acid catalysts and this presentation would prompt esters of oils (biodiesel). Vegetable oils and fats are never similar. There are diverse levels of saturated and unsaturated fats in animal fats; and the yields of vegetable oils per acres of land are varied. Therefore, the biodiesel extracted from vegetable oils and animal fats will differ in composition; and consequently the discharges from energies by using these biodiesel will also be largely different depending on the source of biomass from which biodiesel extracted.

Transesterification is the procedure of exchanging the organic group of an ester with organic group of an alcohol in the presence of a catalyst and the innovation is fundamentally used to produce polyesters. Table 1.2 demonstrates the composition of the bio-diesel produced from the animal fats and the waste cooking oil along with the standard properties of bio-diesel. The opposite response, methanolysis is an alternate illustration for tranesterification procedure used to reuse the polyesters into individual monomers transformation of plastics into bio diesel. Tranesterification focused around the high pressure conditions is portrayed by the base catalyst in which the activation volume is in the negative scope of 10^{-3} cm^3. During the esterification

process, the triglyceride is reacted with alcohol in the presence of a catalyst, usually a strong alkaline like sodium hydroxide. The alcohol reacts with the fatty acids to form the mono-alkyl ester, or biodiesel, and crude glycerol. In most production, methanol or ethanol is the alcohol used (methanol produces methyl esters, ethanol produces ethyl esters) and is base catalyzed by either potassium or sodium hydroxide. Potassium hydroxide has been found more suitable for the ethyl ester biodiesel production, but either base can be used for methyl ester production. After the transesterification reaction and the separation of the crude heavy glycerin phase, the producer is left with a crude light biodiesel phase.

Table 1.2: Fuel properties of biodiesel produced from animal fat through transesterification and biodiesel standards from Bhatti et al. (2008)

Properties	**Biodiesel from animal fat**	**Biodiesel from waste cooking**	**Biodiesel standards**
Density (kg/l)	0.867	0.890	0.86-0.9
Viscosity (kg/m.s)	0.00625	-	< 0.005
Cloud point (^{o}C)	-5	1	-
Pour point (^{o}C)	-6	-	-
Moisture content (wt %)	0.01	0.015	< 0.05
Ash content (wt %)	0.022	-	< 0.02
Acid value (mg KOH/g)	0.25	0.48	< 0.8
Cetane value	61.0	54.5	58
Saponification value (mg KOH/g)	251.23	-	< 312.5

1.5.2. Bio-chemical conversion technologies

Bio-chemical conversion of biomass involves the use of bacteria, microorganisms, and enzymes to breakdown biomass into gaseous or liquid fuels, such as biogas or bioethanol. The most popular bio-chemical conversion technologies are anaerobic digestion (or biomethanation),

hydrolysis and fermentation. The three major steps involving the bio-chemical conversion technique are pretreatment, enzymatic hydrolysis, anaerobic digestion followed by fermentation. The details of the process are discussed here in detail.

1.5.2.1. Hydrolysis

Hydrolysis is the process of converting biomass polymers to fermentable sugars (Verardi et al., 2012). The process of hydrolysis involves cleaving the polymers of cellulose and hemicellulose into their monomers (Taherzadeh and Karimi, 2007). Complete hydrolysis of cellulose leads to the formation of glucose, whereas the hemicellulose gives rise to several pentoses and hexoses.

$$Cellulose \xrightarrow{Hydrolysis} Glucose \xrightarrow{Ferementation} Ethanol$$

$$Hemicellulose \xrightarrow{Hydrolysis} Pentoses\ and\ Hexoses \xrightarrow{Ferementation} Ethanol$$

The hydrolysis of biogas to produce bio-oil can be chemical hydrolysis and enzymatic hydrolysis. The details of these two processes are depicted in Figure 1.6**.**

1.5.2.2. Chemical Hydrolysis

Chemical hydrolysis involves the exposure of lignocellulose materials to chemical for a period of time at a specific temperature, resulting in sugar monomers from cellulose and hemicellulose polymers. The acids which are predominant for the chemical hydrolysis process are sulfuric acid (Harris et al., 1945), and HCl (Hasheem and Rashad, 1993). In general, the hydrolysis by dilute acids occur at high temperatures and pressures with a short residence time, resulting the degradation of hemicellulose and cellulose. Thereby the glucose yield is low due to the higher decomposition rate of glucose and high formation rate of undesirable products such as

levulinic acid, acetic acid, uronic acid, vanillin, phenol, formaldehyde, etc. (Larsson et al., 2000, Taherzadeh, 1999). Due to the severity of acid together with high temperature and pressure, chemical hydrolysis lead to high utility cost with additional burden of downstream neutralization.

1.5.2.3. Enzymatic hydrolysis

Enzymatic hydrolysis in which enzymes facilitate to depolymerize the lignocellulose biomass into biofuels and bio-chemicals. It is naturally a very slow process because of the structural parameters of the substrate (e.g. lignin and hemicellulose), surface area, and cellulose crystallinity. The process of conversion of cellulose to glucose is carried out by the cellulose enzymes that are highly specific catalysts. The hydrolysis is performed at mild conditions of temperature between 40^{o}C -50^{o}C and pH ranging between 4.5 - 5.0. This reduces the corrosion problems, low utility consumption, low toxicity of hydrolysates, etc. The process of cellulose degradation to glucose majorly depends on the three major classes of enzymes namely endo-glucanases, exo-glucanases, and β-glucosidases. In addition to this, enzymatic hydrolysis is an environmental friendly process, whereas it has a disadvantage of longer hydrolysis time, however, enzymes are more expensive than acids and the end product inhibition may occur.

1.5.2.4. Fermentation

A Group of chemical reactions induced by microorganisms or enzymes that split complex organic compounds into relatively simple substances, especially the anaerobic conversion of sugar to carbon dioxide and alcohol. The common biomass that is used in the fermentation process is rich in sugar compounds majorly lignocellulose biomass (sugarcane, sweet potato and corn) consisting of fermentable sugars namely cellulose and hemicellulose along with non-

fermentable sugars like lignin. The lignin fraction is high in energy and can be utilized for the generation of heat and electricity. Various product outputs are targeted through fermentation process depending on the type of feedstock majorly ethyl alcohol from lignocellulose biomass.

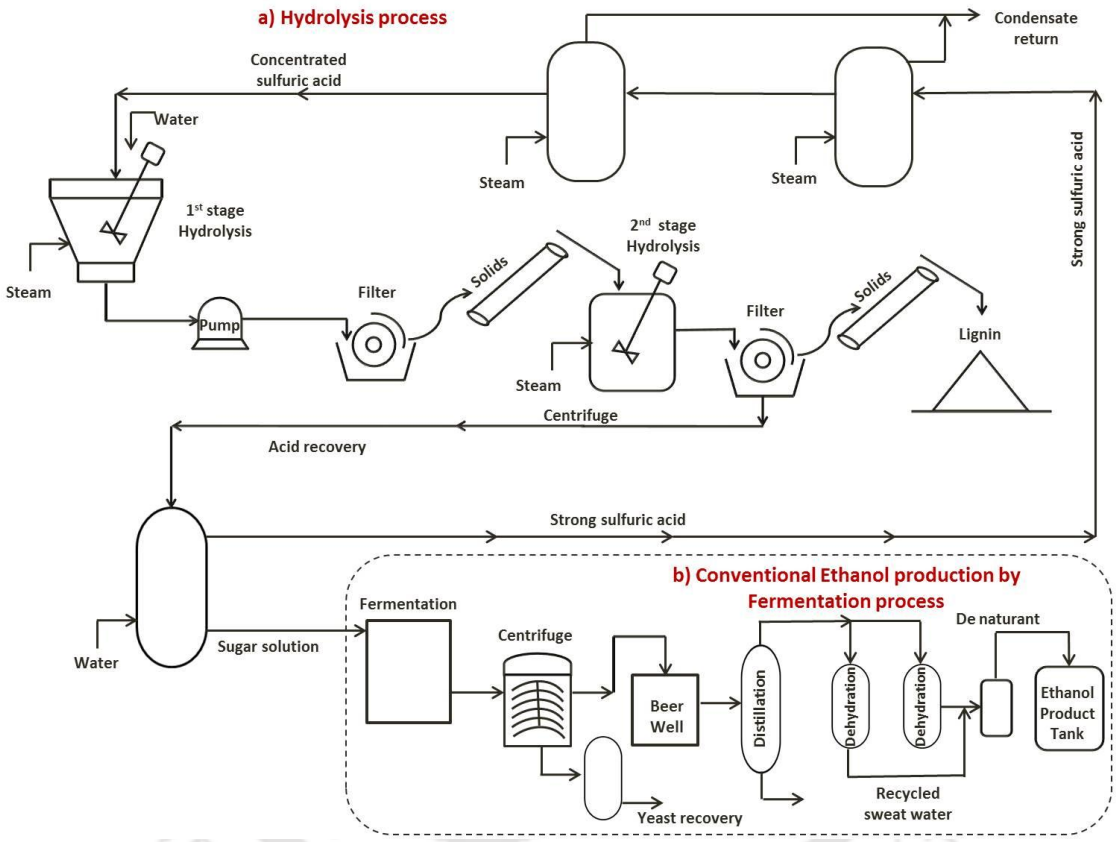

Figure 1.6: Bio-chemical conversion process a) hydrolysis b) fermentation

(Source: www.arkenol.com/Arkenol.Inc/tech01.html)

The yeast or the enzyme that is commonly used in the fermentation to breakdown glucose into fructose and sucrose for the ethanol production are schizosaccharomyces pombe, saccharomyces cerevisivae. The ethanol produced is distilled and dehydrated to get a higher concentration of alcohol to attain to the required immaculateness (higher concentration) for the utilization as automotive fuel. The solid residue from the fermentation process is utilized as a cattle feed and

in the case of sugarcane; bagasse is used as a fuel for boilers. Although decomposition of the material into fermentable sugars is complicated, the processing steps of dehydration, distillation, fermentation processes are interlinked and are identical for either agricultural crops or lignocellulose biomass.

1.5.2.5. Anaerobic Digestion

This process not only decreases the greenhouse gases but also reduce dependence on fossil fuels for energy requirements. It is a microbiological conversion of organic matter to methane in the absence of oxygen. The decomposition is mainly caused by the natural bacterial action in various stages. It takes place in variety of natural anaerobic environments including water sediments, water logged soils, natural hot springs, ocean thermal vents and stomach of various animals. The process generates three main products.

- Biogas: A mixture of carbon dioxide and methane which is used to generate heat and electricity.
- Fiber: It is used as a nutrient rich soil conditioner
- Liquor: It can be used as a simple liquid fertilizer.

There are two types of anaerobic digestion processes

- Mesophilic digestion
- Thermophilic digestion

Mesophilic digestion is most commonly used process for anaerobic digestion, in particular waste sludge treatment. Decomposition of volatile waste suspended solids is around 40% over a retention time of 15 - 40 days at a temperature of $30^{o}C$ – $40^{o}C$, that requires larger digestion tanks. Whereas thermophilic digestion is less common and not as mature a technology as

Mesophilic digestion. The digester is heated to 55^{o}C and held for a period of 12-14 days. This technology provides higher biogas production, faster throughput and improved pathogen and kills virus, but the technology is more expensive more energy is needed and it is necessary to have more sophisticated control and instrumentation.

Anaerobic digestion Process

Figure 1.7 presents an anaerobic digestion system for converting biomass feedstock to bio-oil. The initial stage of this process involves shredder where the feed streams are passed into it and the particles are shredded into 12 mm size as per the regulations of EU and UK and less than the biogas and the liquor/fiber, known as digestate. The biogas generated from the digestion tank finally will be sent to gas storage.10mm as per Indian standard. From the shredder, particles are transferred to input buffer which is simply a sealed tank that holds the shredded material.

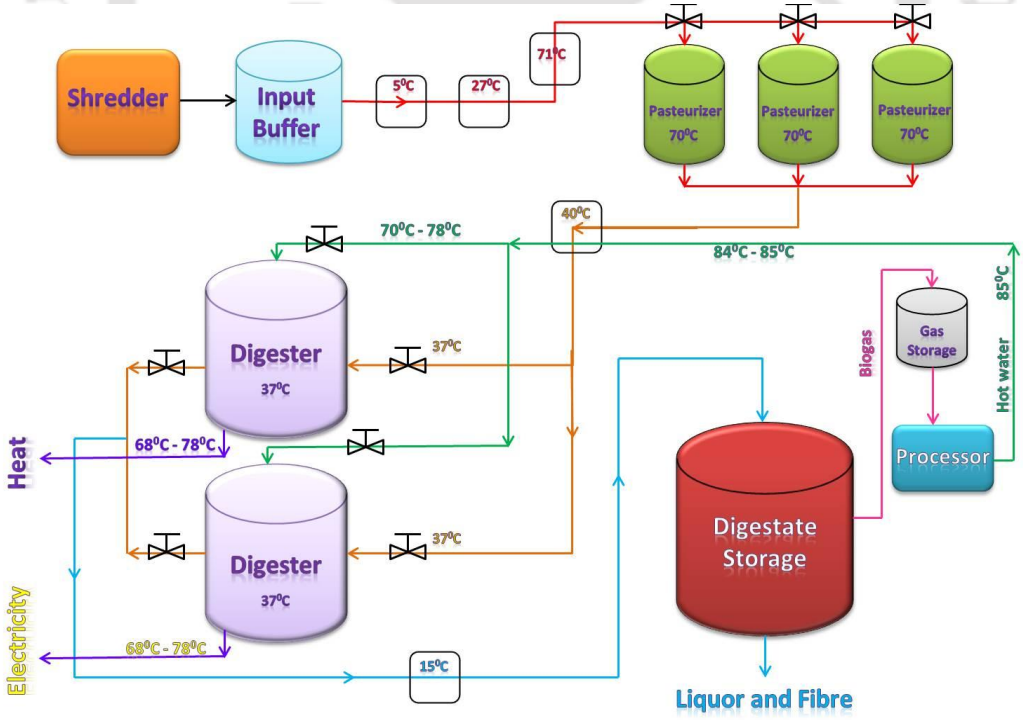

Figure 1.7: Anaerobic digestion system (bio-chemical method) for processing biomass feed stock to bio oil. (Source: Energy systems research unit- University of Strathclyde; www.esru.strath.ac.uk/EandE/Web_sites/03-04/biomass/background info8.html).

This allows controlling the flow to further processing steps. It also allows excess storage in case of any unforeseen amount of feed stream offered. Then feedstock is allowed to pass to pasteurizer where the temperature is maintained at $70^{o}C$ for at least one hour. This temperature is enough to destroy the pathogens in the feedstock which prevents the bacterial competition in the digestion stage. To allow a constant supply of feed to digestion stage three pasteurizers are used. Further the material is transferred to digestion tank where the majority of bio gas is produced. The anaerobic bacteria convert a quantity of organic matter into biogas in a sealed container. This is continuously stirred and heated to $35^{o}C$ and the average retention time is approximately 18 days. This allows a significant percentage of organic solids to be converted to biogas. The outflows of biogas are in two forms, the biogas and the liquor/fiber, known as digestate. The biogas generated from the digestion tank finally will be sent to gas storage.

1.5.3. Thermo-chemical conversion technologies

The thermo chemical conversion of biomass involves three major steps namely

- Pyrolysis
- Gasification
- Liquefaction

1.5.3.1. Pyrolysis

Figure 1.8 presents the pyrolysis process for the thermo-chemical degradation of biomass to bio oil. It is the thermal decomposition of organic matter in the absence of air which is also

referred to devolatization. The thermal decomposition takes place in less than two seconds; is the primary chemical reaction that is precursor for both the combustion and gasification processes. This thermal decomposition of biomass through pyrolysis leads to the formation of bio-oil, bio char, methane, hydrogen, carbon-dioxide and carbon-monoxide. This process involves simultaneous and successive reactions when organic material is heated in an inert atmosphere. In Pyrolysis, the thermal decomposition of organic components of biomass starts at 350^{o}C – 450^{o}C and goes up to 700^{o}C – 800^{o}C in the absence of air/oxygen.

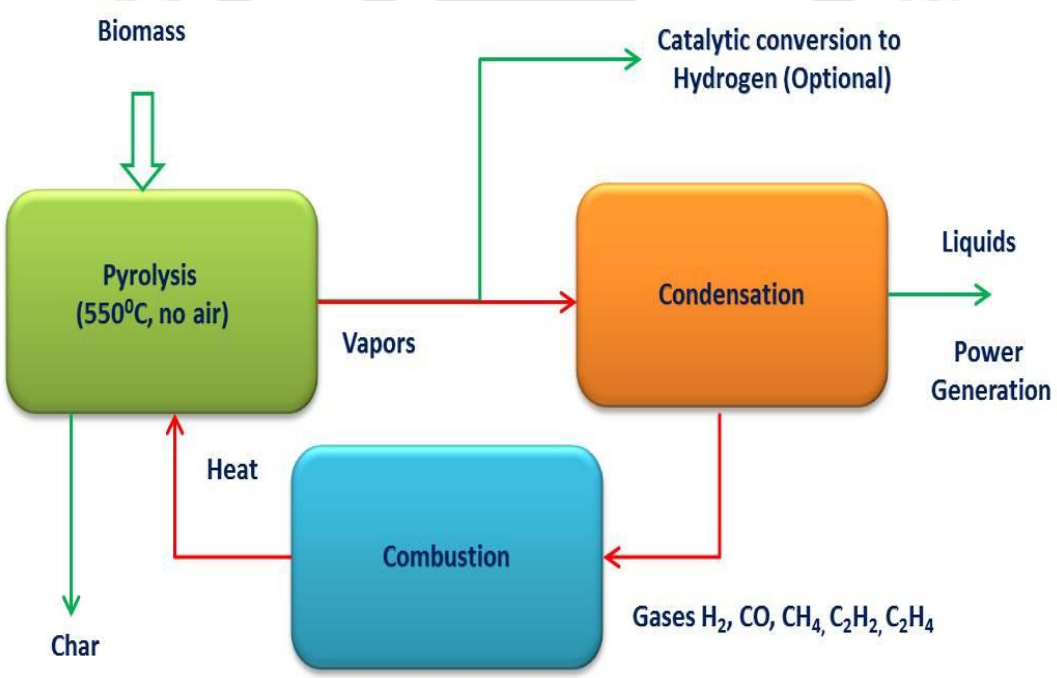

Figure 1.8: Pyrolysis process (thermo-chemical method) for producing bio-oil from biomass feedstock.
(Source:www.altenergymag.com/content.php?issue_number=09.02.01&article=pyrolysis)

The long chains of carbon bonded with hydrogen and oxygen breaks into smaller ones in the form of gases, condensable vapors, and solid charcoal under pyrolytic conditions. The extent of decomposition and rate of reaction is dependent on the process parameters and reaction

temperatures, pressure, reactor configuration and feedstock. The pyrolysis process under lower temperatures (450^{o}C) and when the heating rate is quite slow, the biomass yields bio-char; whereas at higher temperatures i.e., above 800^{o}C, pyrolysis of biomass yields gases with rapid heating rates. At intermediate temperatures and relatively higher heating rates pyrolysis of biomass yields bio-oil. Pyrolysis process can be categorized as slow or fast pyrolysis. Slow pyrolysis takes several hours to complete the process and results in bio-char as the main product. On the other hand, fast pyrolysis yields 60% bio-oil, and takes seconds for complete pyrolysis. In addition, it gives 20% bio char and 20% syngas. Thus, the fast pyrolysis is currently used most widely.

Further in this method, there are three main components, namely, combustion zone, reaction zone and pyrolysis zone. In the combustion zone, the combustible solid substance which is the feed stock is made out of elements carbon, hydrogen and oxygen. From the combustion chamber the carbon dioxide is obtained from carbon and water is obtained from hydrogen in the form of water vapor. The reactions that are taking place inside a combustion chamber are exothermic and yield a theoretical oxidation temperature of 1450^{o}C. The products obtained from partial combustion in combustion zone will now pass through a reaction zone consisting of a red hot bed of charcoal where the reduction reaction takes place. These reactions are endothermic and the temperature may be in the range of 800^{o}C -1000^{o}C. Further, the pyrolysis zone is an intricate process that is not completely out broken. The product formation is dependent upon temperature, pressure, residence time, and heat losses. In this pyrolysis zone the temperature is maintained at 700^{o}C. Up to 200^{o}C only water is driven off. Between 200^{o}C -280^{o}C carbon dioxide, acetic acid and water are given off. The real pyrolysis, which takes place between 280^{o}C

-500^{o}C, producing large quantities of tar and gases containing carbon dioxide. Besides large tars, some methyl alcohol is also formed.

Advantages of biomass pyrolysis

- Biomass pyrolysis can be carried out at small scale and at remote areas which improve energy density of the biomass asset and diminish transport.
- This methodology offers an alluring method for changing over organic matter into energy products which is utilized for the generation of high heat, power and electricity.
- This process has been accumulating much consideration because of its high productivity and great natural execution qualities.
- The char delivered from pyrolysis can be sequestered which has an enormous effect in the fossil fuel outflows overall and goes about as a significant player in the worldwide carbon market (trading of carbon emissions specifically targeted for CO_2) with its vigorous, clean and straightforward engineering.

1.5.3.2. Gasification

Biomass gasification includes the partial combustion of solid fuel at the temperature of 1000^{o}C inside a reactor termed as gasifier and the procedure is known as low temperature gasification. In contrast, high temperature results the elevated amounts of hydrocarbons, flammable and combustible gases like CO, H_2, tar, dust, and traces of methane also known as producer gas. The producer gas is utilized in internal combustion engines, as a substitute for furnace oil in immediate heat applications and to deliver in a financially feasible way. Different types of gasifiers for the gasification of solid fuels are shown in Figure 1.9.

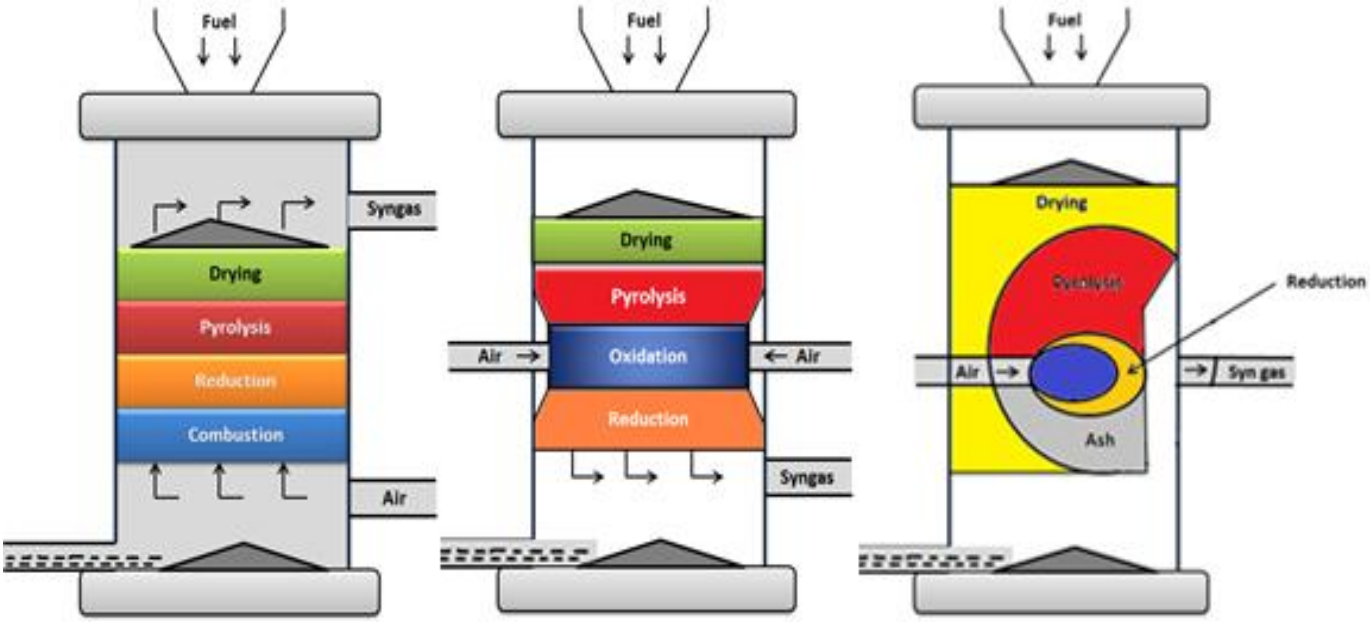

Figure 1.9: Types of gasifier a) Downdraft gasifier b) updraft gasifier c) cross draft gasifier (Source: www.soi.wide.ad.jp/class/20070041/slides/05/index_42.html)

The generation of these gasses is by response of water vapor and carbon dioxide through a shining layer of charcoal. Along these lines the way to gasifier outline is to make conditions such that a) biomass is lessened to charcoal and b) charcoal is converted to CO and H_2. Since there is an association of air, oxygen and biomass in the gasifier, they are characterized by the way air and oxygen is presented in it.

1.6. Bio-oil

The fast pyrolysis bio oil is a guaranteed second era fluid fuel, which can be obtained from fast pyrolysis of lignocellulose (a combination of hemicellulose, cellulose, and lignin) biomass with yield up to 75 wt. %. The bio-oil obtained by pyrolysis are often considered as "*unprocessed bio-oil*" and are not suitable for direct use as transportation fuel because of various reasons as discussed in later sections. Because of such reasons the liquid oil obtained from

pyrolysis is often termed as bio-oil (or unprocessed bio-oil) but not bio-fuel. Bio oil obtained from biomass pyrolysis is dim tan in shade, free flowing with smoky smell. The properties of bio oil rely on upon different variables, for example, feedstocks, bio-oil preparation procedures, and other operating conditions. The physical properties of bi-oil demonstrate that bio-oils are a complex mixture of more than 300 compounds derived from the depolymerization and fragmentation reactions of cellulose, hemicellulose and lignin.

The organic compounds present in unprocessed bio-oil are acids, alcohol, ethers, ketones, aldehydes, phenols, esters, sugar, furans, and nitrogen mixes. The phenolic compositions are structured by the decomposition of lignin, while different oxygenates, for example, sugars, and furans are produced by the depolymerization of cellulose and hemicellulose of biomass. The esters, acids, alcohols, ketones and aldehydes are obtained by the decomposition of random little oxygenated compounds. As a consequence of exceedingly gooey/viscous, thermally precarious, and highly corrosive nature of unprocessed bio-oils renders these bio-oils less helpful as an option to routine fuels. The unprocessed bio-oils are less steady ascribed to the action of oxygenated chemicals, because of the negative chemical properties like presence of acids, ethers and esters, aldehydes, ketones, alcohols, and other high oxygen substances. Accordingly the viscosity of the bio-oil may be increased amid the storage and experiences several chemical reactions amid the aging of bio-oils. The viscosity of unprocessed bio-oil differs from 25 cSt to 1000 cSt relying upon feedstock, water substance of bio-oil, and pyrolysis procedure utilized. As the bio-oil has high thickness, it counts for higher pressure drop, hence increasing venture/investment (stock).

Low temperature heating is a transcendent answer to lessen viscosity. The viscosity can be likewise controlled by adding solvents like alcohols to unprocessed bio oil before

upgradation. Besides, lignin obtained from the softwood biomass material has mostly three forerunners and to be specific they are pocumaryl alcohol, coniferyl alcohol, and sinapyl alcohol. Lignin is the highest temperature resistant in the three noteworthy parts of biomass and regularly disintegrates at 208^{o}C - 500^{o}C. Because of this decay results char formation prompting the simple blockage of spouts. The presence of high oxygen and high moisture substance lessens the heating value, and serious corrosivity due to acid richness. These unprocessed bio-oils have low heating values when contrasted with petroleum fuels. The higher heating value of plant based bio-oils is larger than wood and farming based bio-oils. There are numerous different attributes of unprocessed bio oil are low H/C proportion, nitrogen and sulfur vicinity, stage division, poisonous quality, high temperature affectability, extreme ignition delay.

Disadvantages of unprocessed Bio-oils

- Biofuels are not less expensive in terms of both financial aspects and ecology.
- Researches contend that the energy needed to create the one gallon of bio fuel is equal to the vitality creation of a few gallons of the petroleum fuel.
- Variation of bio fuel quality is an alternate critical issue to be explored. The nature of the bio fuel created differs for product to harvest plant to plant. Such a variety of unsaturated oils leave sticky deposits which needs further handling includes extra cost.
- Biofuels doesn't toll much better. In light of the higher than petroleum gel purpose of numerous biodiesel-creating oils, a biodiesel motor can be troublesome if not difficult to begin in icy climate. The issue is far and away more terrible for the unadulterated vegetable oils. A percentage of the oils created from these plant and rural plants have higher thickness which lessens the fuel stream to the practically identical.

- Bio-oils possess higher viscosity leads to ageing problem while it is stored; maintaining high pressure drops in pipelines during transportation leads to higher maintenance of equipment.
- Bio-oil is highly non-homogenous which leads to the layering or partial separation of phases also causing filtration problems.
- Lower values of pH of bio-oil refers to higher acidic nature which leads to the corrosion problems.
- Bio-oils contain higher alkali metals causing solid depositions in combustion chambers, boilers reduces the efficiency of the equipment
- The higher water content of bio-oil makes severe complications in terms of increasing viscosity, reducing heating values, decreases the stability, and also leads to phase separation.

1.7. Upgradation of unprocessed Bio-oil to Bio-fuel

The immediate application of bio oil as customary petroleum fuels is restricted by the issues of high viscosity, high oxygen substance, highly corrosive, high moisture content, and their thermal flimsiness/instability. Accordingly, bio-oils ought to be upgraded utilizing legitimate strategies before they can be utilized as a part of diesel or gasoline engines. The focal objective of the upgradation is to convert the oxygen rich, and high atomic weight lignin into hydrocarbons that are contrasted with today's petroleum derived fuels. Just constrained data is accessible on hydrotreatment of biomass determined oils. Numerous substances, for example, aromatics, olefins, pitches, and so on can be separated from the pyrolysis bio-oil for useful modern application. The hydrotreatment techniques accessible for the upgradation methodology utilizing a solid catalyst included are hydrodeoxygeneation (HDO), hydrodesulphurization (HDS), hydrodenitrogenation (HDN), hydrodemetallization (HDM), and hydrogenation (HYD).

The burning of fuels creates NO_x and SO_x discharges which are naturally determined for the evacuation of sulfur and nitrogen mixes from the bio oil.

Advantages of processed/upgraded bio fuel

The bio fuel obtained from pyrolysis can have the following industrial use.

- The upgraded bio-fuel can be used as combustion fuel, transportation fuel.
- Used for power generation
- Production of resins and chemicals, anhydro-sugars like levoglucosan
- Can be used as liquid smoke
- Used as binders for palletizing and briquetting of combustible organic waste materials
- Bio-oil can be used as a wood preservative, and adhesives.

1.7.1. Hydrodeoxygenation

To beat the issues brought about because of the pernicious materials in the bio oil because of oxy-rich antecedents like sugars and so on an upgradation procedure is to be conveyed. Among the different upgradation procedures, the hydrodeoxygeneation (HDO) strategy has attained a lot of attention so that the unprocessed bio-oil can be converted into bio-fuel. HDO is the hydrogenalysis process and the centrality of the HDO methodology lies with the measure of oxygen evacuation as water present in the oxy rich bio oil and upgradation of substantial buildups. According to the gauges of American Petroleum Institute (API) the normal estimation of the oxygen substance ought not surpass 0.5 wt% while the oxygen substance of pyrolysis bio oil is around 1.2 wt%. These hydrotreating of transforming components utilize high pressures to evacuate oxygen and hydrogen and heterous molecules out of the bio-oil. HDO

procedure is less relevant to the tradition petroleum as the substance of oxygen is under 3000 ppmw in petroleum.

Yet in the hydroprocessing of biomass feedstock, HDO assumes a significant part in the upgradation process subsequent to the biomass feedstock have enormous measure of oxygen substance of around 500000 ppmw with a little measure of sulfur. The methodology is extremely productive because of the high carbon productivity (hypothetically carbon effectiveness of 100% as all carbons are converted to hydrocarbons without CO_2 outflows). The utilization of the solid catalyst and the severity of the operation needed for accomplishing high HDO transformations rely upon the substance and sort of the oxygen compounds in the feed. Approximate compositions of feed varying from the starting point of source are recorded in Table 1.3.

The upgrading technique is complex network due to the involvement of the complex compositions of bio oils. The general reaction for the hydrodeoxygenation is given as

$$(CH_2O) + H_2 \xrightarrow{Catalyst} (CH_2) + H_2O$$

The other possible reactions during the HDO process are as follow:

- Dehydration reaction due to condensation polymerization.
- Decarboxylation reaction in which oxygen is removed in the form of water
- Hydrogenation reaction involves the saturation of unsaturated compounds
- Hydrogenalysis reaction related to the breakup of C-O bonds
- Hydrocracking reactions resulting the breakdown of higher molecular components into smaller molecules.

Table 1.3: Composition (wt.%) of feed for HDO from different sources of oil stocks (Furimsky 2000)

Characteristic	Conventional crude	Coal derived naptha	Oil shale crude	Bio-oil	
				Liquefied	Pyrolyzed
Carbon	85.2	85.2	85.9	74.8	45.3
Hydrogen	12.8	9.6	11.0	8.0	7.5
H/C	1.8	1.4	1.5	1.3	2.0
Sulphur	1.8	0.1	0.5	< 0.1	< 0.1
Nitrogen	0.1	0.5	1.4	< 0.1	< 0.1
Oxygen	0.1	4.7	1.2	16.6	46.9

Some of the important findings of the HDO process are presented herein:

- The ketone group is easily and selectively hydrogenated into a methylene group above 200^{o}C.
- Carboxyl groups are hydrogenated under HDO conditions but parallel decarboxylation also occurs at comparable rates to form alkanes.
- Guaiacol caused deactivation of a few catalysts due to coking reaction.
- Water contents decreased the catalytic activity to one-third of initial activity of catalyst.
- Conventional catalyst show very low activity for the HDO in aqueous phase while using the super critical solvent extraction, the conversion of cresol to aromatic hydrocarbons is increased tremendously. Usage of supported noble metal catalysts enhance the properties of HDO bio-fuel.

Finally**,** Figure 1.10 shows the production of upgraded bio-oil from biomass through various possible processes.

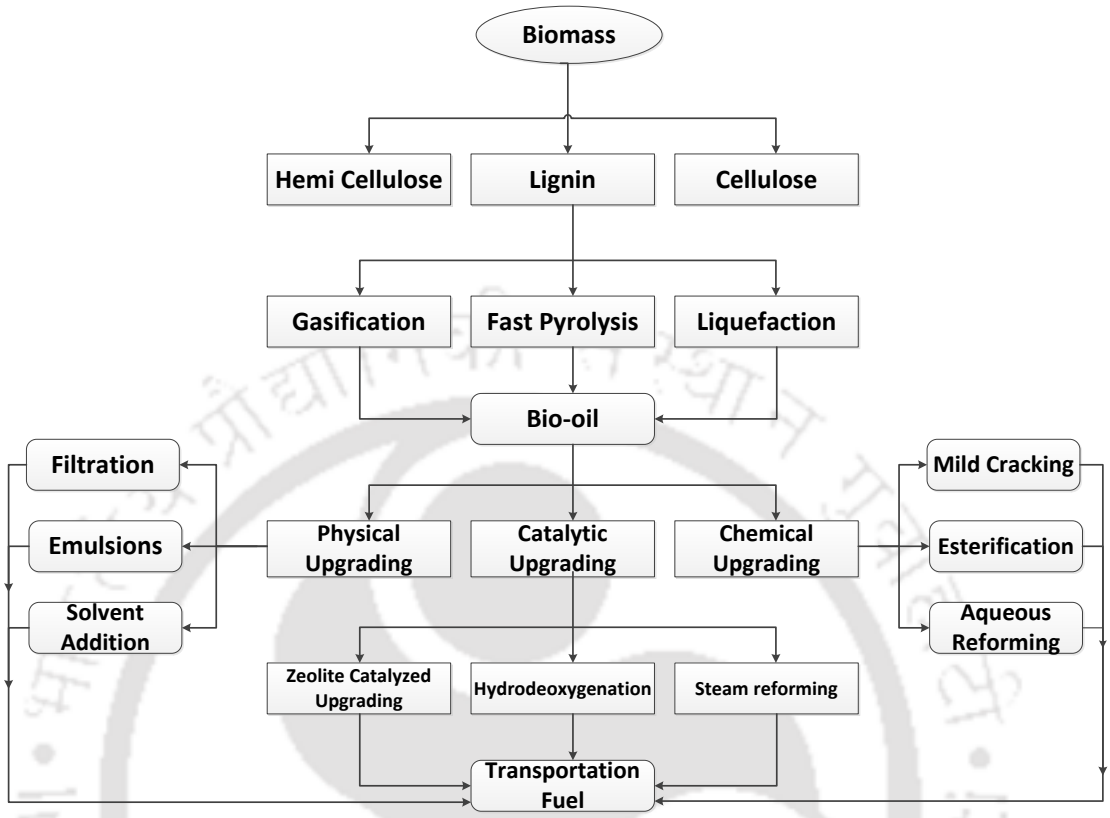

Figure 1.10: Upgradation of bio-oil flow sheet (adopted from Saidi et al. (2014))

1.7.2. Catalysts for HDO

HDO involves the presence of a catalyst phase and a gas (H_2) phase at a moderate temperature (300^oC - 600^oC) in which oxygen is removed in the form of water. An active and stable catalyst plays a crucial role during HDO process. Till date transition metal sulfides (Wildschut et al. 2009), carbides (Ramanatham and Oyama, 1995), nitrides (Ramanatham and Oyama, 1995), oxynitrides (Lippitz and Hubert, 2005), phosphides (Phuong et al., 2012), noble metals (Wang et al., 2011), precious metals (Gutierrez et al., 2009), metal oxides (Heng Shi et al., 2014) have been used as the active catalyst phases for the HDO process. Details of roles of some of these catalysts are presented below.

1.7.2.1. Transition metal sulfides

Ni-Mo and Co-Mo supported on Al_2O_3 are the conventional transition metal sulfides catalysts that are used mostly in the HDO processing (Gutierrez et al. 2009). The sulphided catalyst show Bronsted acid character since groups such as H^+ and SH^- exist in the catalyst surface. Thus they remove oxygen from HDO reactions. Additives like phosporous (Yang et al., 2009), potash (Centeno et al., 1995), and platinum (Centeno et al., 1995) are added to Co-Mo or Ni-Mo catalyst and the promotion effect of phosporous (Zhong and Xianqin, 2012) is resulted as follows:

- Formation of new Lewis and Bronsted acid sites on the catalyst surfaces.
- Formation of compounds that are easily reducible and sulphidable.
- Increase in Mo dispersion due to solubility of molybdate by the formation of phosphomolybdate complexes.

1.7.2.2. Noble metals

The conventional industrial hydrotreating catalysts are less suitable for bio-oil HDO due to the economy of sulphur usage, product contamination, and poor stability in the presence of H_2O. Therefore development of sulphur free catalysts for bio-oil upgrading is more suitable, as they are environmental friendly and economically favorable. HDO process in the presence of noble catalysts is accepted particularly because they are efficient in activating molecular hydrogen atoms under mild conditions since hydrogen is easily activated and split on the surface to react with reactants. Thus it is expected that noble metal catalysts can achieve better activity and stability on supports other than alumina. However the main challenge lies in the availability of the catalyst, cost, and higher sensitivity towards poisoning such as iron and sulphur.

1.7.2.3. Non precious metals

Fe based catalyst (Olcese et al., 2012)

Fe/SiO_2 is the common iron based catalyst used for the HDO process of guaiacol. Metallic Fe activates hydrogen; guaiacol is activated by acidic OH sites from SiO_2. The products obtained using this catalyst is benzene and toluene. The operating temperatures for the specific catalyst are in the range of $350^oC – 450^oC$.

Ni based catalyst (Yakovlev et al., 2009)

Metallic Ni based catalyst such as Ni/Al_2O_3 is found to be very active (HDO degree of 95%). Bi metallic Ni-Cu catalysts such as $Ni\text{-}Cu/Al_2O_3$ are even more active than Ni, with HDO degree of 99.2%.

1.8. Types of Reactors

The implementation of new technologies which are focused on the heavier (significant amount of asphaltenes and fractions boiling above 524^oC) oil feed stocks processing involves the conversion of heavy, high boiling feedstock molecules into lower boing point products through carbon bond breakage, along with hydrogenation process sequentially. In order to facilitate hydrotreating and/or hydrocracking of the heavier feed stock various reactors are already been developed (or in developing stage) and some of them which are available in the market. Some of important type of reactors can be used for HDO of bio-oil are fixed bed, moving bed, ebullated bed, and slurry bed reactors. A few key information about these reactors are presented below:

1.8.1. Fixed bed reactors (FBR)

Figure 1.11 shows the schematic of fixed bed reactors most economically utilized as a part of hydrotreatment operations because of the way that they are basic and simple to work. The

effortlessness of the reactor is constrained to hydrodesulphurization of the lighter feeds. On account of HDS of naptha in a fixed bed reactor the response continues in two stages. In the first stage the naptha is completely vaporized and in the second stage, when the amount of feed to the distillation column is increased, three phases are found such as partially vaporized gas liquid mixture, hydrogen gas and solid catalyst. This later can be processed in a type of fixed bed reactor namely trickle bed reactor where the liquid and gas phases flow counter current downwards through the catalyst bed where the reaction takes place. In this reactor the gas is considered to be continuous phase and the liquid as dispersed phase. The reaction on the surface of the catalyst between the reactants is possible only when the phase of hydrogen has to be converted from gas to liquid.

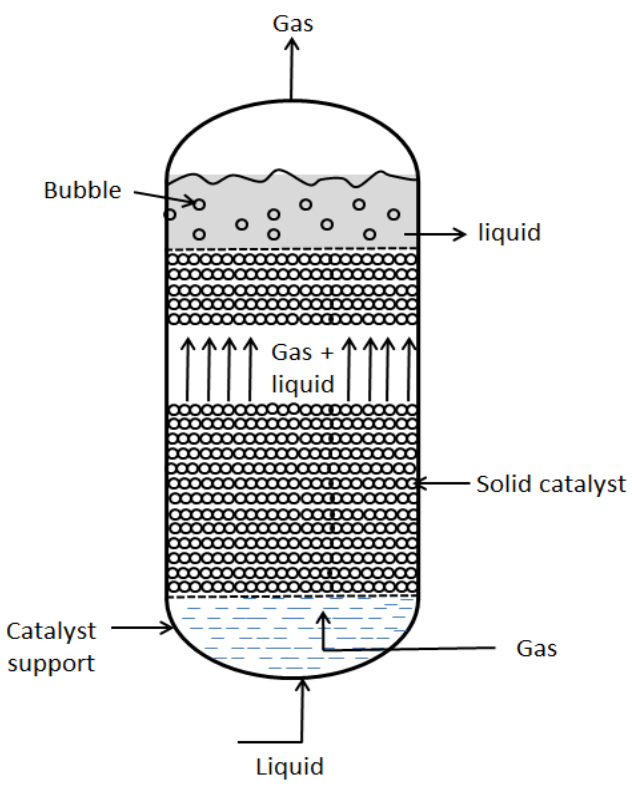

Figure 1.11: Fixed bed reactor (Ancheyta and Speight, 2007)

This change of phase is to maintain the balance between the bulk partial pressure and also equilibrium concentration because of the mass transfer resistance in gas film is negligible. When the reaction is completed again the gas reaction products are transferred to gas phase and liquid reaction products are transferred to liquid phase. The another important feature of theses reactors are to maintain the proper superficial velocities which is low in the case of pilot plants and varies significantly when comes to commercial plants.

1.8.2. Moving bed reactors (MBR)

In the moving bed reactors (Figure 1.12) the catalyst is flowing in descending bearing because of the gravitational force. The crisp/fresh catalyst is entering at the highest point of the reactor and the spent catalyst is leaving to the base of the reactor.

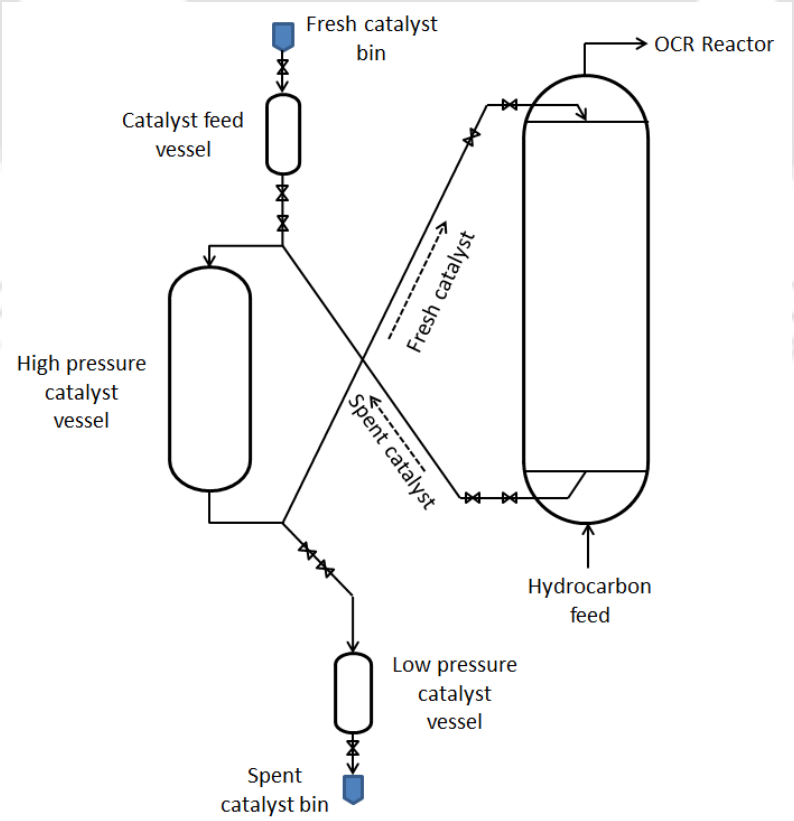

Figure 1.12: Moving bed reactor (Ancheyta and Speight, 2007)

The hydrocarbons goes in either counter or cocurrent direction through the reactor. The catalyst in the moving bed reactors are homogeneously stacked by metal sulfides. The catalyst utilization is greatest on account of moving bed reactors, furthermore catalyst is particular in nature like scraped spot safe/ abrasion resistant, solid. The tolerance to metals and different contaminants in the moving bed reactor is high as contrasted with fixed bed reactors. The countercurrent mode of operation for the moving bed reactor is the best suitable arrangement for the operation. In this arrangement the fresh catalyst is introduced at the top and the feed from the bottom. Both the catalyst and feed moves in a countercurrent flow causing the feed with utmost impurities; the spent catalyst is withdrawn from the bottom of the reactor and a new batch of the catalyst is added at the top. In this way the process is advantageous in terms of lower catalyst utilization, and continuous without any interruption for the catalyst replacement.

1.8.3. Ebullated bed reactor (EBR)

Figure 1.13 presents the recent novel multiphase catalytic reactors, namely, ebullated bed reactors (EBR), picked up consideration in applications like hydrodesulphurization, hydrodeoxygeneation, hydrocracking, generation of adiponitrile, methanation, waste water treatment, Fischer-Tropsch combination and so forth. The renowned importance of usage of EBR has considerably increased due to the increased processing of heavier petroleum feed stocks using hydrocracking and refining. These heavier feeds are hard to process because of the higher substance of sulfur, nitrogen, metals, (for example, vanadium, nickel), asphaltenes which has a significant negative effect on the dependability and the movement of the catalyst. The issues arised in fixed bed reactor are overcome by the presentation EBR. In EBR the hydrocarbon feed and hydrogen gas are fed up flow through a catalyst bed.

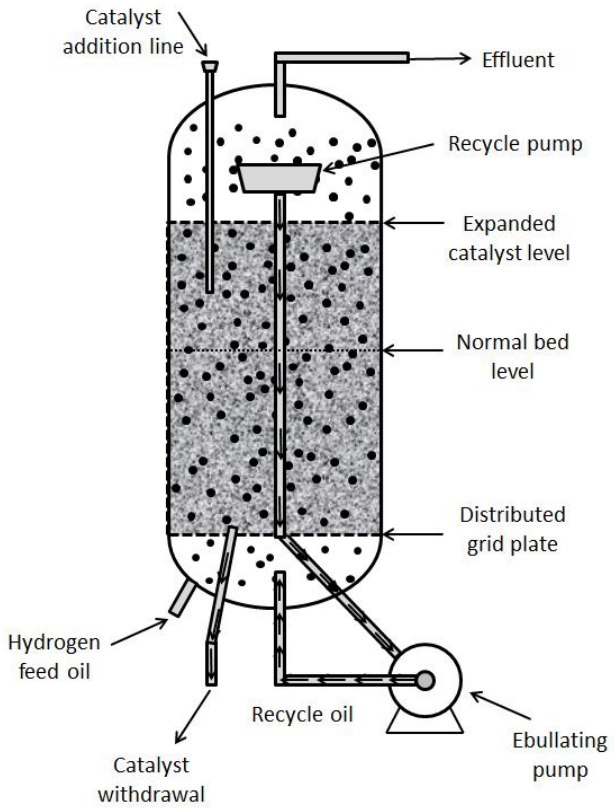

Figure 1.13: Ebullated bed reactor (Ancheyta and Speight, 2007)

This result in expansion of bed, back mixing inside the reactor which reduces the plugging of the bed and also reduces the pressure drop problems. The feed that is entered into the plenum chamber of the reactor is thoroughly mixed through a specially designed mixer, and spraggers attached to the catalyst support plate. The quality of the product is maintained at a high rate due to the constant withdrawal of spent catalyst and addition of new batch of catalyst incorporates on stream catalyst expansion, withdrawal, and killing the shutdown issue for the impetus substitution. The hydroprocessing of the feed stocks oil is separated from the catalyst at the top of the reactor and recirculated to the bottom in order to mix with new feed and hence the reactor behaves like a continuous stirred tank reactor. The reactor is provided with an ebullated pump to maintain the liquid circulations within the reactor. The liquid circulations maintain the

isothermal conditions within the reactor and require no further quenching. The unconverted heavy feed stock is recycled to the reactor by adding some diluent to improve fluidization and overall conversion. The common commercial addition rate of the catalyst is 90 to 100 g catalysts/barrel of liquid feed. Catalyst bed expansion can be controlled by the adjustment of the circulating pump flow. These reactors are designed to have an expanded catalyst bed of 130 to 150% of the settled catalyst bed, in order to achieve a maximum fluidization, good contact between the oil, gas and catalyst phases.

1.8.4. Slurry bed reactors (SBR)

Slurry bed reactor **(see** Figure 1.14**)** is mainly used to hydroprocess the feeds with heavier metal contents in order to obtain low boiling products.

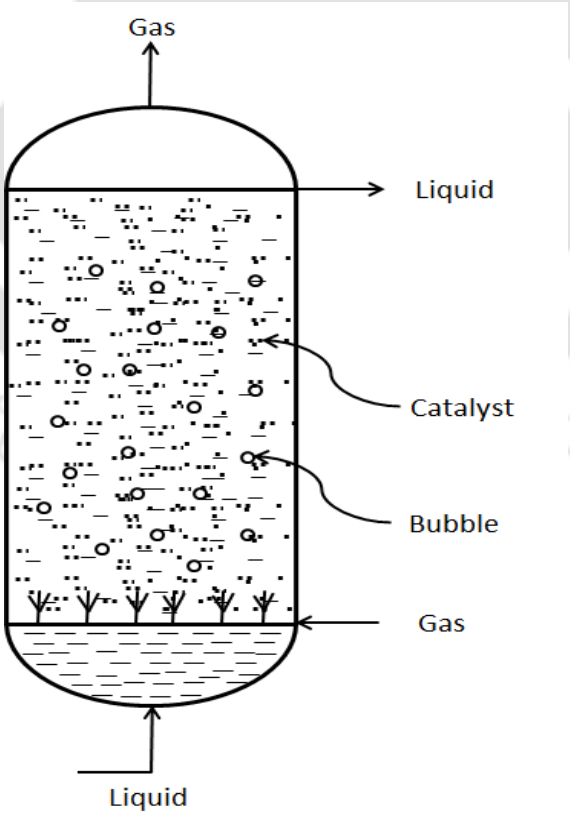

Figure 1.14: Slurry bed reactor (Ancheyta and Speight, 2007)

This reactor operates similar to the fluidized bed reactor in terms of intimate contact of oil and catalyst with a lower degree of back mixing; however a small amount of fine powder typically in the range of 0.1 to 3.0 wt% as an additive or a catalyst precursor. In this reactor the catalyst is mixed with the feed (oil) to form slurry and fed upward with hydrogen gas through a reactor. In the rector the liquid-powder mixture behaves as a homogeneous phase due to the small size of the catalyst particles. The catalyst dispersion into the feed inhibits the coke formation during the reaction inside the reactor. When the reaction is completed, the spent catalyst leaves the reactor together with some traces of oil and remains as an unconverted residue. However, every type of reactor mentioned above have their own advantages and disadvantages shown in Table 1.4 and Table 1.5 respectively **(Ancheyta and Speight, 2007).**

Table 1.4: Advantages of the different types of reactors for hydrotreatment of bio-oil **(Ancheyta and Speight, 2007).**

Fixed bed reactor	Moving phase reactor	Ebullated bed reactor	Slurry bed Reactor
High conversion per unit mass of catalyst	Catalyst regeneration is easy	Operation is very flexible (high and low conversion modes)	Usage of disposable catalyst enables higher catalyst utilization
Low operating cost and simple design	These reactors possess plug flow reactors	The catalyst can be withdrawn or added into the reactor without an interruption to the reactor and the process and to maintain the catalyst activity	The spent catalysts are not hazardous which does not require separate handling procedures.
Continuous operation	This reactors requires low catalyst handling cost	Sufficient space between the particles allowing entrained solids to pass through the bed without plugging or increased pressure drop.	Residue conversions are very higher which is up to 95% sometimes at higher values of space velocities in comparison to the other reactors.
No moving parts to wear out	These reactors possess high conversion rates	The coke formation is minimized in the reactor by reducing the overheating of catalyst	This reactor enhances the external mass transfer

Table 1.5: Disadvantages of the different types of reactors for hydrotreatment of bio-oil **(Ancheyta and Speight, 2007).**

Fixed bed reactor	**Moving phase reactor**	**Ebullated bed reactor**	**Slurry bed Reactor**
Undesired heat gradients	The flow of solids are not easy to maintain	Catalyst consumption rate is quite high	Poor product quality
Lower catalyst effectiveness, due to the usage of large catalyst particle size.	Poor heat transfer characteristics	Sediment formation	Catalyst particles size has to be designed accurately in order achieve higher dispersion.
Limited to reasonably fast reactions.	Fluid reactant may bypass catalyst bed, breakup of catalyst may occur due to the impact against the reactor walls	Absence of kinetic flow regime which is more favorable than well mixed regime.	These reactors are still at demonstration stage and not commercially competitive yet.
Limitations on the use of liquid and foaming liquids	Solid distribution is difficult to maintain	The reactor requires a larger volume due to the small size of the catalyst, lower catalyst holdup.	Higher coke formation

1.9. Organization of Thesis

The present dissertation is aimed to numerically investigate catalytic upgradation of bio-oil by hydrodeoxygenation using different catalysts in ebullated bed reactors over a wide range of temperature, pressure and WHSV values. This dissertation is organized into five chapters as follows.

In Chapter 2, the literature on the hydrodeoxygenation of bio-oil upgradation processes are critically reviewed. Also critical reviews of literature for the individual compounds upgradation into upgraded bio-oil species are presented. This enabled the research gap and set the objectives for the preliminary studies on the upgradation process numerically.

Chapter 3 deals with the statement of the problem and its mathematical formulation. It also presents various hydrodynamic model and reaction kinetics of the bio-oil upgradation. It also, presents the mathematical equations underlying assumptions, appropriate boundary conditions, parameters and the operating conditions for the present research in details.

Chapter 4 signifies the numerical methodology for studying the upgradation process of bio oil using Ansys fluent solver. This chapter also specifies the methodology adopted to solve the mathematical equations including the chemical reaction kinetics.

Chapter 5 deals with the results and discussions of different cases considered in the study. To be more specific the first section deals with the catalytic upgradation of bio oil using Pt/Al_2O_3 catalyst, by varying WHSV, temperature and pressure. Similarly, the second and third sub sections of the chapter deals with this upgradation process but using different catalysts namely $Ni\text{-}Mo/Al_2O_3$, and $Co\text{-}Mo/Al_2O_3$ catalysts.

Chapter 6 summarizes the key findings of the research with a possible scope for further research.

2.1. Previous work

An important challenge that the society is facing today is securing a sustainable fuel supply for the transportation sector. The transportation sector currently relies almost exclusively on liquid hydrocarbons as its energy source. According to the global statistics, approximately 79% of the World's energy demand is compensated by the fossil fuels. But now the trading between the demand and supply of the fossil fuels to the global needs are not counterbalanced due to the depletion of the global oil reserves. Further, this leads to the dramatic fluctuations of fossil fuel prices makes the life even more difficult which questions the dependability of fossil fuels as primary energy fuel. Despite the increasing energy demand, its utilization as an energy source is also being increasingly controversial from environmental standpoint and growing concern on their usage is best portrayed via today's catastrophic greenhouse effects. Hence, renewable energy has become an indispensable contributor to the energy portfolio to renovate the energy source structure, reduce the dependency on fossil fuel resources and provide opportunities to mitigate the greenhouse gases and production of chemicals. In the vicinity of energy crisis, extensive motivation of research turned up in the field of renewable energy i.e., bio-oil production from various modes of conversion of biomass. Thus the strategy should be to increase the biofuels production to improve energy security and reduce greenhouse gas emissions. Production of liquid fuels from biomass can help solve the problem of CO_2 emission from the transportation sector because CO_2 released from vehicle exhaust is captured during biomass growth. Currently, there are two major routes for conversion of biomass to liquid fuels: biological and thermo-chemical. Bio-oil produced as such has an energy content that is nearly half of petroleum and is similar to original biomass (~17 MJ/kg) due to extremely high O_2

contents (~35-40 wt.%) according to Agarwal et al. (2009). Furthermore, such bio-oils do not asily blend with petroleum products. Bio-oil formed directly from fast pyrolysis, however, may not be suitable for replacement of diesel or gasoline due to its low heating value, solid content, high viscosity, chemical instability, etc. Further, most biomass derived bio-oil has high oxygen content which lowers fuel quality and heat value. Upgrading biomass or biomass intermediates into high quality hydrocarbon fuels thus requires removal of oxygen. The bio-oil containing oxygen may be in the form of an ester, carboxylic acid or hydroxyl groups. Accordingly, bio-oil upgrading may be performed by catalytic hydrotreatment. Removal of oxygen by catalytic reaction with hydrogen is referred to as hydrodeoxygenation (HDO). This reaction may be conducted with conventional fixed-bed bimetallic hydrotreating catalysts such as sulfided nickel molybdenum (Ni-Mo) or cobalt-molybdenum (Co-Mo) which are commonly used in refineries. Use of supported novel catalysts may enhance the physiochemical properties of bio-oil similar to that of conventional fossil fuels according to Ramanatham and Oyama (1995) and Furimsky (2000). Therefore, in order to improve the physiochemical properties of bio-oil for its practical applications, upgrading is highly desirable. However the process of upgradation is highly complex due to the bio-oil compositions. Despite, the fact of complexity, several researchers attempted various analogies and techniques to upgrade the bio-oil obtained through various feed stocks using a wide range of parameters. This chapter gives a gist of some of the available techniques of bio-oil upgradation for a wide range of parameters and also put forward some recommendations based on the current research status of upgradation process. The bio-oil containing oxygen may be in the form of an ester, carboxylic acid or hydroxyl groups. Accordingly, bio-oil upgrading may be performed by catalytic hydrotreatment. Removal of oxygen by catalytic reaction with hydrogen is referred to as hydrodeoxygenation (HDO). This

reaction may be conducted with conventional fixed-bed bimetallic hydrotreating catalysts such as sulfided nickel molybdenum (Ni-Mo) or cobalt-molybdenum (Co-Mo) which are commonly used in refineries. Use of supported novel catalysts may enhance the physiochemical properties of bio-oil similar to that of conventional fossil fuels according to Ramanatham and Oyama (1995) and Furimsky (2000).m Therefore, in order to improve the physiochemical properties of bio-oil for its practical applications, upgrading is highly desirable. However the process of upgradation is highly complex due to the bio-oil compositions. Despite, the fact of complexity, several researchers attempted various analogies and techniques to upgrade the bio-oil obtained through various feed stocks using a wide range of parameters. This chapter gives a gist of some of the available techniques of bio-oil upgradation for a wide range of parameters and also put forward some recommendations based on the current research status of upgradation process. Hydrodeoxygenation of bio-oil can decrease the oxygen substance of numerous sorts of oxygenated chemical groups, for example, acids, aldehydes, esters, ketones, phenols and so on. HDO of bio-oils is typically conducted in a liquid phase under high hydrogen pressures (10-15 MPa) and high temperatures (300^{o}C-600^{o}C) in the presence of a heterogeneous catalyst. Oxygen containing compounds in the bio-oil reacts with hydrogen to form saturated compounds and water. Some research studies reveal that the use of conventional catalysts are very well suited for the upgradation of lignin derived bio oils containing <0.1 wt. % oxygen. But the catalyst stability and the gum formation are identified as major drawbacks. Many of the past research on hydrodeoxygenation of bio-oil used industrial Ni-Mo or Co-Mo sulfide/supported hydrotreating catalysts. To intensify the process several other catalysts including Pt, Pd, Ru as well as carbides and nitrides of transition metals such as Mo,W, V, Nb and Ti are also used by many researchers. However the underlying catalytic chemistry and mechanism including the role of specific

catalyst in deoxygenation of bio-oils are not well understood till date. To the best of our knowledge, the pioneering research work on the upgradation using hydrotreatment reported by White et al. (1968) on upgradation of coal derived liquid from pyrolysis in the presence of Ni-Mo/Al_2O_3 catalyst in the temperature range of 400^oC to 500^oC and in the pressure of 20.6 MPa of H_2. Qader et al. (1968) performed similar study, however, at lower operating parameters such as H_2 pressure of 10.5 MPa and temperature range of 300^oC to 500^oC in the presence of WS_2 catalyst. The authors reported that the initial concentration of oxygen in the biofuel is linear with the oxygen conversion rate after the reaction. The calculated rate constants for the temperature ranges are given as $6x10^{-8}$ exp $^{-12000/RT}$ min^{-1}. Later on, Rollmann (1979) investigated the HDO rates of a dibenzofuran, benzofuran, and o-ethyl phenol compounds at a temperature of 344^oC and at a pressure of 5 MPa over sulfided Co-Mo catalyst using first order kinetics to determine the rate constants. These investigations resulted that the compounds are most resistant to HDO and their rate constants are similar as those of HDN of quinolone and indole. Also, HDO rates are effected by the H_2 pressure i.e., the rate constants increased with the increasing pressure and HDO of intermediate phenols is the rate determining step of overall HDO mechanism. Further, Schneider et al. (1979) made an attempt to study the kinetics of removal of total, neutral and phenolic oxygen from a solvent refined coal using first order kinetics in the presence of conventional catalysts such as Ni-W, Ni-Mo and Co-Mo all supported on alumina at a temperature of 350^oC to 400^oC and 17.3 MPa of H_2 gas pressure. The studies revealed that rate of HDN of the feed was slowed down, and the presence of phenolic oxygen of higher concentration does not affect the removal of total and neutral oxygen. Another similar study was performed by Krishnamurthy et al. (1981) on the kinetics of HDO of dibenzofuran and of related phenols at temperatures and H_2 pressuresof 343^oC to 376^oC and 6.9 to 13.8 MPa, respectively, in

the presence of a sulfided Ni-Mo/Al_2O_3 catalyst. It was assumed that all the reactions were first order in the reactants. The authors found that the rate constant for the conversion of dibenzofuran into hydrogenated compounds is increased with the temperature, H_2 gas pressure but independent of reactant concentration. This shows that the conversion of dibenzofuran into biphenyl was insensitive to changes in gas pressure and temperature. Similarly, a detailed kinetic study of HDO of naphtha fraction obtained by direct liquefaction of coal due to Ternan and Brown (1982). The work was performed in the temperature range of 300^oC to 500^oC and the pressure range of 1 to 30 MPa in the presence of Co-Mo/Al_2O_3 catalyst using first order kinetics. The authors reported an increasing trend of overall HDO conversion of coal derived liquids with the increase in the temperature, pressure and the residence time. The activation energy for the overall HDO process, based on their experimental data was 84.4 kJ/mol. This value has a good agreement with the models of Krishnamurthy et al. (1981).

Furimsky (1983) presented first review on the HDO of bio-oil model compounds and clearly explained the mechanism of HDO and the rate determining step of HDO process to an acceptable extent. The author showed the lacuna of the work lies on the information of the catalyst structure, optimal ratios of the promoters to active ingredients for HDO of the most O-containing compounds present in synthetic liquids are to be established. Later, **Baker and Elliott (1988)** performed HDO studies on the products of the liquefaction process in the presence of CO at a pressure of 138 bar and at a temperatures ranging between 350^oC-450^oC in a batch reactor. Further, **Johnson et al. (1988**) investigated the conversion of Lignin into phenols and hydrocarbons by mild HDO process in the presence of the Ni-Mo/γ-Al_2O_3 catalyst, along with the phosphorous supports to catalysts. The addition of phosphorous lead to the increase in the production of dealkylated phenols to hydrocarbons without decreasing the overall conversion.

The first numerical monte-carlo simulations on the HDO of lignin was performed by Train (1987) using the kinetics obtained from the experimental results of Jegers and Klein (1982) who designed the reaction pathways for the primary and secondary lignin pyrolysis. Furthermore, Sheu et al. (1988) performed experimental studies on the upgradation of pine pyrolytic oil by HDO process in a trickle bed reactor at different operating conditions of temperatures ranging between 350^{o}C to 400^{o}C, pressures varying between 6996 kPa to 10443 kPa, and space velocity values lies in the range of 2-4 h^{-1} in the presence of conventional Pt, Ni-Mo, Co-Mo supported by SiO_2 and Al_2O_3 catalysts. The authors developed two models, one for the overall oxygen removal and the other for the compositional changes in hydrotreated oil. Further the authors chosen the 5 parameter lumped reaction kinetics to see the upgradation of individual species of the pine pyrolytic oil. In continuation, Baldauf et al. (1994) performed hydroprocessing of flash pyrolysis oil using the conventional Co-Mo, Ni-Mo catalysts. The flash pyrolysis oil containing oxygenated chemical groups like aldehydes, ketones, carboxylic acids, esters, aliphatic and aromatic alcohols are deoxygenated and converted to higher yield aromatic hydrocarbons and the yield of 60% with reduced moisture content by Horne and Williams (1995). A report by Oyama (1996) stated that the HDO process is similar to hydrodenitrogenation (HDN) but 10 times smarter than the later technique over vanadium nitride catalysts. Maggi and Delmon (1997) published a review on the development of catalytic hydrotreating process using bio-oils and industrial sulphided Co-Mo, Ni-Mo supported on alumina catalyst. The author also discussed the reaction schemes, catalytic functions, rate of reaction and the utility of the activated carbon as a support. Similar review by Furimsky (2000) explained the HDO reaction mechanism, complexities in the HDO kinetics, self-inhibiting characteristics of oxygenated compounds and the poisoning effects of the feeds containing sulphur and nitrogen. Oasmaa (1992) reported the

importance of macro studies on the deoxygenation of bio oils by performing catalytic hydrotreatment (HDO) of peat pyrolysis oils in a batch reactor at a higher pressure of 21.5 MPa for two hours at 390^{o}C with 10 wt. % catalyst, 4% Co-O wt. %, 15.5% Mo-O_3 wt. %, on alumina support. The authors reported that the oxygen content is reduced from 22% to 3% in the process. Another review by Furimsky (2000) explained the importance of hydrodeoxygenation (HDO) which occurs during hydroprocessing depends on the origin of feeds. HDO plays a minor role in the case of the conventional feed, whereas for the feeds derived from coal, oil shale and particularly from the biomass, its role can be rather crucial. Complexities in the HDO kinetics have been attributed to the self-inhibiting effects of the O-containing compounds as well as inhibiting and poisoning effects of the S- and N-containing compounds present in the feeds. This is a cause for some uncertainties in establishing the order of the relative HDO reactivity of the O-containing compounds and/or groups of the compounds as well as relative rates of the removal of S, O and N.

Apparently, more stable catalysts are needed to make production of the commercial fuels from the bio-feeds more attractive. Elliott (2007) reviewed the insights and achievements of HDO process in the past twenty five years. The important aspect in HDO process is the hydrogen consumption. The author reported various heterogeneous catalysts used including the precious metals and also pointed out the important processing differences that require adjustments to improve HDO process. Mahfud (2007) schematically presented the reaction stoichiometry of the HDO process and reported that HDO is efficient in terms of carbon efficiency saturates C=C, C=O bonds and aromatic rings while removing oxygen in presence of H_2 and catalysts, resulted for the production of the renewable liquid fuels like gasoline and diesel. Also, stated that the classical hydrotreating (HDT) catalysts (sulfided Co-Mo and Ni-Mo) have been the first and

most extensively tested ones. Another study of Elliott and Hart (2009) on semi-batch HDO experiments using acetic acid and furfural to represent pyrolysis products from hemi- cellulose and cellulose at 250^{o}C obtained a solid polymeric material from furfural. Using Ru/C as catalyst and acetic acid as feed, they observed negligible conversions at low temperatures (< 200^{o}C) and strong gas production at high temperatures (> 250^{o}C). The conversion of furfural already started at low temperature i.e., 83% conversion was obtained by heating at 150^{o}C. For the first time, Bui et al. (2009) reported the impact of co-processing guaiacol as an oxygenated molecule representative of pyrolytic bio-oils with a straight run gas oil (SRGO) in the framework of a hydrodesulphurization. The reaction scheme observed during the hydrotreating of the sole guaiacol in the gas phase was compared to the conversion products observed during the co-processing of guaiacol with SRGO. During the co-processing a decrease of the HDS performance of a reference Co-Mo/Al_2O_3 catalyst was observed at low temperature and high contact time. Above 320^{0}C complete HDO of guaiacol was observed and HDS could proceed without any inhibition. Recent results of Mercader et al. (2010) and Venderbosch et al. (2010) indicate that stabilization of pyrolysis oil by low severity HDO is sufficient for upgradation process and reduce the hydrogen consumption. **Zhang (2010)** conducted an experimental study on the hydrodeoxygenation of bio oil from the fast pyrolysis of bio-oil using first order reaction kinetics mechanism. The authors also studied the effects of temperature, pressure, activation energy, reaction order, and reaction time. The results indicate that deoxygenation and the conversion of reactants to products i.e., yield of higher hydrocarbons are functions of both time and temperature. Another recent review by Mortensen (2011) showed that there are two general routes of upgrading bio-oil to remove the oxygen, namely hydrodeoxygenation and zeolite cracking. The author stated that the usage of traditional catalyst

Co-MoS_2/Al_2O_3 catalysts have lifetime of much more than 200 h than the other catalysts due to the carbon deposition. Of the upgradation methods mentioned by the author, HDO is found to be the suitable way to produce synthetic fuels of acceptable grade for current infrastructure.

Following the aforementioned study Choudhary and Phillips (2011) made a review on renewable fuels via catalytic hydrodeoxygenation of feed stocks namely oil with high content of triglycerides and oils derived from high pressure liquefaction of pyrolysis of biomass. The author divided the gaps into two types optimization gap and technology gap. The inhibition effects of the HDO of triglycerides come under the optimization and on the other hand to enhance the poor quality of the bio-oils (high oxygen content, impurity levels, molecular complexity and coking propensity) come under the technology gap. Although there are several uncertainties associated with new renewable fuels, the economic and environmental importance coupled with enormous challenges of this topic will continue to maintain this as one of the most vibrant areas of the research. He and Wang (2012) proposed another review similar to Mortensen (2011) on hydrodeoxygenation of model compounds and catalytic systems for pyrolysis bio-oil upgrading. The author emphasizes the recent advances in HDO of pyrolysis bio-oils over many different types of catalysts, concentrating on the investigations of reasons why current catalyst have showed poor stability and have hindered pyrolysis oil HDO process in industrial scale. The review has also included the chemistry of the model compounds from pyrolysis oil and the reactions occurring via different routes over different catalysts with different products. Secondly a detailed elaboration on the reaction mechanisms on the catalyst reactions, the importance of catalyst supports and catalyst deactivation mechanism is explained. Also the author explained that the extent of coke formation is majorly dependent on the type of oxy compounds, acidity of the catalyst and operating conditions.

Further, effects of the catalyst on HDO process is mentioned by Bykova (2012) considering Ni based sol gel catalysts stabilized with SiO_2 and ZrO_2. The operating conditions for the bio-oil upgradation for their system is best suited at 320^oC and 17 MPa H_2 gas pressure in order to obtain cyclohexane, 1-methylcyclohexane, 1,2-diol and cyclohexane. Further, the activity of the catalyst is dependent on the Ni loading, higher specific area of the catalyst provided by the formation of nickel oxide-silicate species**. Joshi and Lawal (2012)** studied the hydrodeoxygenation of pyrolysis oil in micro packed bed reactor to estimate the effect of temperature, hydrogen partial pressure (varied by two ways: changing hydrogen flow rate at constant total pressure, and changing the total pressure at constant H_2 flow rate), and residence time using a Ni-Mo/Al_2O_3 catalyst. The authors observed that the high hydrogen consumption along with small oxygen removal suggests that in hydrodeoxygenation of pyrolysis oil hydrogenation cannot be avoided. Xu et al. (2013) proposed two step catalytic HDO of fast pyrolysis oil to hydro carbon liquid fuels. In the first step organic solvents were employed to reduce the coke formation and promote higher rates of HDO process. In the second step conventional reaction mechanism of reactants to products in the presence of catalyst along with hydrogen gas is performed to obtain hydrocarbon fuel. Popov et al. (2013) reported the interaction of aromatic compounds (phenols, ethyl phenols, and guaiacol) of bio-oils with sulfided Co-Mo/Al_2O_3 catalyst in order to determine the origin of catalyst deactivation in HDO. The reaction takes place at 350^oC forming only phenate species on the support of the catalyst during HDO reaction. The author showed that oxygenated compounds adsorbed on the sulfided catalyst poison the sulfide sites and deactivates the catalyst. Leng et al. (2013) proposed a universal catalyst for the hydrodeoxygenation of bio-oil and its model compounds. The author proposed Ni-Fe bimetallic catalyst shows an excellent activity and selectivity for the

hydrodeoxygenation of three typical model compounds of bio-oil. In support to the statement the author showed that the conversion of furfuryl alcohol, benzene alcohol and ethyloenanthate to 2-methylfuran, toluene and heptane is found to be 100, 95.48 and 97.89 % conversion respectively at 400^{o}C. The experiments revealed that that major reaction pathway during this process is the cleavage of C-O rather than C-C. Finally the author showed an increasing trend of heating value with a change in pH as well. One more critical review on upgradation techniques of bio-oil from biomass by Tang et al. (2013) concluded that the one step hydrogenation-esterification method (conversion of furfural and acetic acid over a composite of bi-functional catalyst) is much better than the traditional method. The usage of amorphous catalysts is more novel and economical viable for HDO of bio-oil with high oxygen content. Catalytic pyrolysis promotes the higher production and higher quality of bio-oils using appropriate catalysts (bi-functional catalyst). The author also reported that upgradation through molecular distillation is also a possible alternate for the process but limited due to the poor properties of upgraded bio-oil. Finally, usage of supercritical fluids is not economically feasible to upgrade bio-oil on a large scale due to the high cost of the organic solvents. Recently, Xu et al. (2013) performed two stage catalytic HDO of fast pyrolysis oil for translating pyrolysis oil to transportation grade hydrocarbon liquid fuels. At the first stage various organic solvents were employed to promote HDO of bio oil to overcome coke formation using noble catalyst (Ru/C) at a mild temperature of 300^{o}C at 10 MPa. At the second stage conventional hydrogenation in the presence of Ni-Mo/Al_2O_3 catalyst were used under the condition of 400^{o}C and 13MPa for obtaining hydrocarbon fuel. The author also reported that the coke formation is eliminated significantly and oxygen content decreased from 48 to 0.5% obtaining a high heating value of 46 MJ/kg from 17 MJ/kg obtaining a final product

of C11-C27 aliphatic hydrocarbons and aromatic hydrocarbons. Several challenges for upgrading of bio oil via hydrotreating process was explained by Majhi (2013). The author employed two methods to remove or reduce oxygenates from the deodar and pine bio-oils are fractionation of bio-oil at temperature less than 400^{o}C and hydrodeoxygenation using Pd/Al_2O_3 catalyst. The author found that the fractionation of bio-oil increases the heating value by removing the phenol compounds thereby maintaining the same carbon content. Similar results were obtained by the author with an increasing content of carbon in the case of hydrodeoxygenation principle.

Substantial shift in the paradigm of the upgradation work has started recently and several researchers focused on the primary aspect of upgrading the bio-oil in the recent years of 2013-2015. A brief description of some of the studies is presented here. The amount of the char formed during the HDO process is also needs to be taken proper care. This char formation leads to the catalyst deactivation as mentioned by the several aforementioned studies. In this category Sathish and Steele (2014) explained that pre-treating of bio oil will increase the yield and reduce the char during hydrodeoxygenation to produce hydrocarbons. The method tested by the author is the oxidation pretreatment of raw bio-oil to increase carboxylic acids by conversion of aldehydes and ketones, phenols and other alcohols were also oxidized to some extent. The oxidation pretreatment allowed to perform the hydrotreating step with low hydrogen pressure and reduced hydrogen consumption. The studies revealed that hydrotreated oxidized bio-oil had 30.5% higher organic fraction yield, and char and water content were reduced by 92% and 46.2% with an acid and oxygen content values tending to approximately zero. Similar studies were performed by Kim et al. (2014) on hydrodeoxygenation of bio oil obtained from the fast pyrolysis of biomass in an autoclave reactor at three different reaction factors of temperature ranging between 250^{o}C -370^{o}C, catalyst loading of 0-6 wt. % and the reaction time between

40-120 min under hydrogen atmosphere. After HDO process is done the authors observed gas, char and two immiscible liquid products. The obtained liquid products are less acidic and contained less water than the crude bio-oil with a heating value of 28.7 MJ/kg. An attempt of using carbon support for the catalyst is done by **Elkasabi et al. (2014)** on HDO of fast pyrolysis bio-oils from various feed stocks of Eucalyptus and equine manure at 320^{o}C under 2100 psi H_2 for 4 h. The results elucidate the relationship between the feedstock type and the suitability of catalyst for HDO upgrading. The conclusions of the author are Eucalyptus oil exhibited poor HDO efficiency with a large consumption of hydrogen gas, and platinum catalysts generally deoxygenate more efficiently than ruthenium except for the manure bio-oil. Switch grass bio-oil catalyzed with platinum shows the promising upgrading efficiency than the others. Recently, De and Luque (2014) presented a review aimed to emphasize the recent developments on HDO catalysts in effective transformations of biomass derived platform chemicals into hydrocarbon fuels with reduced oxygen content and improved H/C ratio. The author also stated that the liquid hydrocarbon fuels can be obtained by combining oxygen removal processes as well as by increasing the molecular weight via C-C coupling reactions. In the line of the aforementioned review, Sanna et al. (2015) performed HDO of the aqueous fraction of bio-oil with Ru/C and Pt/C catalysts at a temperature of 125^{o}C known as low temperature hydrogenation (LTH) lead to the homogenous reactions within the aqueous phase bio-oil with a WHSV values varying between 1.5 to 3 h^{-1}. The products of the LTH process were ethylene and propylene glycols along with sorbitol with small traces of acetic acid, levenoglucose, furanone, phenols and phenol substitutes. Some other researchers working in the area of upgradation of bio-oil through HDO process are listed below in Table 2.1.

`

Table 2.1: Summary of the literature on upgradation of bio-oil by hydrodeoxygenation

Author	Description/Title	Feed type, operating conditions and reactor details		Remarks
Odebunmi and Ollis (1983)	Catalytic hydrodeoxygenation I. Conversions of O-, p-, m-Cresols	Feed Temperature Pressure Catalyst Reactor	O,p,m cresols 225^{o}C-400^{o}C 6.8MPa CoO-MoO_3/γ-Al_2O_3 Micro batch	The reactivity of the cresols to deoxygenation decreases in order m-cresol > p-cresol > o-cresol.
Laurent and Delmon (1994)	Study of the hydrodeoxygenation of carbonyl, carboxylic and guaiacol groups over sulfided Co-Mo/γ-Al_2O_3 and Ni-Mo/γ-Al_2O_3 catalysts. I. Catalytic reaction schemes	Feed Temperature Pressure Catalyst Reactor	Pyrolysis oil 200^{o}C 1MPa Co-Mo/Al_2O_3, Ni-Mo/Al_2O_3 Batch	Ni-Mo has a higher decarboxylating activity and Co-Mo leads to the conversion of heavy products.
Rocha et al. (1996)	Hydrodeoxygenation of oils from cellulose in single and two stage hydropyrolysis	Feed Temperature Pressure Catalyst Reactor	Oils from cellulose 300^{o}C – 520^{o}C 10MPa Ni-Mo/Al_2O_3 Batch	The first stage hydropyrolysis with iron sulphided catalyst reduced the oxygen content by 20%. In the second stage Ni-Mo catalyst further reduced the oxygen content by another 10%.

`

Wandas et al. (1996)	Conversion of cresols and naphthalene in the hydroprocessing of three - component model mixtures simulating fast pyrolysis tars	Feed Temperature Pressure Catalyst Reactor	O,p,m cresols with naphthalene and n-hexadecane 360^{o}C 7MPa Co-Mo/Al_2O_3 Batch	The experiments revealed that the hydrodeoxygenation efficiency of the cresol isomers decreases in the sequence of para > meta > ortho
De la Puente et al. (1999)	Effects of Support Surface Chemistry in hydrodeoxygenation reactions over Co-Mo/Activated Carbon Sulfided Catalysts	Feed Temperature Pressure Catalyst Reactor	4-methyl-acetophenone, ethyl decanoate and guaiacol dissolves in p-xylene 280^{o}C 7MPa Co-Mo/C Batch	The catalyst supported on carbon offers better activity for the hydrodeoxygenation with negligible coke formations.
Massoth et al. (2006)	Catalytic hydrodeoxygeantion of Methyl-Substituted Phenols: Correlations of Kinetic Parameters with Molecular Properties	Feed Temperature Pressure Catalyst Reactor	Phenol, dimethyl disulfide dissolved in n-heptane and n-decane 300 ^{o}C 2.85MPa Co-Mo/Al_2O_3 Continuous	Hydrodeoxygenation of methyl substituted phenols indicated two different pathways; one leading to aromatic formation and other to cyclohexane formation with adsorption rates remaining constant for both.

`

Yang et al. (2008)	Hydrodeoxygenation of phenolic compounds over MoS_2 catalysts with different structures	Feed Temperature Pressure Catalyst Reactor	Phenol, 4-methylphenol, 4-methoxyphenol 320^oC-370^oC 2.8MPa Ammonum heptamolybdate, molybdenum nathenate, exfoliated MoS_2 in H_2O (TDM-W), exfoliated MoS_2 in decalin (TDM-D) Batch	The hydrodeoxygenation reactivity and the conversion of the phenol substitutes for different catalysts are in the order AHM > TDM-D > Mo Naph > thermal > powder > TDM-W
Gutierrez et al. (2009)	Hydrodeoxygenation of guaiacol on noble metal catalysts	Feed Temperature Pressure Catalyst Reactor	Pyrolysis oil 100^oC-300^oC 8MPa Rh/ZrO_2, $Co\text{-}Mo/Al_2O_3$ Batch	The complete conversion of guaiacol is achieved using noble metal catalyst; H/C ratio similar to gasoline and diesel. The carbon deposition is lower for noble catalyst
Nava et al. (2009)	Upgrading of bio - liquids on different mesoporous silica – supported Co-Mo catalysts	Feed Temperature Pressure Catalyst Reactor	Olive oil 250^oC 3MPa $Co\text{-}Mo/Al_2O_3$ supported on SBA-15, SBA-16, DMS-1 Fixed bed	The CoMo/SBA-16 is most desired catalyst for the production of paraffins and alcohols, removal of oxygen containing products and polyaromatics.

`

Pham et al. (2009)	Hydrogenation and Hydrodeoxygenation of 2-methyl-2-pentenal on supported metal catalysts	Feed Temperature Pressure Catalyst Reactor	2-methyl-2-penetenal 200^{o}C-400^{o}C 0.1MPa Pt/H_2PtCl_6, Pd/$Pd(NO_3)_2$, Cu/$Cu(NO_3)_2$ Tubular	Pt, Pd showed stronger hydrogenation, Cu catalyst showed hydrogenalysis. Cu is best suitable for the production of 2-methyl-pentenol at low temperatures, with high removal of oxygen.
Wang et al. (2009)	Characterization and catalytic properties of Ni–Mo–B amorphous catalysts for phenol hydrodeoxygenation	Feed T P Catalyst Reactor	Phenol 175^{o}C-300^{o}C 4MPa Ni-Mo-B-x(amorphous), Ni-Mo-B-xu(ultrasonic) Fixed bed	The catalyst prepared by ultrasonic-assisted reduction showed better performance over the amorphous catalyst.
Wildschut et al. (2009)	Hydrotreatment of fast pyrolysis oil Using Heterogeneous Noble-Metal Catalysts	Feed T P Catalyst Reactor	Pyrolysis oil 250^{o}C-350^{o}C 10MPa-20MPa Ru/C, Ru/TiO_2, Ru/Al_2O_3, Pt/C, Pd/C Batch	Ru/C catalyst showed better performance of HDO with an HHV of 43 MJ/kg, pH of 2.5-5.8, higher amounts of phenols, alkanes and aromatics.

`

Yang et al. (2009)	Hydrodeoxygenation of bio-crude in supercritical hexane with sulfided CoMo and CoMoP catalysts supported on MgO: A model compound study using phenol	Feed Temperature Pressure Catalyst Reactor	Bio-oil (Phenol as model compound) 375^{o}C-400^{o}C 6.9MPa Co-Mo/Al_2O_3 Batch	The HDO activity of CoMoP/Mgo is high at higher temperatures, and resistant to the coke deposition due to the basic nature of the MgO support resulting 64% benzene formation.
Xu et al. (2010)	Upgrading of liquid fuel from the vacuum pyrolysis of biomass over the Mo–Ni/γ-Al_2O_3 catalysts	Feed Temperature Pressure Catalyst Reactor	Pine-oil 100^{o}C-200^{o}C 3MPa Mo-10Ni /γ-Al_2O_3 Fixed bed	Both hydrotreatment and esterification reactions took place during the upgradation process. The value of the pH is increased, H content is increased, and percent of esters increased to 20.74% from 7.28%.
Ahmad et al. (2010)	Upgrading of Bio-Oil into High-Value Hydrocarbons via Hydrodeoxygenation	Feed Temperature Pressure Catalyst Reactor	Bio-oil (Palm shell) 300^{o}C-450^{o}C 5MPa Co-Mo/Mgo Batch	Simulation study results included the techno economic feasibility of the HDO of pyrolysis oil through a series of reactions. The HDO of cyclohexene to cyclohexane requires higher H_2 pressure.

`

Echeandia et al. (2010)	Synergy effect in the HDO of phenol over Ni–W catalysts supported on active carbon: Effect of tungsten precursors	Feed Temperature Pressure Catalyst Reactor	Phenol 150^{o}C-300^{o}C 1.5MPa Ni-W/C Fixed bed	Activated carbon supported Ni-W catalyst are beneficial in terms of reduced coke formation, promote better HDO. The pathway for the HDO of phenol followed similar lines of Massoth et al. (2006)
Šimácek et al. (2010)	Fuel properties of hydroprocessed rapeseed oil	Feed Temperature Pressure Catalyst Reactor	Rapeseed oil 310^{o}C-360^{o}C 7-15MPa Ni-Mo /Al_2O_3 Fixed bed	The hydroprocessed rapeseed oil composition and the physiochemical properties resembles similar to the high cetane diesel fuel with low pour point.
Romero et al. (2010)	Hydrodeoxygenation of 2-ethylphenol as a model compound of bio-crude over sulfided Mo-based catalysts: Promoting effect and reaction mechanism	Feed Temperature Pressure Catalyst Reactor	2-ethylphenol 340^{o}C 7MPa Mo/Al_2O_3, Ni-Mo/Al_2O_3, Co-Mo/Al_2O_3 Fixed bed	The deoxygenation is mainly due to hydrogenation step in HDO followed by deoxygenation. The acid sites of the alumina support play a role in isomerization for the desired products.

`

Ryymin et al. (2010)	Competitive reactions and mechanisms in the simultaneous HDO of phenol and methyl heptanoate over sulphided NiMo/γ-Al_2O_3	Feed Temperature Pressure Catalyst Reactor	Phenol and methylheptanoate 200^oC-250^oC 7.5MPa NiMo/γ-Al_2O_3 Batch	The reduction reactions (hydrogenation) co-ordinatively unsaturated sites (CUS). Sulphur-saturated sites are needed for the acid catalyzed and decarboxylation reactions. The sulphur adsorbs on these CUS and affects the reactions on this site.
Madsen et al. (2011)	Hydrodeoxygenation of waste fat for diesel production: Study on model feed with Pt/ Al_2O_3 catalyst	Feed Temperature Pressure Catalyst Reactor	Waste fat 325^oC 2MPa Pt /γ-Al_2O_3, Ni /γ-Al_2O_3, Pd/γ-Al_2O_3 Batch	Pd/γ-Al_2O_3 is found to be active than the Pt/γ-Al_2O_3, Ni/γ-Al_2O_3 with higher decarboxylation, decarbonylation, hydrogenation. The increase in the temperature increased the conversion of oleic acid from 6% to 100%.
Popov et al. (2011)	IR study of the interaction of phenol with oxides and sulfided CoMo catalysts for bio-fuel hydrodeoxygenation	Feed Temperature Pressure Catalyst Reactor	 350^oC 0.0002MPa Co-Mo/Al_2O_3, Ni-Mo/Al_2O_3 Batch	The interaction of the phenol on silica support is mainly due to the hydrogen bonding whereas on alumina it dissociates into adsorbed phenolates. On sulphided support phenol again dissociates with weaker interaction of phenol with sulphided CoMo catalyst.

`

Wang et al. (2011)	Amorphous Co-Mo-B catalyst with high activity for the hydrodeoxygenation of bio-oil	Feed Temperature Pressure Catalyst Reactor	Phenol, benzoldehyde and acetophenone 250^{o}C-275^{o}C 4MPa Co-Mo-B -	The amorphous catalyst possesses low cost, simple preparation, high thermal stability, and high HDO activity.
Kyung et al. (2011)	Catalytic deoxygenation of liquid biomass for hydrocarbon fuels	Feed Temperature Pressure Catalyst Reactor	Canola oil 300^{o}C-400^{o}C 1.8MPa-8.5MPa Ni-Mo/γ- Al_2O_3 Batch	The effect of temperature, pressure, catalyst loading, oxygen removal conditions. The formation of the gaseous products increases with the temperature.
Chen et al. (2011)	Aqueous-phase hydrodeoxygenation of carboxylic acids to alcohols or alkanes over supported Ru catalysts	Feed Temperature Pressure Catalyst Reactor	Carboxylic acids 100^{o}C-400^{o}C 0MPa-10MPa Ru/C, Ru/ZrO_2, Ru/Al_2O_3 Trickle bed	The C-C bond cleavage by means of hydrodeoxygenation favors the order Ru/C > Ru/ZrO_2 > Ru/Al_2O_3

`

Sepulveda et al. (2011)	Hydrodeoxygenation of 2-methoxyphenol over Mo_2N catalysts supported on activated carbons	Feed Temperature Pressure Catalyst Reactor	2-methoxyphenol 300^oC-400^oC 5MPa Mo_2N/Norit Batch	The selectivity of the Mo_2N/Norit catalyst is majorly depending on phenol/catechol ratio where the demethylation and demethoxylation reactions are dependent.
Bui et al. (2011)	Hydrodeoxygenation of guaiacol Part II: Support effect of CoMoS catalysts on HDO activity and selectivity	Feed Temperature Pressure Catalyst Reactor	Guaiacol 380^oC-450^oC 0.002MPa Commercial catalysts with Al_2O_3, ZrO_2, TiO_2 Batch	Methylation reaction occurs with the alumina support, hydrogenation reaction is favored by CoMoS/TiO_2 and highest activity is found for CoMoS/ZrO_2
Wang et al. (2011)	Hydrodeoxygenation of dibenzofuran over noble metal supported on zeolite.	Feed Temperature Pressure Catalyst Reactor	Dibenzofuran 200^oC 4MPa Pt/ZSM-5, Pt/Al_2O_3 Fixed bed	Pt/ZSM-5 showed better performance over Pt/Al_2O_3 due to the wormhole like intra crystalline meso-pore channel.

`

Zhao et al. (2011)	Hydrodeoxygenation of guaiacol as model compound for pyrolysis oil on transition metal phosphide hydroprocessing catalysts	Feed Temperature Pressure Catalyst Reactor	Guaiacol 300^{o}C 0.1MPa Ni_2P/SiO_2, Fe_2P/SiO_2, MoP/SiO_2, Co_2P/SiO_2, WP/SiO_2 Packed bed	The activity of the HDO of guaiacol follows the order Ni_2P > Co_2P > Fe_2P, WP, MoP. The metal phosphide catalysts possess no catechol formation as compared to the regular commercial catalysts.
Bu et al. (2012)	A review of catalytic HDO of lignin-derived phenols from biomass pyrolysis	Feed Temperature Pressure Catalyst Reactor	Phenols from lignin - - Co-Mo/Al_2O_3, Ni-Mo/ Al_2O_3, noble metals -	The review summarized the techno-economic feasibility of HDO of lignin derived phenols is possible through optimizing the reaction kinetics, improved catalysts, alternative to H_2 source.
Ardiyanti et al. (2012)	Catalytic hydrotreatment of fast-pyrolysis oil using non-sulfided bimetallic Ni-Cu catalysts on a δ- Al_2O_3 support	Feed Temperature Pressure Catalyst Reactor	Anisole, Fast pyrolysis oil 150^{o}C-350^{o}C 0.1MPa-10MPa Ni-Cu/δ-Al_2O_3 Fixed bed	The catalyst is slightly lesser active than Ru/C because of metal leaching. The coking tendency is improved with improved stability in hydrocarbons.

`

Ausavasukhi et al. (2012)	HDO of m-cresol over gallium-modified beta zeolite catalysts	Feed Temperature Pressure Catalyst Reactor	m-cresol 450^{o}C 0.1MPa Ga/HBEA, Ga/ZSM-5, Ga/SiO_2 Continuous flow	The experiments are conducted with and without presence of H_2 gas and Ga/HBEA catalyst is more active for HDO of m-cresol.
Boonyanwan et al. (2012)	Unsupported MoS_2 and $CoMoS_2$ catalysts for hydrodeoxygenation of phenol	Feed Temperature Pressure Catalyst Reactor	Phenol 160^{o}C-220^{o}C 2.8MPa CoMoS-A-x, MoS-A Parr Reactor	Multilayered amorphous MoS_2 catalyst had a greater activity than crystalline MoS_2. This is due to the stronger bond strengths of the molybdenumm and sulphur in amorphous form than the crystalline.
Zhao et al. (2012)	Comparison of kinetics, activity and stability of Ni/HZSM-5 and Ni/ Al_2O_3-HZSM-5 for phenol hydrodeoxygenation	Feed Temperature Pressure Catalyst Reactor	Phenol 200^{o}C-300^{o}C 4MPa Ni/Al_2O_3-HZSM-5, Ni/ HZSM-5 Batch	The phenol rates increased in the sequence of phenol hydrogenation < cyclohexane hydrogenation < cyclohexane dehydration. Ni/Al_2O_3-HZSM-5 has higher phenol HDO rate than Ni/HZSM-5.

`

Liu et al. (2012)	Hydrodeoxygenation of benzofuran over activated carbon supported Pt, Pd and Pt-Pd catalysts.	Feed Temperature Pressure Catalyst Reactor	Benzofuran 340^{o}C 3MPa Pd/C, Pt/C, Pt-Pd/C Continuous flow	The bi-metallic Pt-Pd/C catalyst had the highest deoxygenation levels, conversion of benzofuran increases with temperature, contact time. Ketone isomerization reaction is taking place by the use of activated carbon supported noble metal catalyst.
Olcese et al. (2012)	Gas-phase hydrodeoxygenation of guaiacol over Fe/SiO_2 catalyst	Feed Temperature Pressure Catalyst Reactor	Guaiacol 350^{o}C-450^{o}C 0.02MPa-0.09MPa Fe/SiO_2 Fixed bed	The catalyst produces less methane at higher conversion rates. The catalyst is more environmental friendly and suitable for lignin valorization to benzene, toluene, xylene production.
Phuong Bui et al. (2012)	Studies of the synthesis of transition metal phosphides and their activity in the hydrodeoxygenation of a biofuel model compound	Feed Temperature Pressure Catalyst Reactor	Biofuel 300^{o}C-450^{o}C 0.1MPa Silica supported metal phosphides Packed bed	The order of activity is Ni_2P > WP > MoP > CoP > FeP > Pd/Al_2O_3. Phosphide supported iron group produces pentane and butane, and tungsten supported by phosphides produce pentene.

`

Wang et al. (2012)	From biomass to advanced bio-fuel by catalytic pyrolysis / hydroprocessing: hydrodeoxygenation of bio-oil derived from biomass catalytic pyrolysis	Feed Temperature Pressure Catalyst Reactor	Bio-oil 200^{o}C 4MPa Pt/ZSM, Pt/Al_2O_3 Continuous flow	Complete deoxygenation is possible with the Pt/ZSM-5 catalyst than the conventional alumina support. This is due to the mesoporous structure and the active sites where the acidity of the bio-oil leads to the catalytic action for the removal of oxygen.
Ying et al. (2012)	Upgrading of fast pyrolysis liquid fuel from biomass over Ru/ɣ- Al_2O_3 catalyst	Feed Temperature Pressure Catalyst Reactor	Pyrolysis oil 300^{o}C 3MPa Ru/γ- Al_2O_3 Fluidized bed	The addition of the second metal (Co) to the catalyst improving the catalytic activity and the HDO of the pyrolysis oil.
Chaiwat et al. (2013)	Upgrading of bio-oil into advanced biofuels and chemicals. Part II. Importance of holdup of heavy species during hydrotreatment of bio-oil in a continuous packed – bed catalytic reactor	Feed Temperature Pressure Catalyst Reactor	Pyrolysis oil (Mallee wood) 175^{o}C-300^{o}C 5MPa-15MPa Pd/C Packed bed	The liquid hour space velocity is not the accurate parameter to determine the residence time, and species concentrations inside the reactor.

`

Jiraporn et al. (2013)	Pt/ Al_2O_3-catalytic deoxygenation for upgrading of Leucaena leucocephala-pyrolysis oil	Feed Temperature Pressure Catalyst Reactor	Leucaena leucocephla (rice straw) 340^oC 4bar Pt/Al_2O_3 Fixed bed	The deoxygenation process is carried using N_2 gas. The process is in the lines of steam reforming, water-gas shift, methanation and dehydration reactions.
Zhang et al. (2013)	Hydrodeoxygenation of lignin-derived phenolic compounds to hydrocarbons over Ni/SiO_2-ZrO_2 catalysts	Feed Temperature Pressure Catalyst Reactor	Lignin derive phenols 300^oC 5MPa Ni/SiO_2-ZrO_2 Continuous fixed bed	The selectivity of the process is 98% with 100% conversion at 300^oC and 5MPa for Ni/SZ-3 catalyst. Also SZ provides amphoteric character provides recyclability, anti-coking characteristic.
Wang et al. (2013)	Hydrodeoxygenation of p-cresol on unsupported Ni-Mo-W-S sulfide catalysts were prepared by one step hydrothermal method	Feed Temperature Pressure Catalyst Reactor	p-cresol 300^oC 4MPa Ni-Mo-W-S Batch	Adjusting the ratio of the W/Mo increases the active sites, promotes dispersion of active phases, and shortens the slab length of MoS_2.

`

Iino et al. (2014)	Kinetic studies on hydrodeoxygenation of 2-methyltertrahydrofuran on a Ni_2P/SiO_2 catalyst at medium pressure	Feed Temperature Pressure Catalyst Reactor	2-methyltetrahydrofuran 350^oC 0.5MPa Ni_2P/SiO_2 Continuous flow	C-O bond cleavage of the furanic ring to produce 2-pentanone or 1-pentanal was the rate determining step followed by hydrogen transfer to produce oxygen free compounds such as n-pentane or n-butane.
Güvenatam et al. (2014)	Hydrodeoxygenation of mono- and dimeric lignin model compounds on noble metal catalysts	Feed Temperature Pressure Catalyst Reactor	Mono, dimeric lignin 200^oC 2MPa Pt/C, Pd/C, Ru/C Packed bed	The removal of oxygen is associated with the mineral acids where noble catalyst provides requirements. Pt/C showed the optimal reactivity than the others due to the higher activity polar carbonyl moieties.
Zhang et al. (2014)	Aqueous-phase hydrodeoxygenation of lignin monomer eugenol: Influence of Si/Al ratio of HZSM-5 on catalytic performances	Feed Temperature Pressure Catalyst Reactor	Eugenol 240^oC 5MPa Pd/C, HZSM-5 Batch	The decrease in the ratio of the Si/Al increases the acid sites which improves deoxygenation performance and vice versa. With Si/Al=12.5 the conversion is 86.5%.

`

Wan et al. (2014)	Kinetic investigations of unusual solvent effects during Ru/C catalyzed hydrogenation of model oxygenates	Feed Temperature Pressure Catalyst Reactor	2-butanone, 2-pentanone and phenol 35^{o}C 1.4MPa Ru/C Batch	The solvent effect of low temperature hydrogenation and strong interaction between protic solvents and 2-butanone by hydrogen bonding using Ru/C catalyst lower the activation energy barrier and enhances the hydrogenation rates.
shi et al. (2014)	Catalytic deoxygenation of methyl laurate as a model compound to hydrocarbons on nickel phosphide catalysts: Remarkable support effect	Feed Temperature Pressure Catalyst Reactor	Methyl laurate 300^{o}C-340^{o}C 3MPa Nickel phosphide catalysts Fixed bed	The deoxygenation pathways are mainly affected by the electron density of Ni site and the interaction of the Ni site and the acid site. The stronger Bronsted acid site promotes the HDO and C11/C12 ratio.
Nei and Resasco (2014)	Kinetics and mechanism of m-cresol hydrodeoxygenation on a Pt/SiO_2 catalyst	Feed Temperature Pressure Catalyst Reactor	m-cresol 300^{o}C 1.4MPa Pt/SiO_2 Batch	The author used Langmuir-Hinshelwood kinetic fitting with numerous parameters by the combination of differential and integral reactor.

`

Jęczmionek and Semczuk (2014)	Hydrodeoxygenation, decarboxylation and decarbonylation reactions while co-processing vegetable oils over NiMo hydrotreatment catalyst. Part II: Thermal effects – Experimental results	Feed Temperature Pressure Catalyst Reactor	Olive oil 320^{o}C 3-6MPa Ni-Mo Continuous	Total conversion of the hydroraffinates into paraffins was confirmed by the absence of any triglycerides
Jin et al. (2014)	Catalytic HDO of anisole as lignin model compound over supported nickel catalysts	Feed Temperature Pressure Catalyst Reactor	Anisole 180^{o}C-220^{o}C 0.5MPa-3MPa Ni/Al_2O_3 Batch	The combination of the acidic sites of the supports and good dispersion of the metal contributing to the cleavage of C-O bonds and leads to higher HDO. And also the activity is a strong function of temperature by methoxylation.
Oh et al. (2014)	Investigation of chemical modifications of micro- and macromolecules in bio-oil during hydrodeoxygenation with Pd/C catalyst in supercritical ethanol	Feed Temperature Pressure Catalyst Reactor	Bio-oil (Miscanthus) 250^{o}C-350^{o}C 3MPa Ni/Al_2O_3 Continuous reactor	The chemical modification of the low molecular weight compounds and high molecular weight compounds is determined by reaction time, increased polymerization by the rise in temperature.

`

Le et al. (2014)	Hydrodeoxygenation of 2-furyl methyl ketone as a model compound in bio-oil from pyrolysis of Saccharina Japonica Algae in fixed-bed reactor	Feed Temperature Pressure Catalyst Reactor	2-fury –methyl- ketone 400^{o}C-500^{o}C 6MPa CoP/γ-Al_2O_3 Fixed bed	The results indicate the HDO is achievable even at atmospheric pressure which is possible using CoP/γ-Al_2O_3.
Hong et al. (2014)	The catalytic activity of Pd/Wo_x/γ-Al_2O_3 for hydrodeoxygenation of guaiacol	Feed Temperature Pressure Catalyst Reactor	Guaiacol 50^{o}C-300^{o}C 2MPa Pd/WOx/ γ-Al_2O_3 Batch	Tungsten loading directly affects the HDO activity, and surface acidity of the catalyst. This leads to form the acidic mono layer of tungsten with 32% wt loading of Pd for highest activity of HDO.
Yang et al. (2014)	Effect of metal-support interaction on the selective hydrodeoxygenation of anisole to aromatics over Ni-based catalysts.	Feed Temperature Pressure Catalyst Reactor	Anisole 290^{o}C-310^{o}C 0.3MPa Ni/ γ-Al_2O_3 Continuous flow	The aromatic production is higher at higher temperatures and lower space velocities and also depends on the catalyst support. The presence of the acid sites enhances the hydrogenalysis reaction and then converts the reactants to cyclohexenes.

`

Ayodele et al. (2015)	Hydrodeoxygenation of oleic acid into n- and iso-paraffin biofuel using zeolite supported fluoro-oxalate modified molybdenum catalyst: Kinetics study	Feed Temperature Pressure Catalyst Reactor	Oleic acid 360^{o}C 2MPa FMoOx/Zeol Semi-batch reactor	The kinetic data reveals that sequential hydrogenation of OA into stearic acid (SA) was faster than the HDO of SA into biofuel with activation energies of 98.7 and 130.3 kJ/mol, respectively.
Hellinger et al. (2015)	Catalytic hydrodeoxygenation of guaiacol over platinum supported on metal oxides and zeolites	Feed Temperature Pressure Catalyst Reactor	Guaiacol 250^{o}C 0.5MPa Pt/SiO_2, Pt/Al_2O_3, Pt/ZrO_2, Pt/P25, Pt/TiO_2, Pt/ZrO_2, Pt/CeO_2 Batch	HDO is a strong function of the catalyst support especially acidic supports shows the higher activity followed by Pt/SiO_2 > Pt/Al2O_3 > Pt/ZrO_2 > Pt/P25 > Pt/TiO_2 > Pt/ZrO_2 ≈ Pt/CeO_2. Guaiacol is almost converted to cyclohexane at T > 150^{o}C.
Sankaranarayanan et al. (2015)	Hydrodeoxygenation of anisole as bio-oil model compound over supported Ni and Co catalysts: Effect of metal and support properties	Feed Temperature Pressure Catalyst Reactor	Anisole 220^{o}C 0.5MPa Ni, Co supported by ZSM-5, SBA-15, Al-SBA-15 Batch	The interaction of the metallic species with porous support, and their dispersion is strongly affected by the presence of Al. Co species in particular shows a stronger interaction with Al-SBA-15 and H-ZSM-5.

2.2. Research Gap

Due to the demand for the fuels, the increased buildup of CO_2 in the atmosphere, and the general fact that the oil reserves are depleting, the need for the renewable fuels is evident. Biomass derived fuels in this context is a promising route being the only renewable carbon resource with a sufficiently short reproduction cycles. Problems with biomass are associated with the cost of transport due to low mass and energy density. To circumvent this, local production of bio-oil seems to be a viable option, being a more energy dense intermediate for processing of the biomass. This process is further applicable with all types of biomass. However, bio-oil suffers from high oxygen content, rendering it acidic, instable, and giving it a low heating value. Utilization of bio-oil therefore requires further processing in order to use it as a fuel. Various techniques are available for the processing/upgradation of bio-oil comprising of catalytic cracking, hydrodeoxygenation, steam reforming, esterification, emulsification, supercritical fluids etc. An abundance of literature is available on these techniques but for the individual compounds of the bio-oil. There is no specific reaction mechanism for overall pyrolysis bio-oil upgradation till date. Among the various techniques mentioned hydrodeoxygenation (HDO) seems to be the most promising route for the upgradation of bio-oil as it is economically viable, and with production prices equivalent to conventional crude oil, however challenges still exist with this field. The reaction mechanism or the inside chemistry of the hydrodeoxygenation of bio-oils is not clearly known. Another great concern with the field is the catalyst choice. Much effort and focus were around the commercial Co-Mo, Pt, Ni-Mo supported by sulfides, or noble metal supports, but due to the high affinity of carbon formation, makes the method limited to lab scale but not commercially fit as of now. Another important aspect is that the usage of the noble metal supports which are not easily available and economically not feasible, hence the search for

the alternative is under progress. Overall summary of this review is that a series of fields still have to be investigated before HDO can be in industrial scale. Further tasks include:

- Catalyst development: investigating appropriate catalyst desired for the specific upgradation mechanisms.
- Improved understanding of carbon formation mechanism from classes of compounds.
- Better understanding of kinetics of HDO of model compounds and bio-oil.
- Influence of impurities like sulfur (poisoning catalyst) in bio-oil for the performance of different catalyst.
- Decrease of the reaction temperature and pressure which is economically viable in industrial scale.
- Defining the requirement of the oxygen removal in the context of the further refining bio-oil.
- Selection of appropriate reactor type and its design.

2.3. Objectives of the Thesis

The detailed literature review clearly presents the actual picture on the hydrodeoxygenation procedure for the various feedstocks, using different catalysts. On the other hand, results on the basis of CFD simulation are not available for the upgradation of the bio-oils to the best of our knowledge. Further, the implementation of reaction kinetics mechanism in CFD software is very critical but leads to analyze some critical parameters which are not possible through experimental studies. Therefore the present dissertation aimed to numerically investigate the following objectives:

- CFD modeling and simulations of the upgradation process of bio-oils using three different heterogeneous catalysts namely (Pt/Al_2O_3, $Ni\text{-}Mo/Al_2O_3$, $Co\text{-}Mo/Al_2O_3$) using HDO.
- Introduction of lumped reaction kinetic species parameters into the CFD model and to analyze the product species composition after the HDO reaction.
- Analyzing the effect of the catalyst loading on the product species composition.
- Analyzing the effects of temperature and pressure on the HDO reaction and the product species.
- Analyzing the suitable catalyst for the specific reaction mechanism considered in this dissertation work.

Problem Statement and Mathematical Description Chapter-3

Catalytic hydrodeoxygenation of bio-oil in ebullated bed reactors is very complicated process both hydrodynamically and chemically. In other words in this process hundreds of organic/inorganic compounds present in the unprocessed bio-oil react with hydrogen gas whose reaction kinetics are very complex and most of them are unknown till date. Even the reaction pathway of many of these compounds is unknown in the presence of remaining compounds of bio-oil. Therefore modeling such reactive system is a very tough task without having proper information about their kinetics. On the other hand, the hydrodynamics of this process involves complicated random interactions amongst three phases (i.e., bio-oil liquid phase, H_2 gas phase and catalyst solid phase) involved in hydrodeoxygenation process. Further in such multiphase reactive systems, the hydrodynamics will be turbulent in nature.

Therefore, in this section attempts were made to present the hydrodynamic models which may produce the results as much closer to real life physics as possible. Attempts are also made to present models for reaction mechanism of hydrodeoxygenation process so that to attain results in line with experimental results for validation purpose. Once validated model comprising of hydrodynamics and reaction kinetics of hydrodeoxygenation of unprocessed bio-oil, will further be used to obtain new results for a variety of catalysts and operating conditions. The new results obtained from this work will be analyzed to obtain optimum conditions for this process. However before presenting hydrodynamics and reaction models, it is mandatory to present the statement of the problem in details.

`

3.1. Principles of ebullated bed reactor

Ebullated reactor is a specific type of fluidized bed reactor wherein not only the hydrogen gas is used as fluidization medium but also the liquid oil phase is fed from the bottom into the reactor which is partially filled with catalyst solid phase. The ebullated bed technology utilizes a three phase reactor (liquid, gas and catalyst) applicable for exothermic reactions and for feed stocks like vacuum residues, heavy crude oils, bio-oils, etc. where the contaminants are dominant. Gas-liquid-solid ebullated/fluidized beds can be operated with different hydrodynamic regimes depending on gas-liquid velocities and properties.

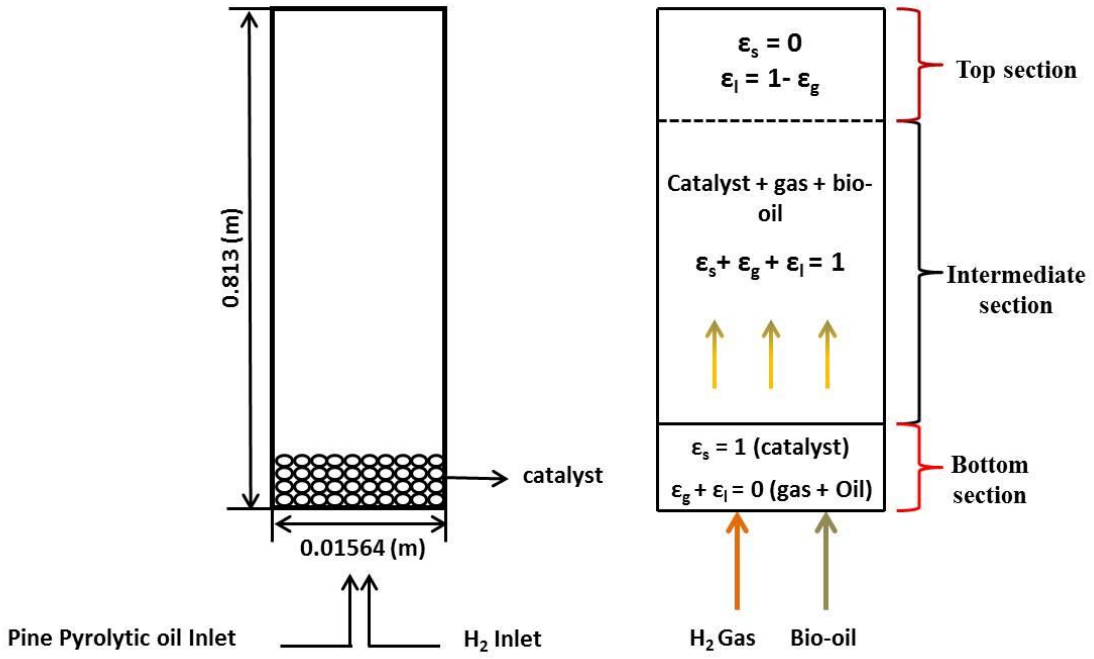

Figure 3.1: a) Schematic model of an ebullated bed reactor for bio-oil upgradation using HDO and b) volume fractions in respective sections

The important hydrodynamic transitions within gas-liquid-solid ebullated/fluidized beds are characterized by the minimum fluidization velocity of gas. Above the minimum fluidization velocity, there exists a good contact between the gas, liquid and solid phases which is essential

`

for proper heat and mass transfer among the phases. Other inherent advantages of these reactors are good back mixing which enables temperature control, eliminate bed plugging and channeling, and maintain low and constant pressure drops over several years of continuous operation with a fluidized catalyst. The catalyst used is held in a fluidized state through the upward lift of liquid reactants (feed oil) and gas entering the reactor. The height of ebullated catalyst bed can be controlled by volume fraction of catalyst, and the flow rate of the input liquid or gas feed. Because of these advantages, ebullated beds are well suited for applications requiring a long uninterrupted run such as for pretreatment of fluid catalytic cracking unit (FCCU) feed stocks. Another advantage associated with the ebullated bed reactors are they can be operated at high pressures (10-200 bar) and temperatures (100-500^{o}C) which are very much essential for the HDO process because the oxygen atoms are very complex to separate from the residues of bio-oil feed stocks at low to moderate temperature and pressures.

3.2. Volume fraction distribution inside the reactor

The schematic shown in Figure 3.1a denotes the reactor domain used for the present simulation studies. This reactor domain is divided into three sections as shown in Figure 3.1b. Further Figure 3.1b denotes the distribution of volume fraction of the three phases (bio-oil, H_2 gas and solid catalyst) inside the reactor. Initially only catalyst particles are preloaded with a solid volume fraction of $\varepsilon_s = 1$ at the bottom of the reactor; whereas the volume fraction of the other two phases (bio-oil, gas) is considered to be zero in this bed region. This means that there is no oil, gas phases present inside the reactor at the inception of reaction process. The arrows at the inlet of the reactor denote the H_2 gas and oil through put to the reactor is distinguished by two different color schemes. The mentioned conditions are pertinent to the startup of the reaction

`

process i.e., at t=0sec. In the reactor and the fluidized conditions are maintained such that these catalyst particles can be fluidized only up to 0.508m of the reactor height. As the oil and gas feeds enters the reactor, mixed with the solid catalyst particles, enabling the balance of volume fractions between phases in such a way that the aggregate of the mixture is unity. The intermediate section denotes the mixing pattern inside a reactor at a specific time. Finally as the reaction process is completed i.e., the bed has reached steady state where there is no significant deviation in the composition is observed and also the height of the bed is constant; and in the upper most section the volume fraction of the gas phase is predominant constituting no solid catalyst particles and a negligible amount of liquid phase.

3.3. Problem statement

Computational fluid dynamics (CFD) approach is economical and most effective tool to study the complex phenomenon of upgradation of bio-oil. Due to the complexity of the simulation, this study is regulated to 2-D approach. A two-dimensional computational domain of ebullated fluidized bed reactor used for the present simulation studies is shown in Figure 3.1. The height and width of the ebullated fluidized reactor are 0.813m and 0.01564m respectively. **The catalyst particles used for the present simulation studies are Pt/Al_2O_3, $Ni\text{-}Mo/Al_2O_3$ and $Co\text{-}Mo/Al_2O_3$. These are filled at the bottom of the reactor (with some interstitial spaces) to a specific volume fraction of 0.0286 in the case of Pt/Al_2O_3, 0.75 in the case of $Ni\text{-}Mo/Al_2O_3$ and $Co\text{-}Mo/Al_2O_3$ catalysts**. At the bottom of the reactor the inlets are fed with two fluids (bio-oil, and H_2 gas) moving in the upward direction. In this study the gas phase is treated as primary phase, bio-oil phase as the secondary phase and solid catalyst particles as tertiary phase. The flow rates of the bio-oil are varied according to the WHSV values and are given as 3.3×10^{-8} m^3/s for 2 h^{-1}, 4.9×10^{-8} m^3/s for 3 h^{-1}, and 6.6×10^{-8} m^3/s for 4 h^{-1} respectively;

`

while, the H_2 gas is introduced with a minimum fluidization velocity of 100cc/min per gram of pine pyrolytic oil. The detailed list of flow rates pertained to different catalysts under various values of WHSV are presented in Table 3.5. The fluidization is used in order to maintain nearly uniform temperatures even in highly exothermic reactions. For a bed of small particles ($d_p \leq 0.1$ mm), the flow conditions are such that the Reynolds number is relatively small ($Re \leq 10$) so that the Kozney-Carman equation is used to establish the point onset of fluidization. This equation is a simplified form of Ergun equation which is applicable to viscous flow dominant regime and is given by

$$u_{mf} = \frac{(\rho_p - \rho_f) g d_p^2}{150 \mu_f} \frac{\varepsilon_{mf}^3}{(1-\varepsilon_{mf})} \tag{3.3.1}$$

The other operating parameters used for the present simulation studies are the temperature ranging between $623 \leq T \leq 673$ K, pressure in the range of $6996 \text{ kPa} \leq P \leq 10443$ kPa and residence time in terms of WHSV varying between $2 \leq \text{WHSV } (h^{-1}) \leq 4$. Also, the heterogeneous chemical reactions of bio-oil reacting with H_2 gas in the presence of catalyst is studied through finite rate/eddy dissipation model. The finite rate/eddy dissipation model takes into account the effects of temperature, pressure and turbulence eddies to calculate the rates of reactions. **Further the thermo-physical properties in the present range of temperature are assumed to be constant.** The choices of operating parameters for the present simulation studies are in lieu with Sheu et al. (1988) and are presented in Table 3.1. Further, according to approach of Sheu et al. (1988), the bio-oil composition is characterized by five major groups namely heavy non-volatile (HNV), light non-volatile (LNV), phenols, alkane and aromatics. This lumping of the bio-oil compounds is due to the fact that bio-oil upgradation process has several complicated reactions amongst hundreds of its compounds in the presence of H_2 and a catalyst. Thus in order

`

to reduce the complexity of the simulation the compounds are lumped in such a way that the major residues come under non-volatiles which are the major reactants converted to desired products.

The details of the pertinent lumped species are given below.

Table 3.1: Typical reactor operating conditions

Gas feed (H_2)	2.7×10^{-8} m^3/s per gram of pine pyrolytic oil (m/s)
Pine oil feed	3.3×10^{-8} m^3/s - 6.6×10^{-8} m^3/s
Weightily hour space velocity	2 h^{-1} to 4 h^{-1}
Temperature conditions	623 K – 673 K
Operating pressures	6996 kPa – 10443 kPa
Catalyst bed	60 gms per each load

Table 3.2: Initial conditions used in the simulation studies

Mass fraction of heavy non-volatiles (HNV) wt.%	0.4932 *
Mass fraction of light non-volatiles (LNV) wt.%	0.3690 *
Mass fraction of phenols wt.%	0.1232 *
Mass fraction of Alkane +Aromatics wt.%	0.0146 *
Mass fraction of gases +Coke	0
Volume fraction of solid in bed	0.5080
Volume fraction of Gas-H_2 in bed	0.4920
Volume fraction of Gas-H_2 free board	1.0000
Volume fraction of solid free board	0

* Same as from Sheu et al. (1988)

3.3.1. Non-volatiles

Bio-oil accounts for almost 37% of the non-volatile fractions/residues needs to be processed in order to obtain alkanes and aromatics and also small traces of phenols. The non-volatiles are majorly due to the presence of sugars and oligomers in the biomass feed stock. The

`

major fractions of the non-volatile compounds comprising (sugars, oligomers, carboxylic acids, aldehydes, ketones, carbohydrates, degraded lignin, and water). The heavy non-volatile fractions have higher molecular weights which are cracked to smaller fractions by means of catalytic cracking. During this process of catalytic cracking the smaller non-volatile fractions are converted to the volatile compounds by the polymerization reaction. In addition some of the components also react to form coke by Rashid Khan (2011). On the other hand they are highly oxygenated which reduces the heating value of the bio-oil. Hence in order to improve the elemental characteristics of bio-oil, these non-volatile fractions need to be processed to obtain higher yields of alkanes and aromatics.

3.3.2. Phenols

Phenol is one of the major compound present in bio-oil constituting 2-5 wt.%. Substituted phenols make up a larger portion of the bio-oils. Phenols from bio-oils of pine consist of 3-methoxy groups with a wide variety of other functional groups. Phenols and substituted phenols yield the corresponding cyclohexanes when hydrogenated. The phenol formation during HDO process is majorly accompanied during the stabilization occurring below $300^{o}C$ in order to avoid coking formation and polymerization of the oxy-compounds i.e., biphenols, ethers and methoxypehnols present in non-volatiles are converted to phenols.

3.3.3. Alkane and Aromatics

During the catalytic hydrodeoxygenation process to upgrade bio-oil, aromatics are considered as the prominent compound. The presence of aromatic compounds reduces the weight % yield of the bio-oil because oxygen is being removed as water, CO, CO_2. Thus the aromatics have a higher heating value than the typical bio-oil because of their reduced oxygen

content. However the presence of aromatics increases the density and viscosity of the bio-oil; the strong interaction between C=C bonds and aromatic rings from oxy-compounds with active sites on the catalyst surface lead to the formation of carbon instead of hydrocarbon fuel and hence desired and optimal conditions are to be maintained to avoid ageing, coking effects of the bio-oil. Aromatic character of the upgraded bio-oils, (unsaturated aromatics) has a higher octane number value comparing with the saturated cyclic hydrocarbons (Elliott 2007). Therefore the presence of aliphatic and aromatic hydrocarbons enhances the quality of liquid bio-fuel by (Aho et al., 2008; Antonakou et al., 2006; Triantafyllidis et al., 2007; Williams and Nugranad, 2000; Zhang et al., 2009).

The initial composition of the bio-oil, gas, and solid catalyst at the inlet condition which are used for the present simulation studies are presented in Table 3.2. The properties of the three phase i.e., (bio-oil, H_2 gas, solid catalysts) used for the present simulation studies are listed in Table 3.3. Finally, the reactions amongst lumped groups involved in the simulation studies are shown by a typical pathway (adopted from Sheu et al. (1988)) in Figure 3.2. The reaction kinetics used for the different catalysts for the proposed reaction mechanism is listed in Table 3.4.

Table 3.3: Properties of the three phases used in the present simulation studies

Phase	Compound	Density (kg/m^3)	Viscosity (kg/ms)	Specific Heat (J/kg K)	Thermal Conductivity (W/m K)
Pine pyrolytic Oil	**HNV-(Limonene) (Stowe 1993)**	841.15	0.00092	1833.817	0.127
	LNV-(Heptane) (Raal and Muhlbauer 1997)	679.5	0.00040	2223.19	0.140
	Phenols-(Cresol-o) (Wang et al. 2012)	1030	0.18423	1430.00	0.190
	Aromatics-(Xylene) (Zhu et al. 2013)	880	0.00081	1699.84	0.131
	Alkane-(Methane) (Fluent database)	0.669	0.000018	2222	0.033
H_2 gas Phase	**H_2 (Gas) (Fluent database)**	0.8189	0.000008	14283	0.167
	Water Vapour (Fluent database)	0.5542	0.000013	2014	0.0261
Catalyst	**Pt/Al_2O_3 (Lin et al. 1980)**	21450	0.000017	130	71.6
	$Ni\text{-}Mo/Al_2O_3$ (Arcot and David 1974)	829.75	0.000017	1360.71	0.186
	$Co\text{-}Mo/Al_2O_3$ (Arcot and David 1974)	829.75	0.000017	1243.47	0.2213
	Coke +Ash (Fluent database)	375	1.206	850	0.2

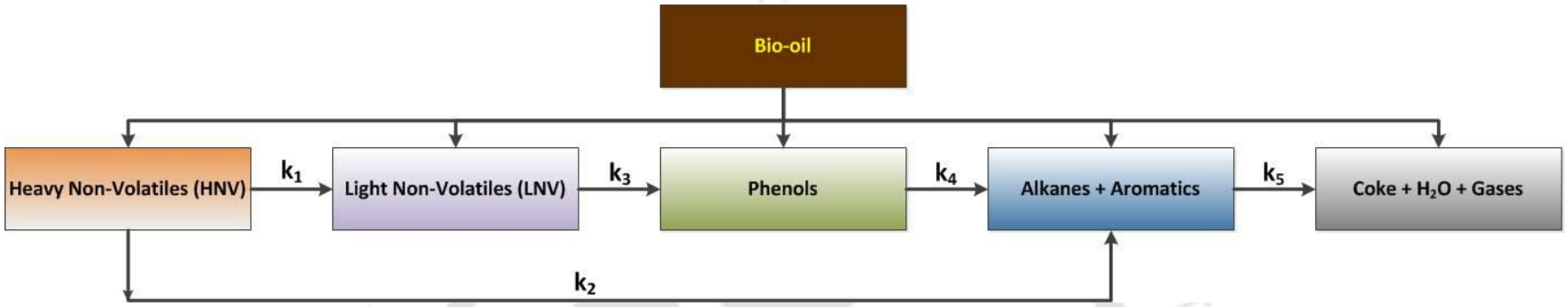

Figure 3.2: Reaction pathways for hydroprocessing of pine pyrolytic oil (adopted from Sheu et al., 1988)

Table 3.4: Reaction pathways, rate expressions, Arrhenius constants & activation energies. (adopted from Sheu et al.,1988).

Pathway	r'	**Pt/Al_2O_3**		**$Ni\text{-}Mo/Al_2O_3$**		**$Co\text{-}Mo/Al_2O_3$**	
		$E \times 10^{-7}$ (kJ mol^{-1})	A (min^{-1})	$E \times 10^{-7}$ (kJ mol^{-1})	A (min^{-1})	$E \times 10^{-7}$ (kJ mol^{-1})	A (min^{-1})
$HNV \xrightarrow{k_1} LNV$	$r_1' = -k_1\rho_1$	74	3860	74.5	3500	82.2	8800
$HNV \xrightarrow{k_2} Alkane + Aromatics$	$r_2' = k_1\rho_1 - k_2\rho_2 - k_3\rho_2$	91.8	75400	96.4	218000	105.8	654000
$LNV \xrightarrow{k_3} Phenol$	$r_3' = k_3\rho_2 - k_4\rho_3$	80.6	8300	81.8	7700	90.4	30600
$Phenol \xrightarrow{k_4} Alkane + Aromatic$	$r_4' = k_2\rho_2 + k_4\rho_3 - k_5\rho_4$	62.3	950	69	3100	68.4	1920
$Alkane + Aromatics \xrightarrow{k_5} Coke + gases + water$	$r_5' = k_5\rho_4$	69.6	4000	55.8	450	74.9	16400

Table 3.5: Flow rates of the bio-oil and H_2 gas phases at different values of WHSV for different catalysts

Catalyst	Catalyst load (kg)	Oil flow rate (m^3/s)	H_2 gas flow rate (m^3/s)	WHSV (hr^{-1})
Pt/Al_2O_3	0.06	3.36×10^{-8}	9.02×10^{-6}	2
	0.06	4.99×10^{-8}	9.02×10^{-6}	3
	0.06	6.67×10^{-8}	9.02×10^{-6}	4
$Ni\text{-}Mo/Al_2O_3$	0.06	3.36×10^{-8}	5.15×10^{-9}	2
	0.06	4.99×10^{-8}	5.15×10^{-9}	3
	0.06	6.67×10^{-8}	5.15×10^{-9}	4
$Co\text{-}Mo/Al_2O_3$	0.06	3.36×10^{-8}	5.15×10^{-9}	2
	0.06	4.99×10^{-8}	5.15×10^{-9}	3
	0.06	6.67×10^{-8}	5.15×10^{-9}	4

3.4. Mathematical formulation

The governing equations for this reactive multiphase flow problem are given below with following phase notations as q^{th} phase refers to primary phase (H_2 gas), p^{th} phase refers to secondary phase (bio-oil), s^{th} phase denotes the tertiary phase (solid catalyst), and r^{th} phase denotes the mixture phase (fluid-solid).

Continuity Equation

$$\frac{1}{\rho_{rq}}\left(\frac{\partial}{\partial t}(\alpha_q \rho_q) + \nabla.(\alpha_q \rho_q \vec{v}_q) = \sum_{p=1}^{n}(\dot{m_{pq}} - \dot{m_{qp}})\right) \quad (3.4.1)$$

Where ρ_{rq} is the **volume averaged density** of the q^{th} phase (H_2 gas) in the solution domain, α_q is the volume fraction of the gas phase, ρ_q is the density of gas, $\dot{m_{pq}}$ is the transfer of mass between p and q phases i.e., between gas and bio-oil.

The volume of q (H_2 gas) phase is given by **Anderson and Jackson (1967) and Bowen (1976).**

$$V_q = \int \alpha_q \, dV \tag{3.4.2}$$

Where the volume fraction of the q[th] phase (H_2 gas) is given by

$$\sum_{q=1}^{n} \alpha_q = 1 \tag{3.4.3}$$

Fluid Phase momentum equations

The conservation of momentum for the fluid phase is given by **Alder and Wainwright (1960)**

$$\frac{\partial}{\partial t}\left(\alpha_q \rho_q \overrightarrow{v_q}\right) + \nabla.\left(\alpha_q \rho_q \overrightarrow{v_q}\overrightarrow{v_q}\right) = -\alpha_q \nabla p + \nabla.\overline{\overline{\tau_q}} + \alpha_q \rho_q \vec{g} + \sum_{p=1}^{n}\left(K_{pq}\left(\overrightarrow{v_p} - \overrightarrow{v_q}\right) + \dot{m_{pq}}\,\overrightarrow{v_{pq}} - \dot{m_{qp}}\,\overrightarrow{v_{qp}}\right) \tag{3.4.5}$$

Where K_{pq} is the interphase force which is dependent on friction, pressure, cohesion and other effects, $\vec{g}$ is the acceleration due to gravity, $\overrightarrow{v_{pq}}$ is the interphase velocity defined by the following conditions. If $m_{pq} > 0$ (i.e., the mass of phase p being transferred to phase q) $\overrightarrow{v_{pq}} = \overrightarrow{v_p}$, if $m_{pq} < 0$ (i.e., the phase q is transferred to phase p) $\overrightarrow{v_{pq}} = \overrightarrow{v_q}$. Likewise if $m_{qp} > 0$ (i.e., the mass of phase q being transferred to phase p) $\overrightarrow{v_{qp}} = \overrightarrow{v_q}$ and if $m_{qp} < 0$ (i.e., the mass of phase p being transferred to phase q) $\overrightarrow{v_{qp}} = \overrightarrow{v_p}$. Here $\overrightarrow{v_p}$ and $\overrightarrow{v_q}$ are the velocities of phase p and q and m_{qp}, m_{pq} characterizes the transfer of mass from phase p to q or vice versa.

Stress tensor is defined as:

$$\overline{\overline{\tau_q}} = \alpha_q \mu_q\left(\nabla\overrightarrow{v_q} + \nabla\overrightarrow{v_q}^T\right) + \alpha_q\left(\lambda_q - \frac{2}{3}\mu_q\right)\nabla.\overrightarrow{v_q}\,\overline{\overline{I}} \tag{3.4.6}$$

$\overline{\overline{\tau_q}}$ is the q[th] phase stress-strain tensor, μ_q is the shear viscosity of the gas phase, α_q is the volume fraction of the gas phase, and λ_q is the bulk viscosity of the gas phase. Similarly, the momentum exchange between the phases is based on the value of fluid-fluid exchange coefficient defined as

$$K_{pq} = \frac{\alpha_q \rho_q \rho_p f}{\tau_p} \tag{3.4.7}$$

K_{pq} is the interphase momentum exchange coefficient, f is the drag force (defined differently for the different exchange coefficient models), ρ_q, ρ_p are the densities of phase p and q and α_q is the volume fraction of phase q.

The drag force is defined as:

$$f = \frac{C_d\, Re}{24} \tag{3.4.8}$$

Here C_d is the drag coefficient based on the Reynolds number *Re*.

The particle relaxation time is defined and given by **Das and Frank (1985)**

$$\tau_p = \frac{\rho_p {d_p}^2}{18\mu_q} \tag{3.4.9}$$

Where d_p is the diameter of the solid particle and μ_q is the shear viscosity if the fluid phase. The drag function also differs for the different exchange coefficient models. In the present study the drag coefficient for the fluid-solid interphase is given as follows (**Schiller and Naumann, 1935**).

$$C_d = \begin{cases} \left\{\dfrac{24(1 + 0.15Re^{0.687})}{Re}\right\} & Re \le 1000 \\ 0.44 & Re > 1000 \end{cases} \tag{3.4.10}$$

where *Re* is the relative Reynolds number for the primary and the secondary phase obtained through (3.4.11) and (3.4.12) equations.

$$Re_{qp} = \frac{\rho_q \left|\overrightarrow{v_p} - \overrightarrow{v_q}\right| d_p}{\mu_q} \tag{3.4.11}$$

$$Re_{pr} = \frac{\rho_{rp}\left|\overrightarrow{v_r} - \overrightarrow{v_p}\right| d_{rp}}{\mu_{rp}} \tag{3.4.12}$$

$$\mu_{rp} = \alpha_p \mu_p + \alpha_r \mu_r \tag{3.4.13}$$

Here μ_{rp} denotes the shear viscosity of mixture phase (fluid-solid), ρ_{rp} denotes the mixture phase density, *Re* is the relative Reynolds number.

Solid Phase Momentum equation

$$\frac{\partial}{\partial t}(\alpha_s \rho_s \overrightarrow{v_s}) + \nabla.(\alpha_s \rho_s \overrightarrow{v_s}\overrightarrow{v_s}) = -\alpha_s \nabla p - \nabla p_s + \nabla.\overline{\overline{\tau_s}} + \alpha_s \rho_s \overrightarrow{g} + \sum_{l=1}^{n}\left(K_{ls}(\overrightarrow{v_l} - \overrightarrow{v_s}) + \dot{m}_{ls}\overrightarrow{v_{ls}} - \dot{m}_{sl}\overrightarrow{v_{sl}}\right) \tag{3.4.14}$$

where α_s, ρ_s are the volume fraction and density of the solid phase, $\vec{g}$ is the acceleration due to gravity, $\overrightarrow{v_{ls}}$ is the interphase velocity of liquid and solid phases and *n* is total number of phases. If $m_{pq} > 0$ (i.e., the mass of phase p being transferred to phase q) $\overrightarrow{v_{pq}} = \overrightarrow{v_p}$, if $m_{pq} < 0$ (i.e., the phase q is transferred to phase p) $\overrightarrow{v_{pq}} = \overrightarrow{v_q}$. Likewise if $m_{qp} > 0$ (i.e., the mass of phase q being transferred to phase p) $\overrightarrow{v_{qp}} = \overrightarrow{v_q}$ and if $m_{qp} < 0$ (i.e., the mass of phase p being transferred to phase q) $\overrightarrow{v_{qp}} = \overrightarrow{v_p}$. Here $\overrightarrow{v_p}$ and $\overrightarrow{v_q}$ are the velocities of phase p and q and m_{ls}, m_{sl} characterizes the transfer of mass from phase solid to liquid phase or vice versa. **But for the present simulation study the transfer of mass between phase is not considered and hence the values of m_{ls}, m_{sl} are considered to be zero.**

K_{sl} is the momentum exchange coefficient between bio-oil and solid catalyst phases and is given by

$$K_{sl} = \frac{3}{4} C_d \frac{\alpha_s \alpha_p \rho_p \left|\overrightarrow{v_s} - \overrightarrow{v_l}\right|}{d_s} \alpha_p^{-2.65} \quad for\ \alpha_p > 0.8 \tag{3.4.15}$$

Where C_d is the drag coefficient and d_s, α_p is the volume fractions of bio-oil phases given by **Wen and Yu (1966)** and **Ergun (1952).**

$$C_d = \frac{24}{\alpha_p Re_s}\left[1 + 0.15\left(\alpha_p Re_s\right)^{0.687}\right] \tag{3.4.16}$$

$$Re_s = \frac{\rho_p \left|\overrightarrow{v_s} - \overrightarrow{v_p}\right| d_s}{\mu_p} \tag{3.4.17}$$

$$K_{sp} = 150\,\frac{\alpha_s(1-\alpha_p)\mu_p}{\alpha_p {d_s}^2} + 1.75\,\frac{\alpha_s \rho_p \left|\overrightarrow{v_s} - \overrightarrow{v_p}\right|}{d_s} \quad for\ \alpha_p \leq 0.8 \tag{3.4.18}$$

Energy equations

In Eulerian multiphase flow, the conservation of energy (enthalpy) is described with a set of mathematical equations as

$$\frac{\partial}{\partial t}\left(\alpha_q \rho_q H_q\right) + \nabla.\left(\alpha_q \rho_q H_q \overrightarrow{u_q}\right) = -\alpha_q \frac{\partial_{pq}}{\partial t} + \overline{\overline{\tau_q}}: \nabla \overrightarrow{u_q} - \nabla.\overrightarrow{q_q} + S_q + \sum_{p=1}^{n}\left(Q_{pq} + \dot{m_{pq}} H_{pq} - \dot{m_{qp}} H_{qp}\right) \tag{3.4.19}$$

where H_q is specific enthalpy of qth phase, $\overrightarrow{q_q}$ is the heat flux, and S_q is source term which includes sources of enthalpy. Further, H_{pq} is interphase enthalpy between p and q phases. m_{pq} is the mass exchange between p and q phases. $\overline{\overline{\tau_q}}$ is the q^{th} phase stress-strain tensor. The rate of energy transfer between fluid-fluid phases is given by **Ranz and Marshall (1952)** whereas for solid-fluid phases it is given by **Gunn (1978).** Q_{pq} is the intensity of heat exchange between q^{th} (continuous gas phase) and p^{th} (bio-oil) phases and is given by

$$Q_{pq} = h_{pq}(T_p - T_q) \tag{3.4.20}$$

Where T_p, T_q are the temperatures of p and q phases respectively, and h_{pq} is the heat transfer coefficient between p and q phases.

$$h_{pq} = \frac{6k_q\alpha_p\alpha_q Nu_p}{d_p^2} \tag{3.4.21}$$

k_q is the thermal conductivity of qth phase, and $\alpha_{p,}\alpha_q$ are the volume fractions of p and q phases. Nu_p is the Nusselt number of pth phase and d_p is the diameter of the particle (catalyst)

From the correlations of **Ranz and Marshall (1952),** Nusselt number of pth phase is given by

$$Nu_p = 2.0 + 0.6{Re_p}^{1/2}Pr^{1/3} \tag{3.4.22}$$

Re_p relative Reynolds number of pth phase and Pr is the Prandtl number of qth phase is given by:

$$Pr = \frac{{C_p}_q\mu_q}{k_q} \tag{3.4.23}$$

Where ${C_p}_q$ is the specific heat capacity of qth phase, and μ_q is the viscosity of qth phase. Nusselt number of solid phase is given by **(Gunn 1978).**

$$Nu_s = \left(7 - 10\alpha_q + 5\alpha_q^2\right)\left(1 + 0.7Re_s^{0.2}Pr^{1/3}\right) + \left(1.33 - 2.4\alpha_q + 1.2\alpha_q^2\right)Re_s^{0.7}Pr^{1/3} \tag{3.4.24}$$

Kinetic theory of Granular flow

The granular temperature for the sth solid phase is proportional to the kinetic energy of the random motion of the particles. The transport equation derived from kinetic theory takes the following form as given by **Gidaspow et al. (1992)**

$$\frac{3}{2}\left[\frac{\partial}{\partial t}(\rho_s\alpha_s\Theta_s) + \nabla.(\rho_s\alpha_s\Theta_s\overrightarrow{v_s})\right] = \left(-p_s\bar{\bar{I}} + \bar{\bar{T}}\right):\nabla\overrightarrow{v_s} + \nabla.\left(K_{\Theta_s}\nabla\Theta_s\right) - \gamma\Theta_s + \emptyset_{ls} \tag{3.4.25}$$

Where $\left(-p_s\bar{\bar{I}} + \bar{\bar{T}}\right):\nabla\overrightarrow{v_s}$ indicates the generation of energy by solid stress tensor

$K_{\Theta_s}\nabla\Theta_s$ represents the diffusion of energy (K_{Θ_s}) is the diffusion coefficient

$\gamma\Theta_s$ represents collisional dissipation energy

$\emptyset_{ls}$is the energy exchange between fluid and solid phase

K_{ls} is the exchange coefficient between fluid and solid phase

ρ_s is the density of the solid, α_s is the volume fraction of the solid, and $\overrightarrow{v_s}$ is the relative velocity of the solid particles

The solid pressure is given by **Ma and Ahmadi (1990)**

$$p_s = \rho_s\alpha_s\Theta_s + 2\rho_s(1+e_{ss})\alpha_s{}^2 g_{0,ss}\Theta_s \tag{3.4.26}$$

The collision dissipation energy is given by

$$\gamma_{\Theta_s} = \frac{12(1-e_{ss}{}^2)g_{0,ss}}{d_s\sqrt{\pi}}\rho_s\alpha_s^2\Theta_s{}^{3/2} \tag{3.4.27}$$

The energy exchange between solid, fluid phases is given by **Gidaspow et al. (1992)**

$$\emptyset_{ls} = -3K_{ls}\,\Theta_s \tag{3.4.28}$$

The diffusion coefficient can be written as

$$K_{\Theta_s} = \frac{150\rho_s d_s\sqrt{\Theta_s\pi}}{384(1+e_{ss})g_{0,ss}}\left[1+\frac{6}{5}(1+e_{ss})g_{0,ss}\alpha_s\right]^2 + 2\rho_s\alpha_s{}^2 d_s g_{0,ss}(1+e_{ss})\sqrt{\frac{\Theta_s}{\pi}} \tag{3.4.29}$$

where ρ_s is the density of the solid phase, e_{ss} is the coefficient of restitution for particle collisions and the default value used is 0.9, $g_{0,ss}$ is the radial distribution function that governs the transition from the compressible condition with $\alpha < \alpha_{s,max}$ with a default value of $\alpha_{s,max}$ = 0.63 and Θ_s is the granular temperature, and d_s is the diameter of solid phase

k-ε Turbulence Model

The model developed and proposed by Launder and Spalding (1972) is used to simulate the mean flow characteristics for turbulent flow conditions. It is a two equation model which gives

the general description of turbulence by means of two transport equations. The first transported variable determines the energy in the turbulence and is called turbulent kinetic energy (k). The second transported variable is the turbulent dissipation (ϵ) which determines the rate of dissipation of the turbulent kinetic energy. The underlying assumption of this model is that the turbulent viscosity is isotropic, in other words, the ratio between Reynolds stress and mean rate of deformations are small in all directions. Transport equations for these two parameters are given by:

$$\frac{\partial}{\partial t}(\rho k) + \frac{\partial}{\partial x_i}(\rho k u_i) = \frac{\partial}{\partial x_j}\left[\left(\mu + \frac{\mu_t}{\sigma_k}\right)\frac{\partial k}{\partial x_j}\right] + G_k + G_b - \rho\epsilon - Y_M + S_k \tag{3.4.30}$$

$$\frac{\partial}{\partial t}(\rho \epsilon) + \frac{\partial}{\partial x_i}(\rho \epsilon u_i) = \frac{\partial}{\partial x_j}\left[\left(\mu + \frac{\mu_t}{\sigma_\epsilon}\right)\frac{\partial \epsilon}{\partial x_j}\right] + C_{1\epsilon}(G_k + C_{3\epsilon}G_b) - C_{2\epsilon\rho}\frac{\epsilon^2}{k} + S_\epsilon \tag{3.4.31}$$

Production of turbulence kinetic energy G_k is given by

$$G_k = -\overline{\rho \mu_i' \mu_j'}\frac{\partial u_j}{\partial x_i} \tag{3.4.32}$$

To evaluate G_k in a manner consistent with Boussinesq hypothesis

$$G_k = \mu_t S^2 \tag{3.4.33}$$

Where S is the modulus of the mean rate-of-strain tensor and is given by

$$S = \sqrt{2 S_{ij} S_{ji}} \tag{3.4.34}$$

$$\mu_t = \rho C_u \frac{k^2}{\epsilon} \tag{3.4.35}$$

The rate of change of turbulent kinetic energy and convection equals the sum of transport by diffusion, rate of production and destruction of kinetic energy and dissipation. Y_M is the fluctuation dilation, and S_k, S_ϵ are the source terms. Here $C_{1\epsilon}$, $C_{2\epsilon}, C_{3\epsilon}$ are the constants with values of 1.44, 1.92, 0.09; σ_ϵ, σ_k are the turbulent Prandtl number for k, ϵ with values 1.0 and

1.3 respectively. G_k, G_b represents of generation of turbulent kinetic energy due to mean velocity gradients and buoyancy. μ_t represents the eddy/turbulent viscosity.

Finally these governing multiphase hydrodynamic equations along with reaction kinetics (Table 3.4) are numerically solved using Ansys Fluent 14.5 to obtain details of upgradation of hydroprocessed bio-oil using hydrodeoxygenation process in the presence of various catalysts in ebullated fluidized bed reactors.

In the present work of reactive three phase fluidization, different solid catalyst materials namely Pt/Al_2O_3, $Ni\text{-}Mo/Al_2O_3$ and $Co\text{-}Mo/Al_2O_3$ are initially at static condition inside the reactor column. The solid catalyst particles are packed to the desired height inside the column according to the calculations shown in the previous chapter. Along with this solid catalyst phase, pine pyrolytic oil is used as a liquid dispersed phase, and hydrogen gas as a continuous gas phase. The liquid and the gas phases are inducted from the bottom side of the reactor so that the fluidization starts when the bed has attained minimum fluidization velocity. The governing conservation equations of mass and momentum along with the appropriate boundary conditions are solved using a commercial solver ANSYS Fluent 14.5 in conjunction with mesh generation software Gambit 6.2.

4.1. Geometry and mesh

The precursor of any CFD simulation study is the geometry creation with proper configuration. Sooner the selection of Ansys Fluent software to solve the fluid flow problem in order to achieve the solution, proper configurations of the domain in which the flow takes is highly needed by the solver. This is achieved through several commercial geometry creating software's like ICem, Gambit, AutoCAD, etc. In the present study Gambit 6.2 has been used to model the geometry with the specified dimensions. Two dimensional geometry with appropriate dimensions of the reactor have been created and meshed to form the grid. Quadrilateral structured meshing has been chosen in the present simulation with regular structured grid of meshing as shown in Figure 4.1a. The zonal view of some portion of the mesh is shown in Figure 4.1 b. The entire two-dimensional domain is structured with quadrilateral grid using total mesh elements of 10000 with 12462 nodes, 12170 faces, and 6000 cells using hexadral mesh. The boundary conditions such as velocity inlet (bottom face), pressure outlet (top face), wall (left and

`

right faces) and default interior have been set. Thus the generated mesh has been exported to Ansys Fluent to obtain the velocity and pressure fields in the entire domain by choosing the $k-\varepsilon$ turbulence flow solver. In the present study Eulerian model for granular flow has been chosen to model the three phase ebullated bed reactor. This Eulerian multiphase flow has a wide range of applications in the field of bubble columns design, risers, particle suspensions and fluidized beds, etc. This model captures the fluidization phenomena in the reactor more effectively. The discrete particle model (DPM) developed in the recent years is more accurate than Eulerian approach however it consumes more CPU time and memory. Thus a tradeoff is required and accordingly Eulerian method is used. The results predicted by this model are promising in most cases and hence it is chosen as a reliable model for the present study.

This model is generally used to solve the set of momentum and continuity equations for each phase in complex multiphase flows. The coupling of equations for continuity, and momentum, is achieved through pressure and interface exchange coefficients and depends on the types of phases involved. The properties of the phases are obtained from the kinetic theory in the case of granular flows. The momentum exchange is also dependent on the type of mixture being used. In this model the fluid and solid phases are treated as interpenetrating continuum phases. Thus the solid particles in such multiphase flows are considered to be identical in terms of diameter and density. Further, the formulation of multiphase model treats each phase as interpenetrating continuum to reconstruct the integral balance of continuity, momentum and energy equations with appropriate operating and boundary conditions. Further certain averaging techniques include the density weighted averaging to predict the flow field variables and the effects of density and fluctuations due to turbulences, and Reynolds averaging to estimate the

`

Reynolds stress terms by Boussinesq hypothesis in the time-averaged conservation equations in order to obtain the momentum balance for the solid phase.

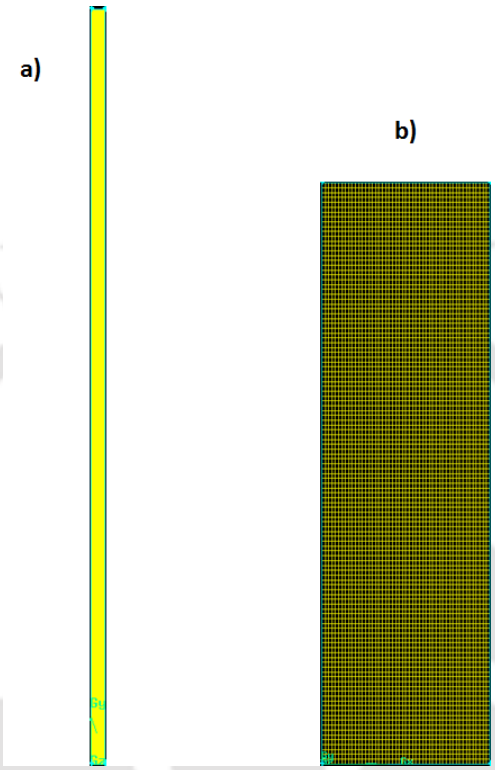

Figure 4.1: Meshing of the reactor used in the present simulation study a) entire domain b) zoomed view of meshing of some portion of the reactor

Table 4.1: Grid independence study

S. No	Total no of mesh elements	Time step	Mass fraction of alkane and aromatics
1	10000	0.001	0.19424
2	15000	0.001	0.19425
3	20000	0.001	0.19428

Table 4.2: Time step dependency study

S. No	Total no of mesh elements	Time step	Mass fraction of alkane and aromatics
1	10000	0.01	Not converged
2	10000	0.001	0.1942
3	10000	0.0001	0.1945

`

The grid sensitivity test is performed using three grids and obtained almost identical values of the mass fractions of alkane and aromatics with all three grids tested (see Table 4.1). Therefore to reduce the computational effort and power, a grid of 10000 elements and 0.001 time step are found to be optimal for the pertinent numerical simulation conditions. Further, using this optimal grid, a time step dependence study is also carried out by varying different time steps and found that for time step 0.01 the solution is not converging as shown in Table 4.2. Further decreasing the time step (less than 10^{-3}) there is no much difference observed in the mass fraction of alkane and aromatics. Therefore finally time steps of 0.001 for all other computations are carried out.

4.2. Solution Methodology

In order to obtain a well posed system of equations, reasonable and realistic boundary conditions needs to be specified to the solver. The velocity inlet and pressure outlet boundary conditions are used for bottom inlet and top outlet faces. For left and right walls of the reactor, standard no slip wall condition is used and for the interior of reactor, default interior is chosen as Eulerian approach used in this simulation study. The composition of the mixture comprised of three phases (bio-oil, H_2 gas and the solid catalyst) is dependent on the individual thermal properties of each phase. The mixture material properties have been chosen to delineate the effects of thermal conductivities on the proposed reaction mechanism and kinetics. The mass weighted mixing law has been chosen to solve the respective governing equations for the solid catalyst particles; incompressible ideal gas law has been adopted for the H_2 gas phase and mixing law in the case of bio-oil phase. H_2 gas phase as the continuous phase, and the bio-oil phase as the secondary phase while solid catalyst particles are treated as the tertiary phase. The heterogeneous stiff chemistry solver to solve the complex reaction mechanisms of the multiphase phase shown in Table 3.4.

`

using finite/eddy rate dissipation model are adopted which is a predefined function in the Ansys Fluent 14.5. In this solver the reactants, products, rate of the reactions, Arrhenius constants, and pre exponential factors are defined as the desired reaction chemistry. For all phases, initial compositions are defined in terms of mass fraction values. The inlet velocity is constant throughout the simulation process for a specific weight hourly space velocity (WHSV) and hence the velocity inlet boundary condition is implemented. The pressure outlet boundary condition is implemented at the outlet of the reactor channel which is set to be 101325 Pa**.**

In order to estimate the effects of turbulence/eddies, turbulence eddy dissipation model is introduced in the present numerical simulation study. But, the velocities of bio-oil and H_2 gas phases are very mild i.e., in the order of 10^{-3} there is no turbulence or back mixing is seen. The similar results were seen with the application of laminar flow condition with no significant changes. Further to avoid the complexities turbulence model is used. The restitution coefficient of solid – solid phases is taken default value of 0.9. The turbulence effects are dealt by using $k-\varepsilon$ turbulence model for mixture momentum equations in order to track the turbulent changes inside the reactor which is discussed in detail in the previous chapter. The phase coupled semi-implicit method for pressure-linked equation (Phase coupled SIMPLE) algorithm along with second order upwind interpolation for the convective kinematics, first order upwind for the volume fraction, and turbulent flow with relaxation parameters of 0.8, 0.8 and 0.2 for turbulent kinetic energy, turbulent dissipation and granular temperature has been chosen as default values. The solution is initialized with respect to all zones and the respective volume fraction of the three phases (bio-oil, H_2 gas and the solid catalyst) are patched as per the numerical calculations. A specific region is adapted with an X_{max} value of 0.01564 and Y_{max} of 0.508 shows that the catalyst particles are patched in that region initially at the start of the process with no other phase

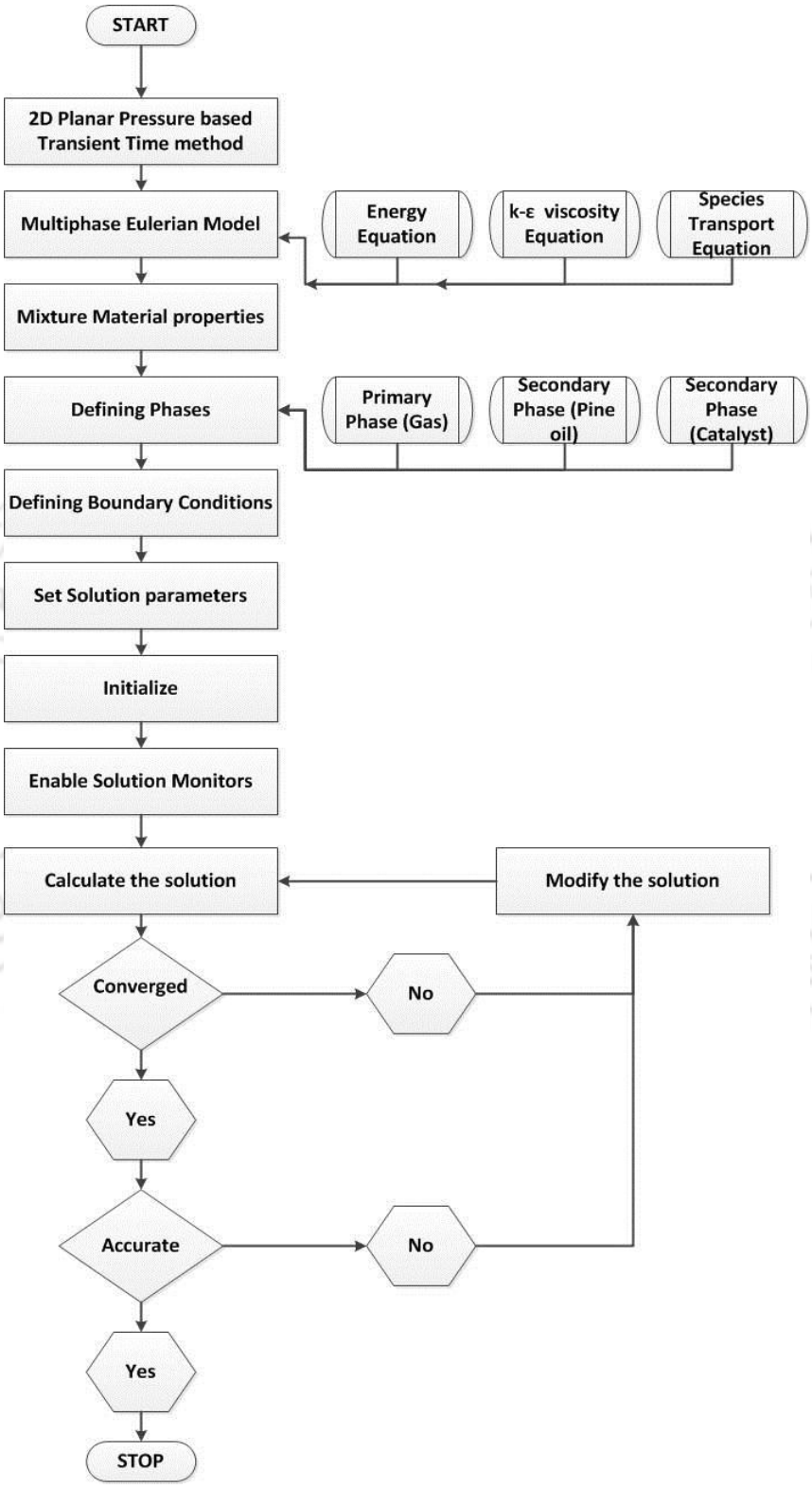

Figure 4.2: Flow chart representing general procedure of simulation using Fluent 14.5

`

The initial volume fraction of the bio-oil and the H_2 phases are maintained to be zero where the catalyst particles volume fraction is patched using the Ansys Fluent software. The flow sheet of the Ansys fluent methodology is presented in Figure 4.2. In order to obtain a fully converged velocity and pressure fields, the residual tolerance for the continuity and momentum equations are set to 10^{-5}. For any set of convergence criteria, the assumption is that the solution is no longer changing with more iteration and when the condition is reached there is an overall mass balance throughout the domain. Then finally, the solution is initialized from all zones by patching a volume fraction of the catalyst as 0.0286 for Pt/Al_2O_3, 0.75 in the case of $Ni\text{-}Mo/Al_2O_3$ and $Co\text{-}Mo/Al_2O_3$ of the static bed height of column has been used, and the volume fractions of the other two phases (oil and gas) are dependent on the calculations. For the present simulation study a pressure based transient solver has been chosen to solve the respective governing equations. A transient solver with a time step size of 0.001 s, 100000 time steps, and maximum iterations of 20 per step has been chosen to obtain optimum numerical values. More details of solution methodology and post processing of results using Ansys post processing are given below with snapshots of each step involved in this simulation study.

4.3. Model Validation

Before presenting the new results, it is mandatory to benchmark the solver with existing experimental results in order to avoid any further errors. For this the solver is validated with the existing experimental results of Sheu et al. (1988). As the research related to the upgradation of bio-oil using HDO process through a numerical approach is very scarce and hence to the best of our knowledge only Sheu et al. (1988) reported results in terms of numeric for the HDO process. The reason behind using the model developed in 1988 for validation is the only available model which is experimentally proven to upgrade the bio-oil through hydrotreatment. The importance of numerical simulation rather than experimental studies is to avoid the laborious effort**, and time to get accurate information**. Further some critical parameters which are difficult to analyze through experimental studies can be studied through numerical simulations. Hence a proper methodology which is validated with the proven or existing literature wills serve the purpose to continue the research further.

Also from the thorough literature survey it is understood that the mass fraction compositions of the inlet feed of three phases were not mentioned elsewhere along with the reaction pathway, Arrhenius constants, activation energies, pre-exponential factors etc., except by Sheu et al. (1988). Finally, the reaction mechanism implemented by Sheu et al., (1988) deals with respect to major compounds of unprocessed bio-oil before and upgradation process including char content and hence, this convinced us to follow their reaction pathway for the present research. **Table 4.3** presents a detailed validation study on the upgradation of bio-oil in a fixed bed reactor in the similar lines of Sheu et al. (1988). The simulated results of the present study are in close proximity with the existing literature values; however the sources of some discrepancy with the literature values may be ascribed to the use of fixed bed reactor in the

present study whereas the experimental work of Sheu et al. (1988) was carried out in a trickle bed reactor. Further it can be noted that such order of discrepencies between experimental and numerical results is not at all uncommon and are often acceptable in such complicated multiphase reactions modeling and simulations. Finally this solver is used to obtain new results in order to check the effects of temperature, pressure and catalyst loading values in the presence of different catalysts namely Pt/Al_2O_3, $Ni\text{-}Mo/Al_2O_3$ and $Co\text{-}Mo/Al_2O_3$ on the hydro-treatment of bio-oil upgradation process.

Table 4.3: Initial operating conditions and the validation of simulation results at T=673 K, WHSV=2 h^{-1} and P=8720 kPa with experimental results of Sheu et al. (1988).

Lumped Species	Initial Mass fractions	Pt/Al_2O_3		$Ni\text{-}Mo/Al_2O_3$		$Co\text{-}Mo/Al_2O_3$	
		Upgraded bio-oil		Upgraded bio-oil		Upgraded bio-oil	
		Sheu et al. (1988)	Present	Sheu et al. (1988)	Present	Sheu et al. (1988)	Present
HNV	0.4932	0.2457	0.2102	0.3602	0.3355	0.3224	0.3526
LNV	0.3690	0.2941	0.4083	0.3258	0.4251	0.3042	0.4196
Phenol	0.1232	0.1063	0.1552	0.1025	0.1318	0.1117	0.1300
Alkane + Aromatic	0.0146	0.1952	0.1962	0.0700	0.0909	0.1003	0.0874
Coke + H_2O +gases	0	0.1587	0.000169	0.1527	0.0167	0.1816	0.0105

5.1. Hydrodynamic Effects

5.1.1. Volume fraction contours of Pt/Al_2O_3 Catalyst

Figures 5.1 - 5.3 denote the prototype volume fraction contours of three phases (i.e., bio-oil, hydrogen gas and the solid catalyst) in the hydrotreatment of bio-oil in the presence of Pt/Al_2O_3 catalyst. The color bar on the left hand side of the image denotes the range of contours of the specific phase at a particular instant. This has been mentioned similarly to the volume fraction of the gas and the oil phases as well. The contour volume fraction of the catalyst bed variation with respect to the different time periods are clearly shown in Figure 5.1. The catalyst bed tends to fluidize at the attainment of minimum fluidization velocity such that the particles tends to rise gradually.

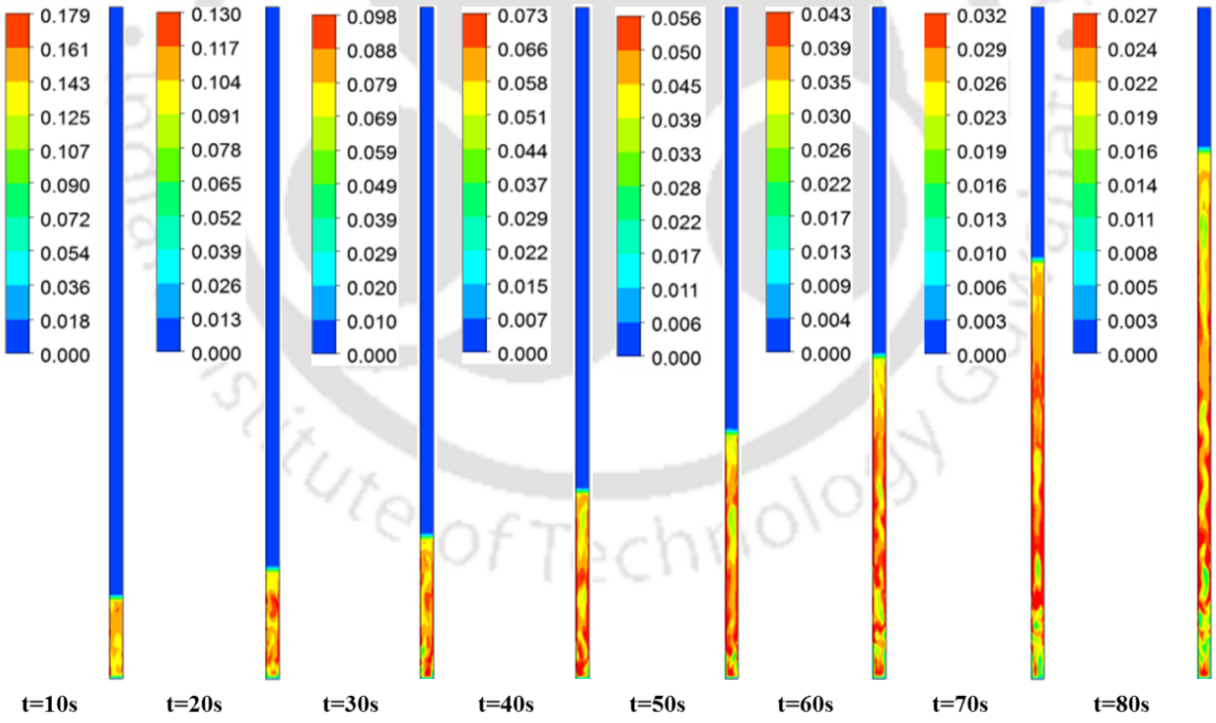

Figure 5.1: Expansion of the Pt/Al_2O_3 catalyst bed **volume fraction** WHSV=3 h^{-1}, T=673 K and P=8720 kPa with increasing time.

As the velocities of the inlet feeds are continuous the bed shows a consistent rise and reaches a point where there is no further change in the height of the bed and also the minimal variations of the compositions. Here the bed has reached a maximum height of the 0.71 m and thereafter the back mixing is taking place inside the reactor. The approximate time taken for the catalyst bed to reach the steady state with the given operating conditions is t = 80sec.

Figure 5.2 illustrates the contour volume fraction changes of the bio-oil phase inside the reactor with respect to the time. There is a gradual change in the height of the bed with respect to the time through the inlets of gas and oil phases such that the complete and proper mixing of the reactants takes place inside the reactor. This is one of the advantages of the ebullated/fluidized bed reactors as compared to the fixed bed reactors.

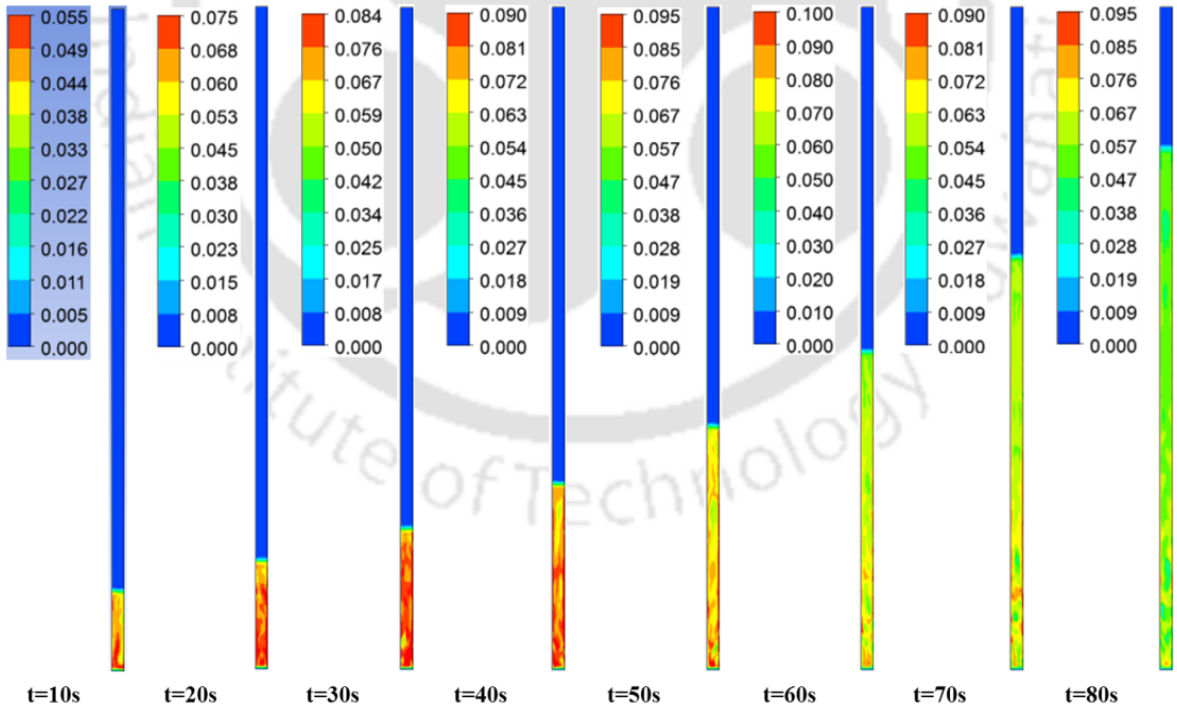

Figure 5.2: Volume fraction of the pine pyrolytic-oil phase with increasing time at WHSV=3 h^{-1}, T=673 K, and P=8720 kPa in the presence of Pt/Al_2O_3 catalyst.

At t = 80 sec the complete mixing of the reaction is taken place and hence the contour density has been changed from the red color (at t=10sec) to mixture of green, yellow and red at t=80sec. Being a lighter medium, the gas occupies the reactor very quickly as compared to the bio-oil, pronounces the initial reaction conditions (seen in Figure 5.3). The stage is set such that the catalyst particles are in close vicinity with the hydrogen gas and when the bio-oil enters the reactor of the solid catalyst particles tends to react with the other two phases and improves the miscibility. Here also it is seen that the gas phase height has been reached to a maximum of 0.71m. The density of the contour varies with respect to time indicates that higher dense is the presence of single phase and the lower dense is the presence of two or more phases introduced into the reactor.

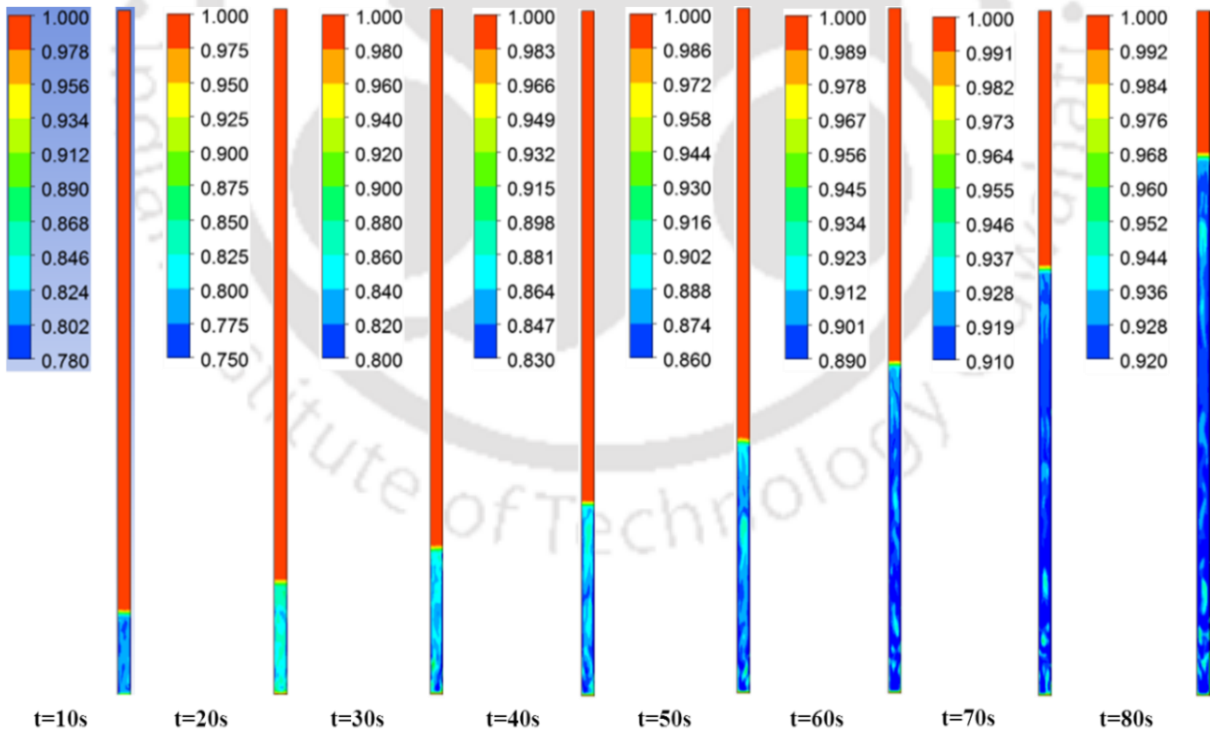

Figure 5.3: Volume fraction of the H_2 gas phase with increasing time at WHSV=3 h^{-1}, T=673 K, and P=8720 kPa in the presence of Pt/Al_2O_3 catalyst.

The detailed summary of the hydrodynamic effects with respect to the pertinent operating conditions are presented in Table 5.1. The steady state variation of volume fraction of processed/upgraded bio-oil with respect to temperature, pressure and WHSV are shown in Figure 5.4. The x-axis denoted the operating pressures used for the present simulation studies ranging between 6996 kPa to 10443 kPa, left y- denotes the variation of volume fractions of oil and the catalyst at the pertinent operating conditions, right y-axis denotes the volume fraction of the gas phase. The solid lines in the Figure 5.4 denotes the volume fraction of processed bio-oil at lower temperatures i.e., T=623 K, dotted lines indicate the moderate temperatures T=648 K, and dashed dot line indicates the higher temperatures T=673 K.

At a steady value of WHSV =2 h^{-1}, the variation in the volume fraction of bio-oil remains unaffected for lower (T=623 K) and moderate temperature (T=648 K) with the increasing pressure; whereas for higher temperature (T=673 K) a decreasing trend is observed with pressure indicate that the solubility of the oil is increased at higher pressures and hence the stability after P=8720 kPa is achieved seen in Figure 5.4a (dash dotted line).

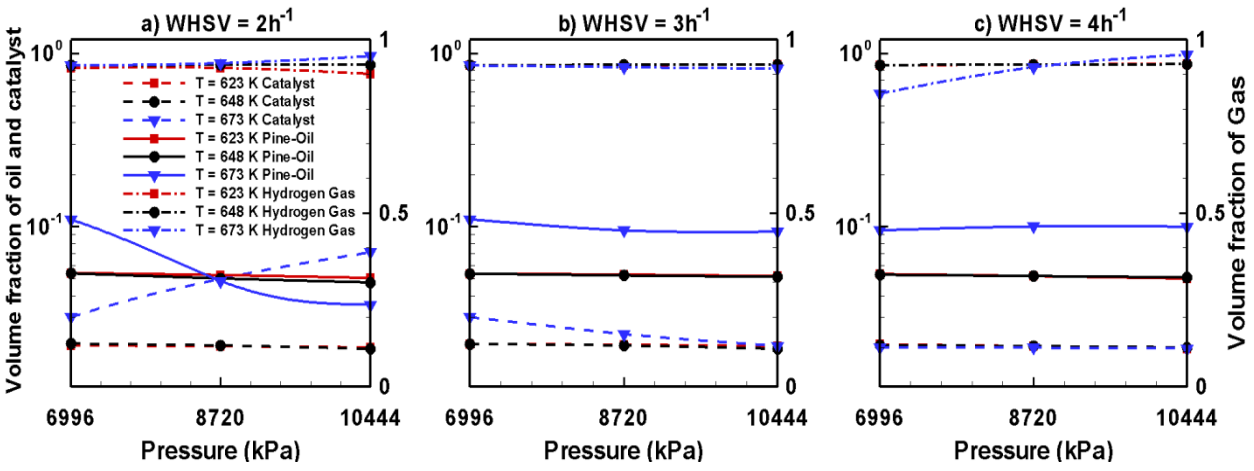

Figure 5.4: Steady volume fractions of pine oil, H_2 gas and Pt/Al_2O_3 catalyst at different temperatures and pressures.

The increase in the solubility ensures the higher availability of hydrogen on the catalyst surface for the reaction to take place. This increases the reaction rate of the catalyst and decreases oil volume fraction in the reactor. With the increase in WHSV the steady state volume fractions of the upgraded bio-oil phase shows a constant trend with no significant deviations irrespective of temperatures, and pressures as seen in Figure 5.4b. The reason could be as the WHSV is increased the residence time for the reaction inside the reactor is decreased and hence the conversion rate of the reactants to products is unchanged. Hence there is no change observed in the volume fraction of the oil phase at WHSV=3 h^{-1} and continued the same trend for WHSV=4 h^{-1} as shown in Figures 5.4b and 5.4c. It is also observed that there is no change noted for the increment in pressure and temperature with the increasing WHSV values.

Figure 5.4b denotes the steady state volume fraction of the gas phase at WHSV ranging between 2 h^{-1} and 4 h^{-1}, temperature vary between 623 K-676 K and the extent of pressure 6996 kPa - 10443 kPa. At constant WHSV =2 h^{-1} the volume fraction of the gas shows a slight variation with respect to operating pressure and temperature. For lower temperatures T=623 K the deviation due to pressure is compensated by the decrement of the oil volume fraction at T=623 K shown in Figure 5.4a. At moderate temperature T=648 K (Figure 5.4a) the trend is constant without any deviation with respect to the varying pressure. At higher temperature T=673 K the volume fraction of gas is slightly increased with the pressure resulting due to the increased solubility of the liquid phase ascribed in Figure 5.4a (T=673 K). This increment in the gaseous fractions are due to the unidentified carbonaceous gases resulted from unconverted oxygenates and insoluble tars of the bio-oil. Further, varying the WHSV to higher values the volume fraction of gases follow a stable trend without much significant deviation to the pertinent operating conditions. This can be clearly seen from Figure 5.4b and Figure 5.4c. Whereas, for the

higher temperatures the volume fraction of catalyst shows a increasing trend with respect to pressure. This increment is resulted due to the transient dispersion of the catalyst to occupy the volume of the reactor. Further, enhancing the WHSV values resulting the steady state values pointing that the equal dispersion of the catalyst throughout the reactor volume is attained with no further deviations as seen in Figure 5.4c. Hence, the effect of the WHSV is majorly attributed to the residence time, reaction rate and higher pressures to the solubility of bio-oil in the vicinity of the catalyst. Table 5.1 presents the numerical values at the pertinent conditions in details.

Table 5.1: Volume fractions of product phases with respect to different operating conditions in the presence of (Pt/Al_2O_3) catalyst

Phase	*WHSV=2h^{-1}*			*WHSV=3h^{-1}*			*WHSV=4h^{-1}*		
				P = 6996 kPa					
	T=623K	T=648K	T=673K	T=623K	T=648K	T=673K	T=623K	T=648K	T=673K
Catalyst	0.0206	0.0211	0.0300	0.0210	0.0210	0.0300	0.0209	0.0207	0.0200
Oil	0.0539	0.0537	0.1100	0.0535	0.0535	0.1100	0.0532	0.0527	0.0950
Gas	0.9180.	0.9250	0.9250	0.9254	0.9254	0.9250	0.9258	0.9265	0.8440
				P = 8720 kPa					
Catalyst	0.0204	0.0206	0.0500	0.0208	0.0206	0.0240	0.0204	0.0204	0.0200
Oil	0.0525	0.0502	0.0486	0.0528	0.0522	0.0950	0.0518	0.0518	0.1000
Gas	0.9180	0.9270	0.9315	0.9262	0.9270	0.9200	0.9277	0.9277	0.9200
				P =10443 kPa					
Catalyst	0.0201	0.0197	0.0710	0.0204	0.0197	0.0205	0.0198	0.0201	0.0198
Oil	0.0505	0.0476	0.0354	0.0517	0.0513	0.0934	0.0501	0.0509	0.0998
Gas	0.9007	0.9282	0.9516	0.9273	0.9282	0.9156	0.9289	0.9285	0.9562

5.1.2. Volume fraction contours of Ni-Mo/Al_2O_3 Catalyst

Figure 5.5 to figure 5.7 denotes the prototype volume fraction contours of three phases (bio-oil, hydrogen gas and the solid catalyst) for the hydrotreatment of bio-oil in the presence of Ni-Mo/Al_2O_3 catalyst. From the Figure 5.5 it is clearly observed that till t=50 sec there is no significant change in the bed is observed and sudden drift in the catalyst bed height is seen till t=70 sec. The bed has reached pseudo steady state at t=70 sec in the presence of Ni-Mo/Al_2O_3 catalyst as compared to Pt/Al_2O_3 (t=80 sec). This clearly proves that the catalyst activity is very much higher in the case of Ni-Mo/Al_2O_3 as compared to Pt/Al_2O_3.

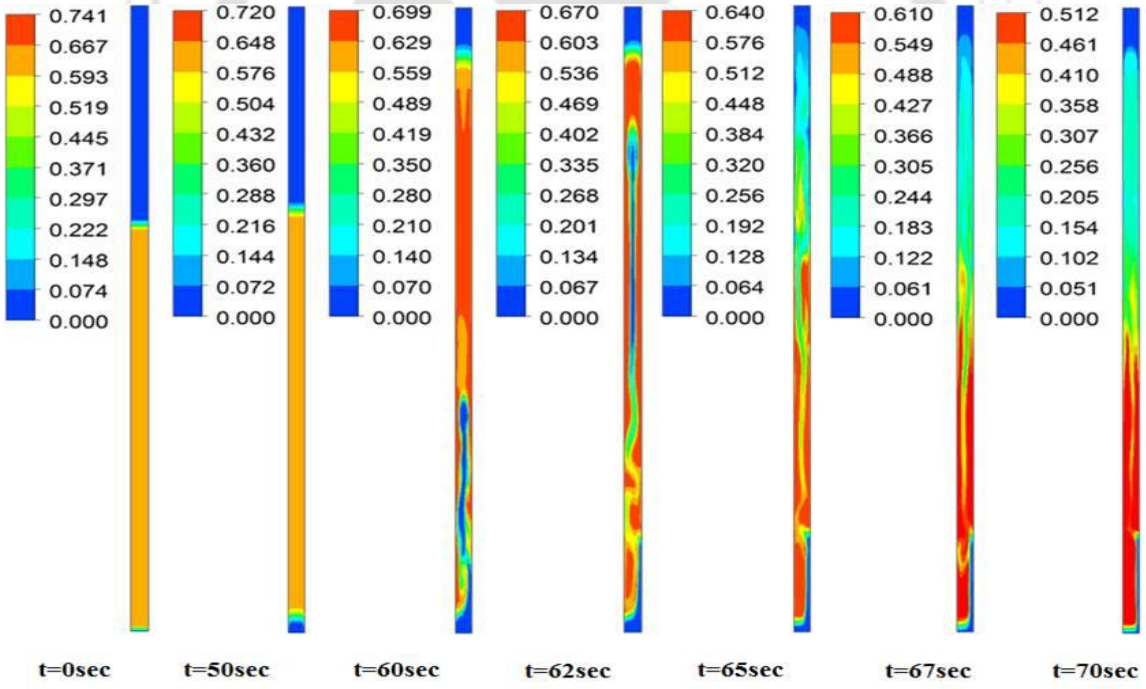

Figure 5.5: Expansion of the Ni-Mo/Al_2O_3 catalyst bed at WHSV=3 h^{-1}, T=673 K, and P=8720 kPa with increasing time

The attainment of the steady state is attributed in two ways both positively and negatively as the higher activity of the catalyst enables the completion of reaction to reach the pseudo

steady state; and the deactivation of the catalyst may be due to the self-inhibiting poisoning nature of the oxygen content reported in the review by Furimsky (2000). The rise of the catalyst bed is in the form of spiral vortex as the major concentration is posed at the center of the reactor and once the steady state has attained the complete mixing of the reactants inside the reactor is seen at t=70 sec. The maximum height of the catalyst bed raised in the present case is 0.802 m which is significantly higher in comparison to Pt/Al_2O_3 catalyst. However the attainment of the steady state of the bed at t=60sec the changes i.e., the rise in the height of the bed and volume fraction values of the bio-oil phase are very minimal.

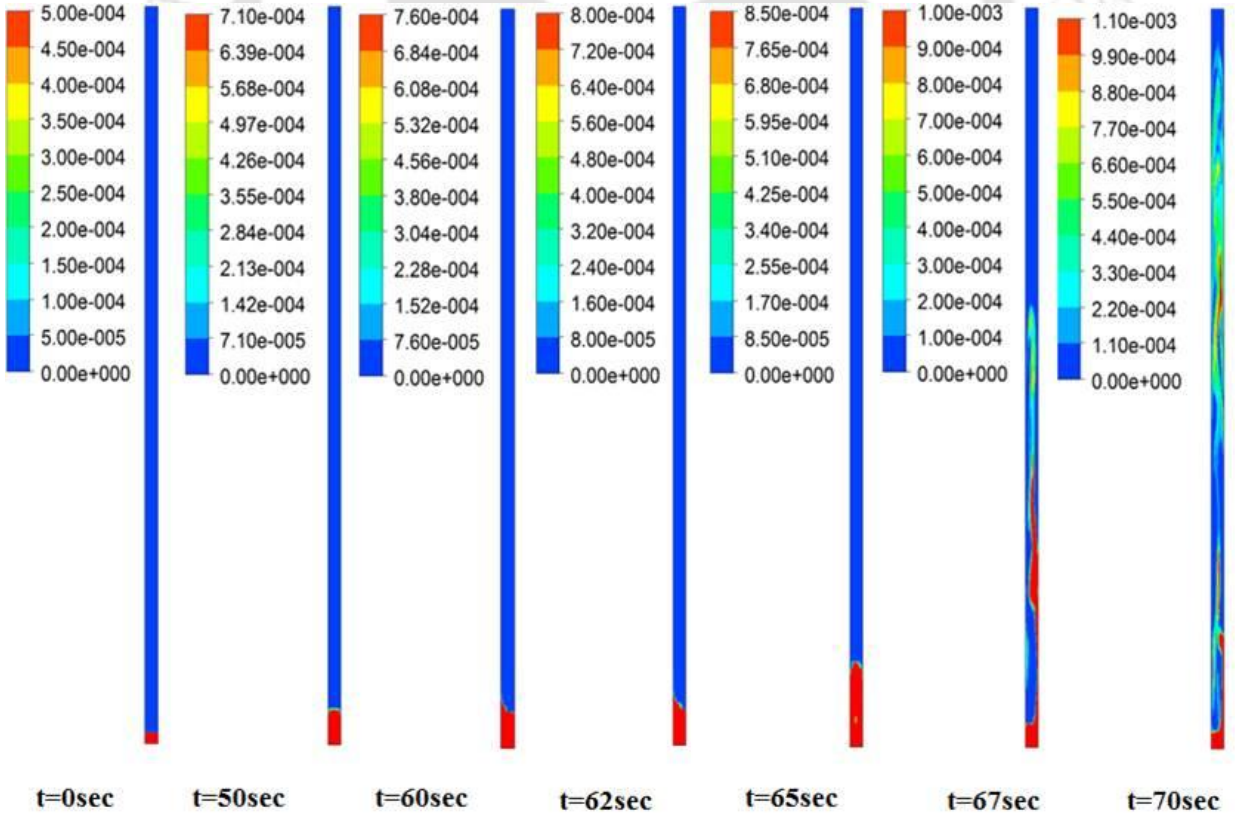

Figure 5.6: Volume fraction of the pine pyrolytic-oil phase with increasing time at WHSV=3 h^{-1}, T=673 K, and P=8720 kPa in the presence of Pt/Al_2O_3 catalyst.

Similarly, the volume fraction contour patterns of the bio-oil phase are seen from Figure 5.6. Till t=50 sec the initial throughput of the oil phase is minimum and once the steady velocity is attained there is a drift in the range of oil volume fractions observed between t=60 sec to t=70 sec.The oil phase has occupied the volume of the reactor which reacts with the other two phases to form a reaction following similar patterns of fluctuating and spiral vortex zones of catalyst phase at the center part of the reactor as seen in Figure 5.6. The similar trends of the volume fractions are observed in the case of H_2 gas varying with respect to time.

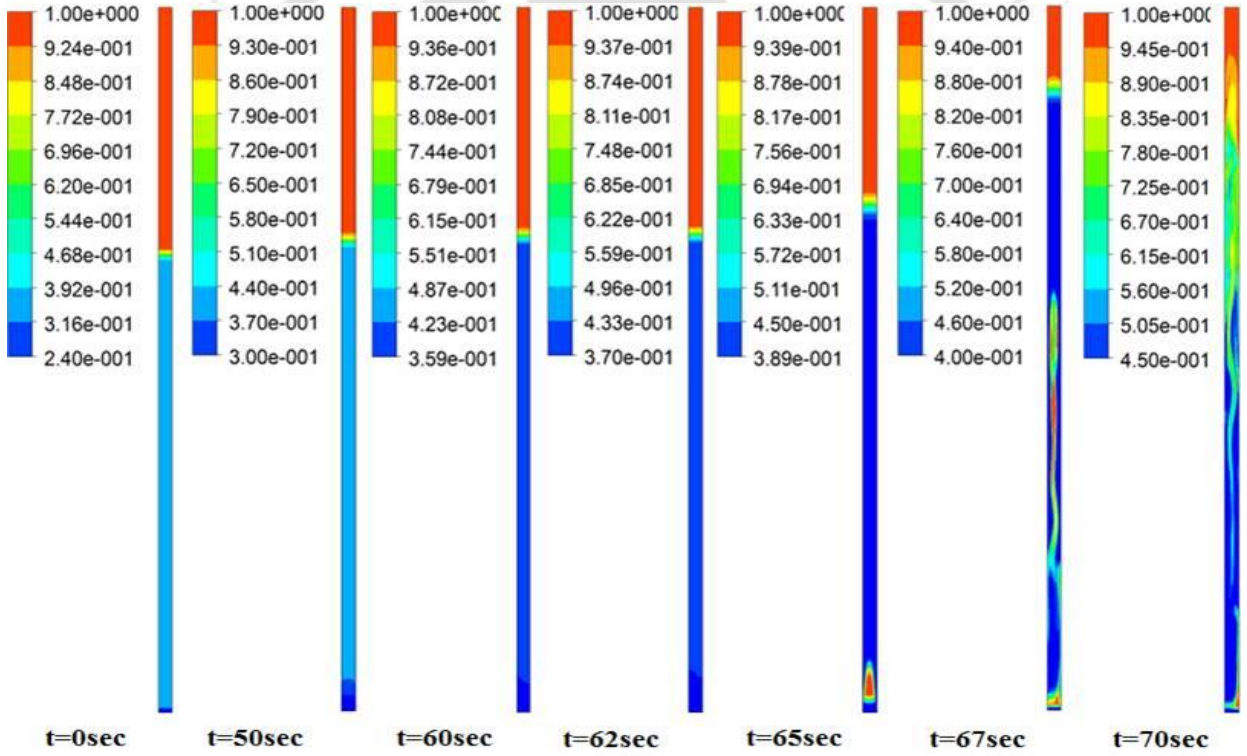

Figure 5.7: Volume fraction of the H_2 gas phase with increasing time at WHSV=3 h^{-1}, T=673 K, and P=8720 kPa in the presence of Pt/Al_2O_3 catalyst.

The volume fraction of the gas occupying the reactor started at t=40 sec-50 sec and there after it takes no time to occupy the total volume of the reactor. The max time taken for the

H_2 gas phase to attain a steady state for a possible reaction with the other two phases is t=70 sec and is seen clearly with the values of the contours from Figure 5.7. The detailed summary on the variation of volume fraction of three phases in the presence of Ni-Mo/Al_2O_3 catalyst at a wide range of operating conditions are presented in Table 5.2. Figure 5.8 specifies the steady state volume fraction of processed/upgraded bio-oil with respect to temperature, pressure and WHSV. The x-axis denotes the operating pressures used for the present simulation studies ranging between 6996 kPa to 10443 kPa, y-axis denotes the variation of volume fractions of oil phases at the pertinent operating conditions, The solid lines in the Figure 5.6 denotes the volume fraction of bio-oil phase at lower temperatures i.e., T=623K, dotted lines indicate the moderate temperatures T=648K, and dashed dot line indicates the higher temperatures T=673K.

Figure 5.8a depicts the volume fraction of the oil phase at WHSV=2 h^{-1} with varying pressure and temperature. At low temperature (T=623 K) the volume fraction of the oil is showing an increasing trend with the increasing pressure.

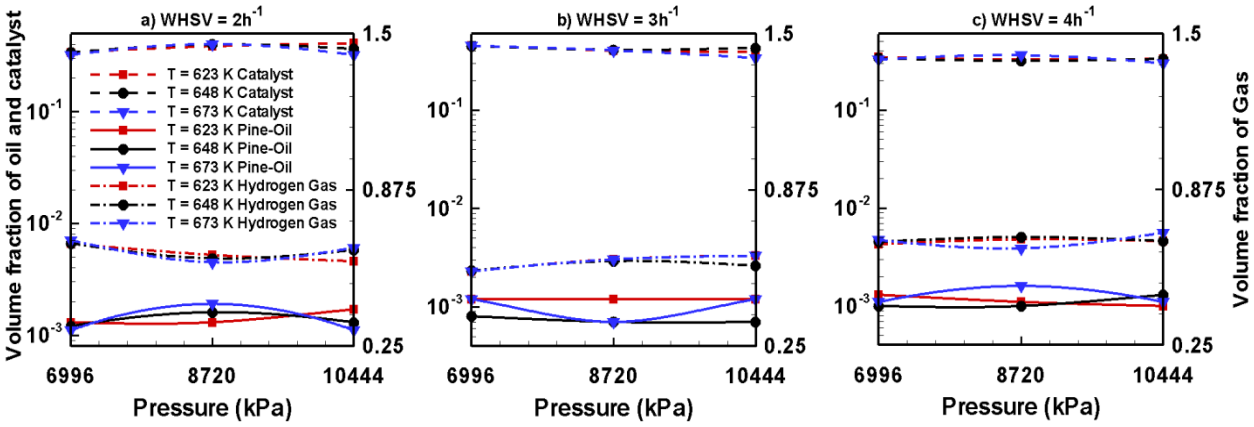

Figure 5.8: Steady volume fractions of pine oil, H_2 gas and Pt/Al_2O_3 catalyst at different temperatures and pressures.

This is due to the fact that with the increase in the pressure the solubility is increased but unfortunately due the sensitivity and inactivity of the catalyst limited the catalyst activity resulted in higher volume fractions of the oil phase given by Olah and Molnar (2003). Whereas, for the moderate (T=648 K) and the higher temperatures (T=673 K) the oil volume fraction shows a mixed trend. The reason may be ascribed for the particular mixed behavior at moderate and high temperatures is due to the formation of intermediate product streams in the form of liquid by Chen (2012) with the increasing pressure up to P=8720 kPa and thereby tends to form the gaseous streams.

The residence time inside the reactor for the reaction is high for the lower values of WHSV has both positive and negative impacts; the activity of the reaction is higher in the case of high residence time and at the same time the formation of undesired secondary products is possible with prolonged reaction at higher pressures. In the present case the formation of the secondary products in the form of gaseous phase is observed at P=8720 kPa and hence a shift from the increasing to decreasing trend of oil volume fraction is observed. Secondly, with the increase in the values of WHSV nothing but reducing the residence time shifted the trends mentioned above i.e., a decreasing trend is observed for the lower temperature (T=623 K) and increasing trend for the moderate and higher temperature regions (T=648 K and T=673 K) seen in Figure 5.8b.

Further, increasing the WHSV to 4 h^{-1} the volume fraction of the pine oil phase has attained a steady state for the case of low (T=623 K) and moderate temperatures (T=648 K) whereas mixed trend is still continued for the high temperature (T=673 K) attributing to the pseudo steady state seen in Figure 5.8c. With the increase in the temperature, at constant WHSV,

and pressure, the volume fraction of the oil phase shows an increasing trend. This is due to the enhanced polymerization of the oxy-organics. These polymerized products are the precursors of coke, which enhances with the rise in temperature. As the temperature is increased aromatic ring condensation followed by hydrogenation reaction in the reaction mechanism proposed by Adjaye and Bakhshi (1995) takes place and hence the volume fraction of the oil phase decreases at higher temperatures and pressures. Figure 5.8 depicts the steady state volume fraction of the gas phase at pertinent operating conditions. From Figure 5.8a it is observed that volume fraction of the gas phase is decreasing with the increasing pressure for all the temperature ranges till P=8720 kPa.

Table 5.2: Volume fractions of product phases with respect to different operating conditions in the presence of (Ni-Mo/Al_2O_3) catalyst

Phase	*WHSV=2h^{-1}*			*WHSV=3h^{-1}*			*WHSV=4h^{-1}*		
				P = 6996 kPa					
	T=623K	T=648K	T=673K	T=623K	T=648K	T=673K	T=623K	T=648K	T=673K
Catalyst	0.3390	0.3380	0.3214	0.4501	0.4486	0.4501	0.3444	0.3346	0.3256
Oil	0.0013	0.0012	0.0011	0.0012	0.0012	0.0012	0.0013	0.0011	0.0010
Gas	0.6590	0.6607	0.6726	0.5486	0.5501	0.5486	0.6541	0.6641	0.6715
				P = 8720 kPa					
Catalyst	0.3847	0.3986	0.4018	0.4026	0.4097	0.4034	0.3248	0.3157	0.3606
Oil	0.0013	0.0016	0.0019	0.0008	0.0007	0.0007	0.0010	0.0010	0.00137
Gas	0.6139	0.5997	0.5846	0.5964	0.5894	0.5957	0.6741	0.6832	0.6379
				P =10443 kPa					
Catalyst	0.4097	0.3645	0.3217	0.3880	0.4283	0.3380	0.3315	0.3315	0.2976
Oil	0.0017	0.0013	0.0011	0.0012	0.0010	0.0012	0.0011	0.0016	0.0011
Gas	0.5885	0.6341	0.6429	0.6106	0.5706	0.6106	0.6672	0.6672	0.7011

Then there is shift observed for the moderate and higher temperature ranges showing an increasing trend with the pressure whereas the lower temperature curve continued with the decreasing trend. The reduction in the oil volume fraction mentioned resulted the formation of the gaseous phase and hence an increment in the values is observed. Further, increasing the value of WHSV to 3 h^{-1} enables the reverse trend as compared to Figure 5.8a. Furthermore, increasing the WHSV to 4 h^{-1} the values of the gas volume fraction are reaching a steady state with the increasing pressure for the moderate and lower temperature curves; however mixed trend is followed at higher temperatures. Finally, in the case of Ni-Mo/Al_2O_3 the volume fraction of the catalyst has no significant effects with respect to WHSV, temperature and pressure denoting the equal dispersion of the catalyst throughout the reactor. In summary, lower values of WHSV have a significant effect on the volume fraction of the oil phase, and gas phase with respect to temperature and pressure; however very minimal changes are observed at the higher values of WHSV.

5.1.3. Volume fraction contours of Co-Mo/Al_2O_3 Catalyst

Figure 5.9 to Figure 5.11 presents the volume fraction contours of three phases (catalyst, bio-oil and H_2 gas) inside the reactor. The color legend on the left hand side presents the variation range of contours at different time steps. The contour volume fractions are projected up to the time at the attainment of the steady state of the bed where there is no significant change in the composition of the hydrotreated bio-oil along with the height of the bed. From Figure 5.9 it is clearly seen that there are no considerable changes in the catalyst bed till t=50 sec. After the attainment of the fluidization state the catalyst bed tends to fluidize vigorously in a span of 20 sec i.e., at t=70 sec and finally reached a pseudo steady state. The maximum height reached by the bed during fluidization is calculated to be 0.803 m which is almost to the brim of the reactor.

At t=70 sec the catalyst bed is completely fluidized where the mixing patterns of the three phases are clearly seen. It is also observed that the reactant species concentration is majorly located at the center of the reactor and hence a jet flow pattern is seen from Figure 5.10 at t=70 sec. Further, it is known that the lighter medium occupies the free board regime of the reactor and hence the gas phase travels quickly and occupies the reactor volume.

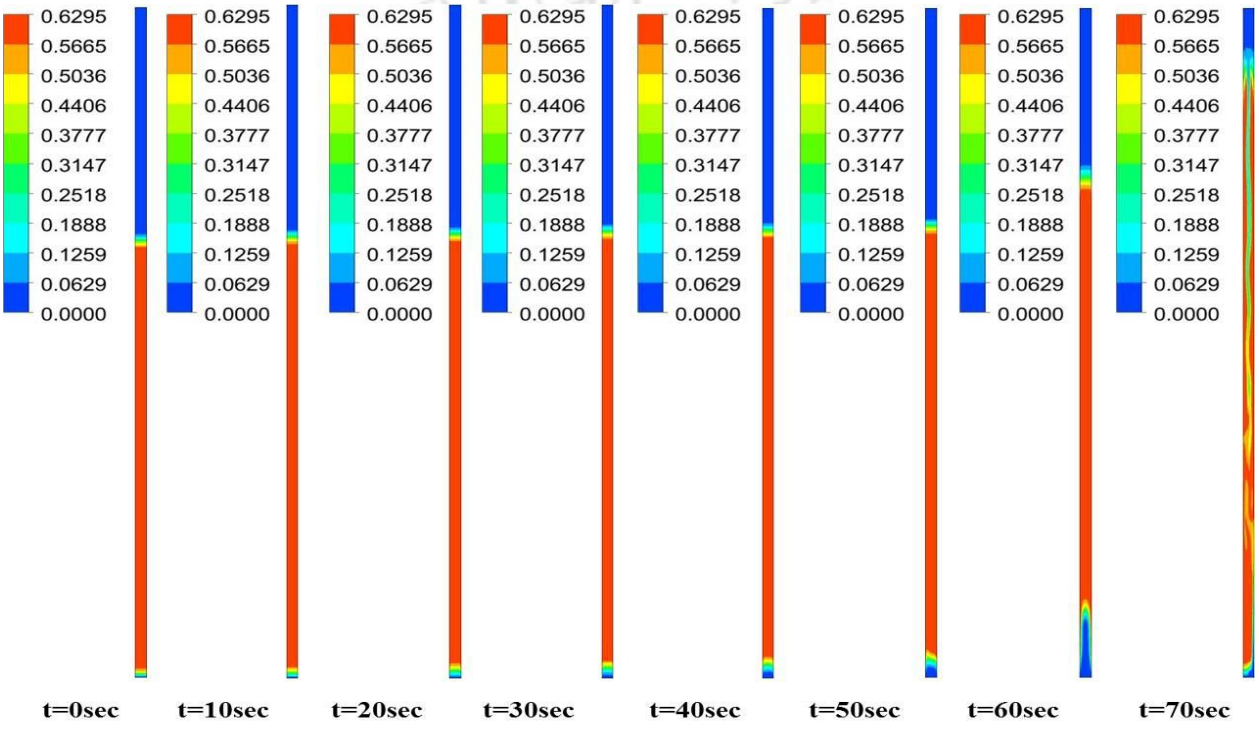

Figure 5.9: Expansion of the Co-Mo/Al_2O_3 catalyst bed at WHSV=3 h^{-1}, T=673 K and P=8720 kPa with increasing time.

The gas enters the reactor at a minimum fluidization velocity such that it doesn't exits the reactor until the reaction process is completed. The time taken for the reaction mechanism to complete a cycle is 70 sec in the present case. In comparison to the other two phases, the volume fraction of the gas phase occupies the reactor from the initial stage and tends to remain steady still till t=50 sec. From then a sudden rise in the gas phase volume

fraction is observed and hence the mixing patterns are seen from the Figure 5.11 at t=70 sec. products followed by Co-Mo/Al_2O_3 and Ni-Mo/Al_2O_3 catalyst. Table 5.3 gives a clear insight about the change in the volume fraction with respect to temperature, pressure and the residence time. Figure 5.12 specifies the steady state volume fraction of processed/upgraded bio-oil with respect to temperature, pressure and WHSV.

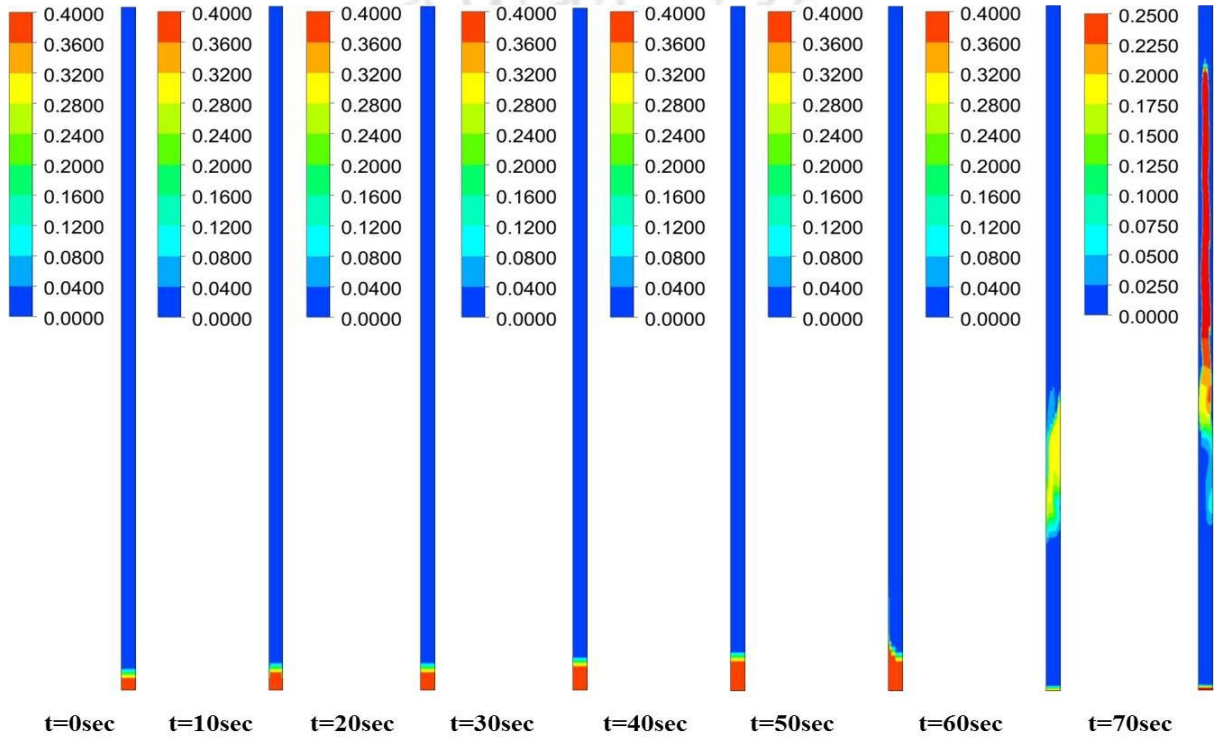

Figure 5.10: Volume fraction of the pine pyrolytic-oil phase with increasing time at WHSV=3 h^{-1}, T=673 K, and P=8720 kPa in the presence of Co-Mo/Al_2O_3 catalyst.

From Figure 5.12a, at constant WHSV=2 h^{-1} the volume fraction of the oil phase with the increase in the pressure shows a decreasing trend specifying the higher activity of the catalyst enabling the higher solubility of the H_2 gas with the bio-oil. Also it is observed from the figure that the conversion of the oil phase is higher at lower temperatures (T=623 K) and relatively less for moderate (T=648 K) and higher temperatures (T=673 K). As the temperature is increased the

activity of the catalyst tends to reduce slowly and hence lower values are observed at higher temperatures (T=673 K). Later, with the increasing WHSV to 3 h^{-1}, the volume fraction of oil

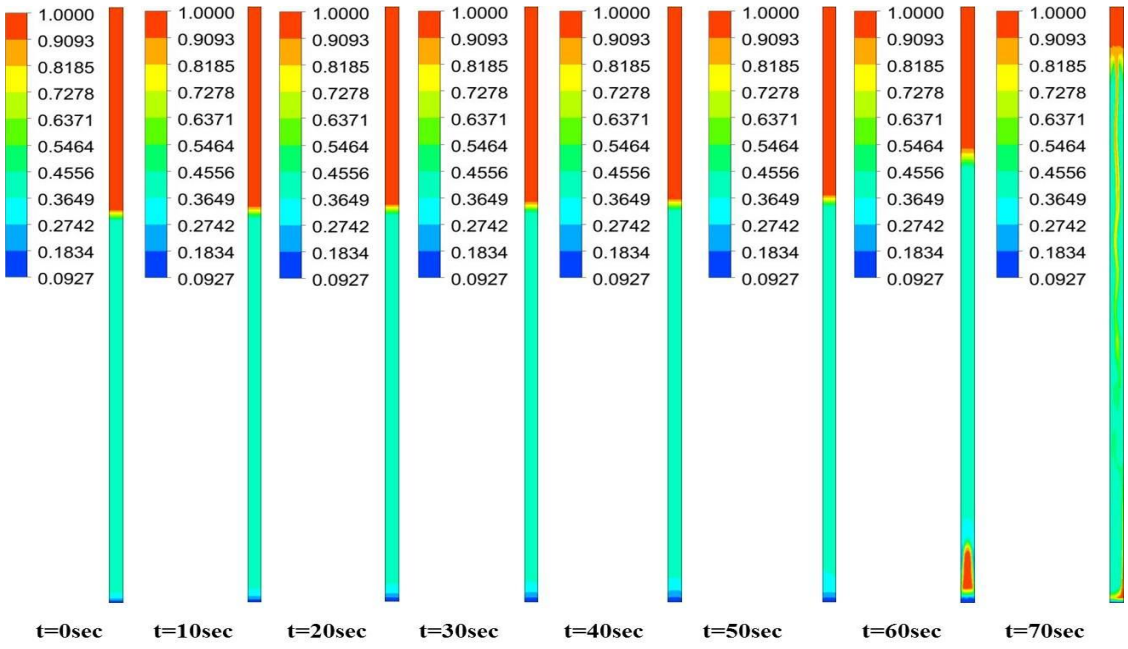

Figure 5.11: Volume fraction of the H_2 gas phase with increasing time at WHSV=3 h^{-1}, T=673 K, and P=8720 kPa in the presence of Pt/Al_2O_3 catalyst.

phase is slightly higher than those of WHSV=2 h^{-1} specifies that the residence time has a considerable effect on the reaction mechanism and hence the unconverted oil phase still remains at higher quantities in the case of WHSV=3 h^{-1}.Further increasing the WHSV values the volume fractions are increasing at lower temperatures as compared to the lower values of WHSV which also signifies that the reaction is not complete due to less residence time On the other hand, the volume fraction of the gas phase tends to show an significant incremental trend with the increasing pressure as seen in Figure 5.12a for a constant WHSV= 2 h^{-1} and T=623 K.

Similarly at a constant WHSV=2 h^{-1} and pressure the incremental trend is still continued with respect to increasing temperature. At a constant WHSV=3 h^{-1} and constant T=623 K, the

volume fraction of the gas phase tends to increase with the increasing pressure and higher values are observed at higher pressures.By maintaining constant WHSV and pressure, the increment forthe gas phase volume fraction is observed merely.

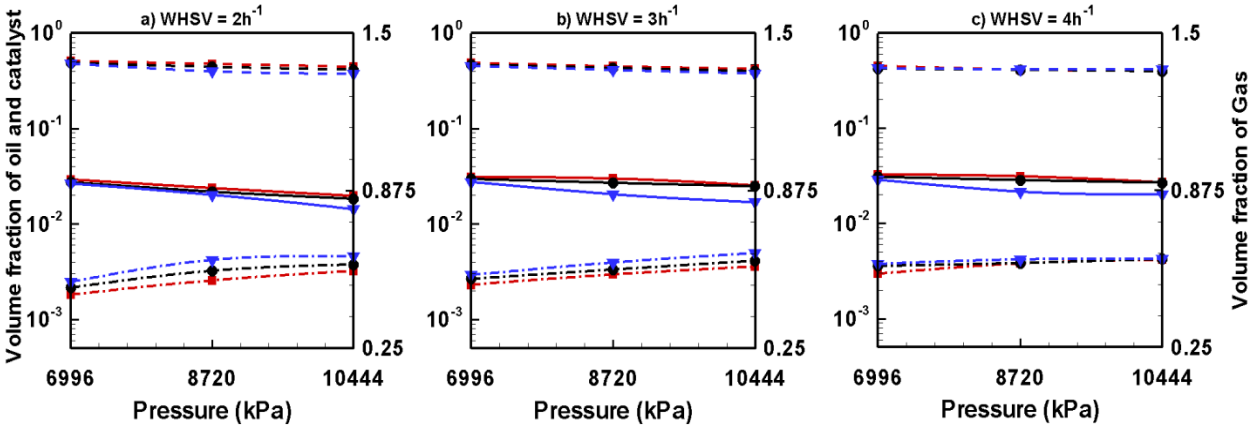

Figure 5.12: Steady volume fractions of pine oil, H_2 gas and Co-Mo/Al_2O_3 catalyst at different temperatures and pressures.

Further decreasing the residence time to 0.25 h and constant temperature T=623 K, similar incremental trends of gas volume fractions are seen with the increasing pressure, and same incremental patterns are recorded with the temperature increase. On the other hand, the volume fraction of the catalyst shows a decreasing trend with the increasing pressure at constant WHSV=2 h^{-1} and same is observed with the increasing temperature as seen in Figure 5.12a. Further shooting up the WHSV to 3 h^{-1} the catalyst volume fraction tries to reach the steady state with the change in temperature and progressive increasing in pressure observed from Figure 5.12b. Besides, the catalyst volume fractions reached a steady state where there is no changes observed at higher values of WHSV=4 h^{-1} with the temperature and pressure effects as seen in Figure 5.12c. From these trends it is seen that the volume fraction of the gas is higher as compared to the oil phase and the catalyst phase which means that the products formed are in the

gaseous form and needs to condense for the liquids. Shortening the residence time favors the limiting of secondary reactions and prevents the coke formation. Also the activity of the catalyst is very high even at high temperatures and pressures; however suitable operating conditions suits the formation of desired products in higher quantities.

Table 5.3: Volume fractions of product phases with respect to different operating conditions in the presence of (Co-Mo/Al_2O_3) catalyst

Phase	*WHSV=2h^{-1}*			*WHSV=3h^{-1}*			*WHSV=4h^{-1}*		
				P = 6996 kPa					
	T=623K	T=648K	T=673K	T=623K	T=648K	T=673K	T=623K	T=648K	T=673K
Catalyst	0.5089	0.4852	0.4762	0.4861	0.4645	0.4511	0.4511	0.4199	0.4260
Oil	0.0291	0.0272	0.0264	0.031	0.0295	0.0274	0.0326	0.0308	0.0286
Gas	0.4619	0.4896	0.5126	0.5012	0.5243	0.5398	0.5422	0.5731	0.5813
				P = 8720 kPa					
Catalyst	0.4736	0.4415	0.3956	0.4466	0.4300	0.4087	0.4113	0.4104	0.4150
Oil	0.0237	0.0217	0.0201	0.0298	0.0269	0.0204	0.0312	0.0285	0.0215
Gas	0.5183	0.5568	0.5995	0.5419	0.5614	0.5892	0.5834	0.5849	0.5994
				P =10443 kPa					
Catalyst	0.4424	0.4116	0.3728	0.4197	0.3974	0.3746	0.4011	0.3958	0.4152
Oil	0.0196	0.0183	0.0142	0.0252	0.0247	0.0168	0.0269	0.0268	0.0201
Gas	0.5561	0.5813	0.6139	0.5734	0.5962	0.6269	0.5979	0.6012	0.6006

5.1.4. Mass fraction contours

The mass fraction values obtained through the hydrotreatment of bio-oil in the presence of different catalyst and variable operating parameters denotes the amount of the unprocessed bio-oil converted into upgraded/processed bio-oil. As mentioned earlier that bio-oil considered in this simulation study comprises of majorly heavy non-volatile, light non-volatile, phenol, alkane and aromatics. During the hydrodeoxygenation process these

compounds are reacting with H_2 gas in the presence of catalyst and converted into the upgraded forms of bio-oil with varying mass fractions compared to the initial mass fractions. In other words, it can be explained as the amount of HNV present/ remained/ unconverted in the product phase denotes the small portion of HNV unconverted from the reactant phase. Similarly the same principle is applicable to the LNV, phenol; whereas for alkane and aromatics it denotes the amount formed/converted from the reactant species. The same terminology of present/ remained/ unconverted/ formed/ converted is applied.

Figure 5.13 to Figure 5.15 shows the contours of mass fractions of individual species of all the three phases obtained after hydrotreating of bio-oil for different catalysts. The legends (colored bars) present on the left hand side denotes range of the product species present inside a mixture. Blue color at the bottom shows the initial value and the red denotes the higher end. From this color bar we can presume the amount of the dominant species in greater composition. The contours presented in this context are concerned to the specific temperature, pressure and WHSV values. All the contour images plotted are at steady state in which there is no further changes in the composition are observed. The numerical values of the plotted contours are presented in Tables 5.4 – 5.6 at subsequent sections. The higher concentration of heavy non-volatiles is seen in the case of Pt/Al_2O_3 catalyst (Figure 5.13) as compared to the other two catalysts (Figures 5.14 - 5.15). This means the conversion of the heavy non-volatiles in the case of Pt/Al_2O_3 catalyst is very low and higher in the case of $Co\text{-}Mo/Al_2O_3$ catalyst seen in Figure 5.15. On the other hand the formation of the phenol traces is very much higher in case of $Ni\text{-}Mo/Al_2O_3$ catalyst seen in Figure 5.14 comparatively with other two catalysts.

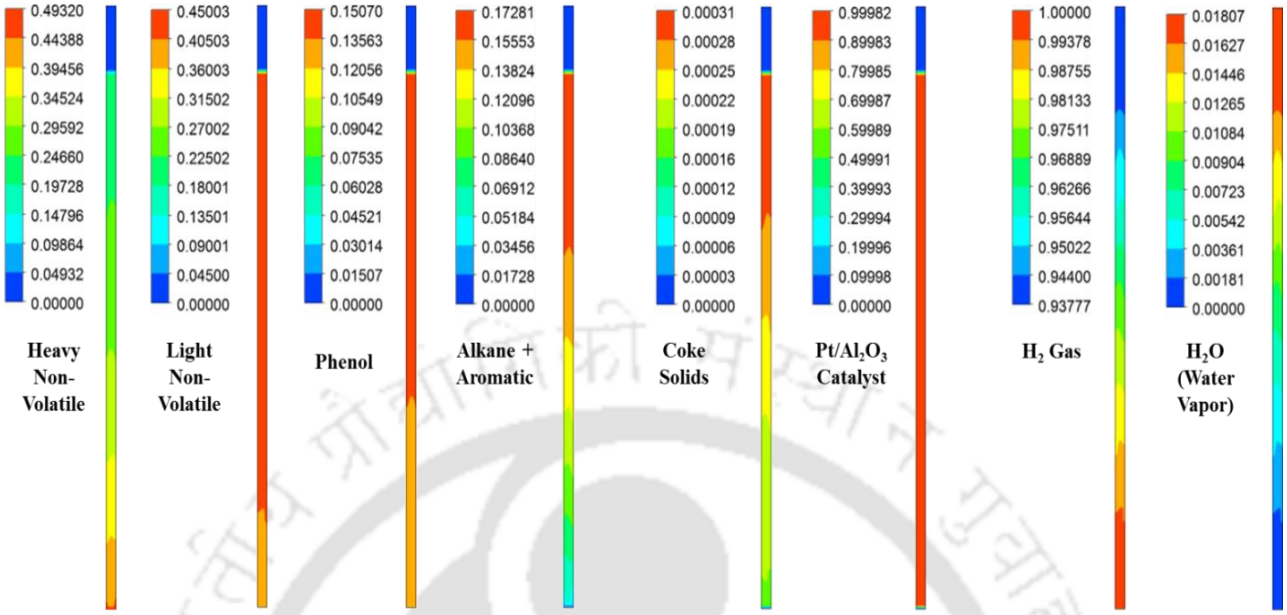

Figure 5.13: Steady mass fraction images of the lumped species of upgraded pyrolytic oil and those of solid and gas/vapor phases in the presence of Pt/Al_2O_3 catalyst at WHSV=$3h^{-1}$, temperature T=673 K and pressure P = 8720 kPa

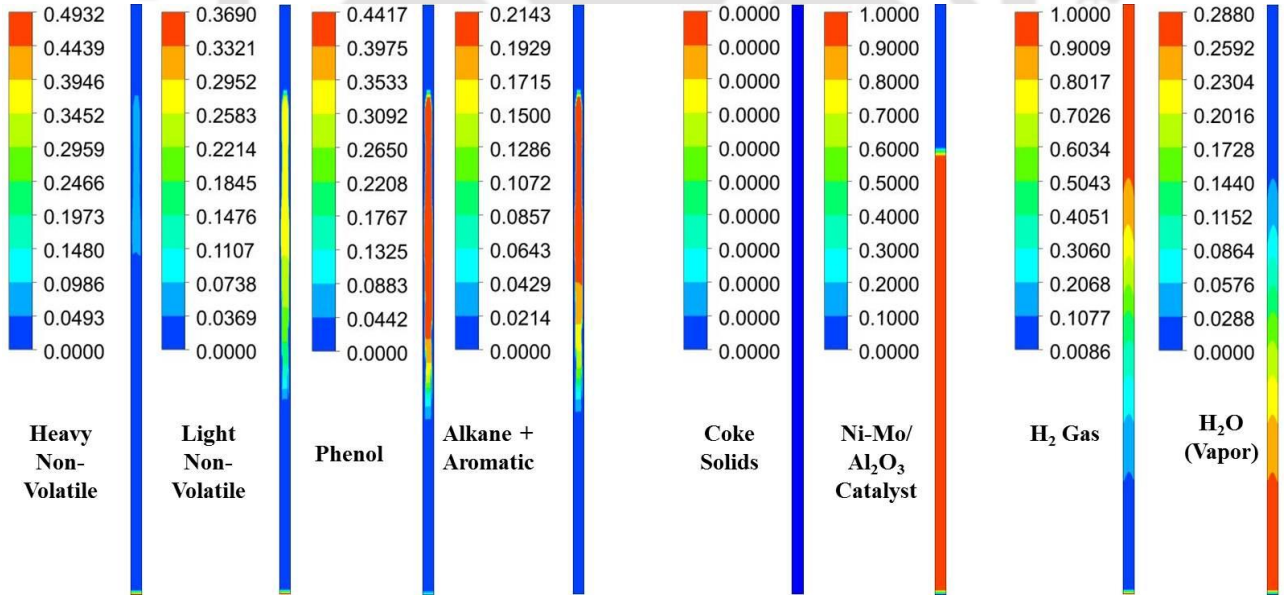

Figure 5.14: Steady mass fraction images of the lumped species of upgraded pyrolytic oil and those of solid and gas/vapor phases in the presence of $Ni\text{-}Mo/Al_2O_3$ catalyst at WHSV=$3h^{-1}$, Temperature T=673 K and pressure P = 8720 kPa

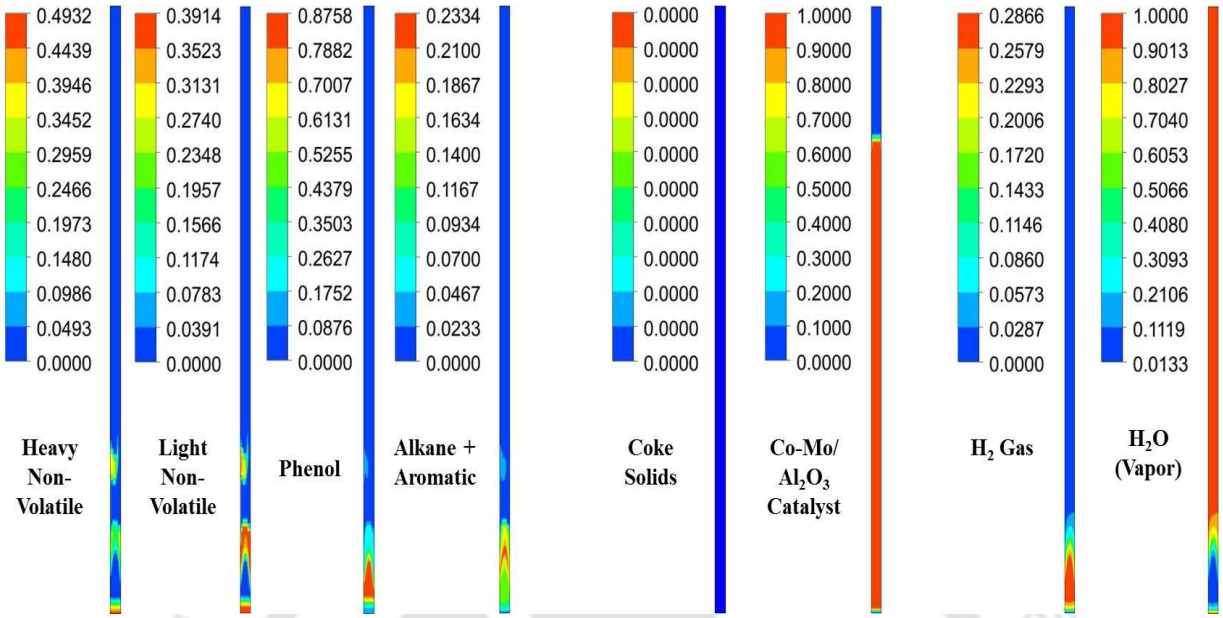

Figure 5.15: Steady mass fraction images of the lumped species of upgraded pyrolytic oil and those of solid and gas/vapor phases in the presence of Co-Mo/Al_2O_3 catalyst at WHSV=3h^{-1}, temperature T=673 K and pressure P = 8720 kPa

Finally from Figure 5.14 it is observed that the amount of alkane and aromatics formed from the reaction of the heavy non-volatiles and phenols are considered to be at higher end by use of Ni-Mo/Al_2O_3 catalyst in comparison to the other two catalysts.

5.3. Effect of Pt/Al_2O_3 catalyst on individual lumped species of bio-oil

5.3.1. Heavy Non-Volatile

Figure 5.16 specifies the percentage mass fraction of the heavy non-volatiles remained after the hydrotreatment of bio-oil in the presence of Pt/Al_2O_3 catalyst. The mass fraction values of HNV and LNV are calculated when the bed has reached a steady state, i.e., no significant variations are observed in the height of the bed and the composition of the fractions. The three different colored lines (blue, black, red) denote the variation of mass fractions of HNV at three different temperatures (higher, moderate and lower) varying with pressure which is same for the

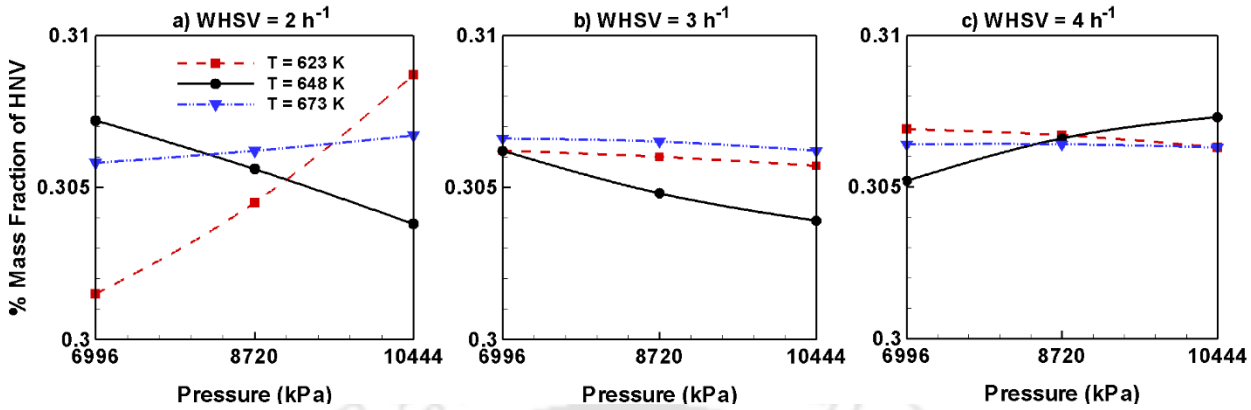

Figure 5.16: Mass fraction of HNV obtained by upgrading pine oil in the presence of Pt/Al_2O_3 catalyst.

other cases. Figure 5.16a portray the effect of temperature and pressure on the conversion of heavy non- volatile residue (a fractional compound of the bio-oil) by hydrotreatment at higher residence time WHSV=2 h^{-1}. From Figure 5.16a it is seen that the higher values of the mass fractions (the amount of unconverted HNV compound after the hydrotreatment of bio-oil) are slowly with the increasing pressure and reported a maximum value at higher pressure i.e., (P=10443 kPa, T=623 K). On the other hand the rise in temperature from T=623 K to 648 K the conversion of heavy non-volatile residues tends to minimize with the increasing pressure.

Further rising the temperature to T=673 K, the conversion of HNV has almost remains unaffected and hence reporting a minimal/negligible deviations with the rise in pressure. From this figure it is understood that at higher residence times the effects of temperature on the conversion of residues has a major role to play particularly at lower temperatures i.e., T=623 K. The heavy non-volatile formation which is observed in the present case is in line with the studies of Adjaye and Bhakshi (1995). The authors reported that the rise in pressure has a significant impact on the higher residence times and enables the phenol substitutes of heavy non-volatiles to undergo polymerization and condensation reaction. Figure 5.16b specifies the effects of

temperature and pressure for conversion of heavy residues of bio-oil at shorter residence times. It is noted that at lower pressure (P=6996 kPa) and lower temperature T=623 K, the mas fraction values are higher in comparison to the values at WHSV=2 h^{-1} as seen Figure 5.16a and similar values of mass fractions are reported for higher temperatures and slightly lower value for the moderate temperature curve. And also the mass fraction values of the residues are higher for all the three temperature curves and tend to decrease with the increasing pressure. This declining trend is significant in the case of moderate temperature (T=648 K); whereas, the trend is following a stable decrement in the case of lower and higher temperature curves. This stability for the lower and higher temperature curves is ascribed due to the reduction in polymerization and condensation reactions, i.e., the shortening of residence time enable reactants to quickly pass through the reactor. During this process there may be a possibility of unreacted species also present and hence the stable values are seen. However, the fluctuating patterns of moderate temperature curve are due to the formation of intermediate boiling fractions. Further shortening the residence time to 0.25 h, the stable patterns of lower and higher temperature curves are persistent; however the fluctuating and patterns of moderate temperatures is continued (seen in Figure 5.16c). In summary, it is observed that, lower values of HNV, i.e., higher conversions of non-volatile heavy residues is better obtained at lower values of WHSV =2 h^{-1}, lower pressure, and lower temperature; and conversion tends to decrease with the increasing WHSV, pressure and temperature in the presence of Pt/Al_2O_3 catalyst.

5.3.2. Light Non-Volatiles

The lighter non-volatile fractions are of very low molecular weighted residues than the heavy non-volatile residues. The name non-volatile signifies the tendency to resist the volatile nature (ready to evaporate) and hence it is very difficult to convert these non-

volatiles to desired fractions of bio-oil through catalytic hydrotreatment. Also non volatiles are heavier fractions which are unconverted while cracking of biomass to bio-oil. These heavier fractions comprises valuable product species needs to be processed through several techniques and convert the heavier residues to the value added products. Figure 5.17a shows the effect of temperature and pressure on the conversion of light non-volatiles at a constant WHSV =2 h^{-1}. The higher values of the LNV denote the lesser conversion and low values of LNV represents the higher conversion. Based on this fact the conversion is higher at higher pressures and lower temperature, and higher values for the moderate temperature curve while the higher temperature falls in between lower and moderate range of temperatures. The higher conversion of light residues with the increasing WHSV is reported at higher temperature (T=673 K) and higher pressure. On the other hand at moderate temperature the conversion seems to be very little; hence reporting the higher values of LNV.

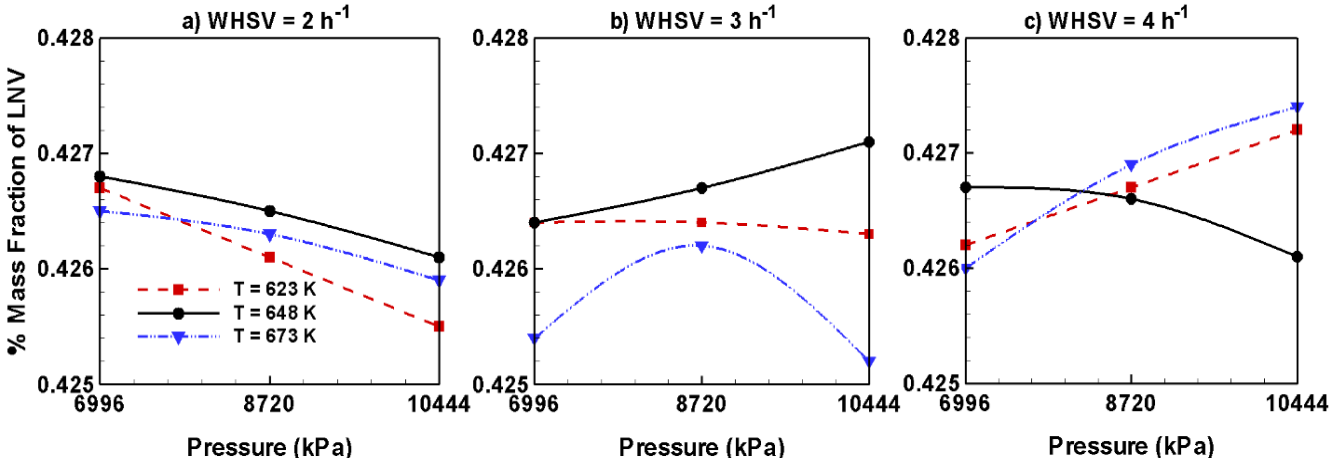

Figure 5.17: Mass fraction of LNV obtained by upgrading pine oil in the presence of Pt/Al_2O_3 catalyst.

In this case, the conversion of LNV tends to fluctuate in between lower and moderate temperature curves as seen in Figure 5.17b. However temperature favors at higher WHSV and lower temperature favors at lower values of LNV is reported at lower pressures with the increasing WHSV to $3h^{-1}$ as compared to WHSV = 2 h^{-1} from Figure 5.17a. Lastly, from Figure 5.17c the values of LNV in the case of lower and higher temperatures reported an increasing trend with the increasing pressure signifies that the conversion is decreasing while shortening the residence time. In other words, shortening the residence time forces the reactants to pass quickly through the reactor and hence suitable mixing with the other two phases is not possible. Thus the reaction is incomplete which signifies that the conversion of LNV is low. But, for the moderate temperatures the fluctuations still continues and reported a higher conversion at higher pressures. Thus, from this it is summarized that the moderate

5.3.3. Phenols

Figure 5.18 illustrates the percentage mass fraction of phenols produced through hydrodeoxygenation (HDO) of bio-oil in the presence of Pt/Al_2O_3 catalyst for the specified operating conditions. The variation in the phenol formations is very much slighter and negligible as the y-axis represents the variation of 0.001. Though the results are plotted in such a way to observe the minute variations with the operating parameters. Figure 5.18a unveil that the higher values of mass fractions are outlined at lower pressure subjected to moderate temperature T=648 K followed by higher temperature and lower temperature curves. At elevated pressures the lump of phenol formation showed a stable rising at low temperature with significant affect is seen for higher temperature. However the declining trend is seen for the moderate temperature T=648 K. Figure 5.18b renders the mass fraction of phenol at shorter residence time 0.33 h, at distinct

operating conditions of temperature and pressure. The deviations with respect to increasing pressure are different for different temperatures as seen clearly from Figure 5.18b.

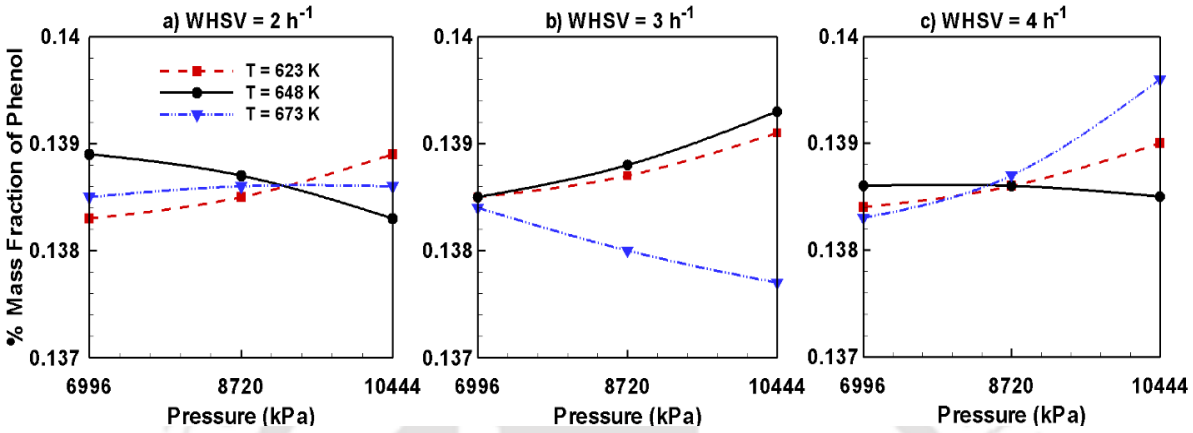

Figure 5.18: Mass fraction of phenols obtained by upgrading pine oil in the presence of Pt/Al_2O_3 catalyst.

A stable increasing pattern is seen for the lower temperature and increasing pressure is continued analogous to Figure 5.18a followed by moderate temperature curve T=648 K. At the same time a drop off is observed for high temperature T=673 K with the rising pressure. Moreover, the conversion of phenols or formation of phenols pageant is immense in the case of higher temperatures and small for the low and moderate temperatures (higher values of phenols means the conversion rate is low or the unspent phenols in the reaction) in lieu of Figure 5.18a. By reducing the reaction time of the reactant species inside a reactor i.e., WHSV=4 h^{-1}, the mass fraction of the phenol product species formed or remained in the reactor after the HDO of bio-oil were presented in Figure 5.18c and the detailed analyses is presented herein. At higher values of pressure the mass fraction of phenol is high which means that the phenol formation or phenols present in the reactor is higher. In other words, the conversion of the lighter non-volatiles to phenols is favored by the higher pressures and shorter residence times. Here also, we can see that

the low temperature curve is steadily rising with respect to pressure which is similar to that of Figures 5.18a, and 5.18b. While the moderate temperature curve reaches the steady state with the increasing pressure but the values are lower in comparison to the lower temperature curve. Finally, the higher temperature curve is pointing an increasing trend which has no comparison with Figure 5.18b and reported a higher value of phenol mass fraction at higher pressure. Though the reported changes are minimal which is almost insignificant/constant, are due to the fact that the oxygen attached to aromatic rings are stronger than the oxygen attached to aliphatic carbons implies the greater bond strength of hindered oxygen in phenolic compounds to resist the HDO conditions. Thus the aromatic carbon containing oxygen is to be converted to aliphatic carbon

Table 5.4. % Mass fractions of product species with respect to different operating conditions in the presence of Pt/Al_2O_3 catalyst

Species	*WHSV=2h^{-1}*			*WHSV=3h^{-1}*			*WHSV=4h^{-1}*		
				P = 6996kPa					
	T=623K	*T=648K*	*T=673K*	*T=623K*	*T=648K*	*T=673K*	*T=623K*	*T=648K*	*T=673K*
HNV	0.3015	0.3072	0.3058	0.3062	0.3062	0.3066	0.3069	0.3052	0.3064
LNV	0.4267	0.4268	0.4265	0.4264	0.4264	0.4254	0.4262	0.4267	0.4260
Phenol	0.1383	0.1389	0.1385	0.1385	0.1385	0.1384	0.1384	0.1386	0.1383
Alkane+ Aromaticc	0.1299	0.1293	0.1289	0.1287	0.1287	0.1285	0.1283	0.1292	0.1278
				P = 8720kPa					
HNV	0.3045	0.3056	0.3062	0.3060	0.3048	0.3065	0.3067	0.3066	0.3064
LNV	0.4261	0.4265	0.4263	0.4264	0.4267	0.4162	0.4267	0.4266	0.4269
Phenol	0.1385	0.1387	0.1386	0.1387	0.1388	0.1380	0.1386	0.1386	0.1387
Alkane+ Aromatic	0.1291	0.1290	0.1287	0.1288	0.1294	0.1280	0.1283	0.1281	0.1286
				P =10443kPa					
HNV	0.3087	0.3038	0.3067	0.3057	0.3039	0.3062	0.3063	0.3073	0.3063
LNV	0.4255	0.4261	0.4259	0.4263	0.4271	0.4052	0.4272	0.4261	0.4274
Phenol	0.1389	0.1383	0.1386	0.1391	0.1393	0.1377	0.1390	0.1385	0.1396
Alkane+ Aromatic	0.1284	0.1286	0.1283	0.1292	0.1301	0.1272	0.1286	0.1272	0.1295

with oxygen bond will enhance the oxygen elimination/deoxygenation. Then H_2 gas pressure through HDO process has a crucial role to play in breaking the phenol compounds to desired alkane and aromatics. Hence, the values are showing a negligible deviation irrespective of the temperature, pressure and residence times, and type of catalyst.

5.3.4. Alkane and Aromatics

Figure 5.19 signifies the alkane and aromatic mass fraction in upgraded bio-oil through catalytic hydrotreatment using Pt/Al_2O_3 catalyst at varying operating conditions. The fluctuations reported in the mass fraction values of alkane and aromatics produced after the upgradation process is very minimal (in the order of 10^{-3}). The results are presented in such a way that the mass fraction of alkane and aromatics formed from the reaction of heavy non-volatiles and phenols with hydrogen in the presence of a catalyst Pt/Al_2O_3 at a specified reaction mechanism. At a constant WHSV =2 h^{-1} i.e., higher residence time and a constant pressure P=6996 kPa, the formation of alkane and aromatics is favored by lower temperature followed by moderate and higher temperatures. On the other side with the increasing pressure alkane and aromatic products tends to decrease gradually, and the decrement is high in the case of lower temperature followed by moderate and higher temperatures is clearly presented in Figure 5.19a. Moving horizontally i.e., increasing the WHSV to 3 h^{-1} (shortening the residence time), the erratic behavior of the temperature curves with the pressure is seen clearly in Figure 5.19b. The constant values of alkane and aromatic products are reported at lower pressure (P=6996 kPa) in the case of moderate and higher temperature curves; whereas the fall of alkane and aromatics product values are seen in the case of low temperature curve. Secondly, with the increasing pressure, the low temperature curve shows a stable trend; while the moderate and higher temperature curves deviates drastically. At higher pressure (P=10443 kPa), and moderate temperature curve yields

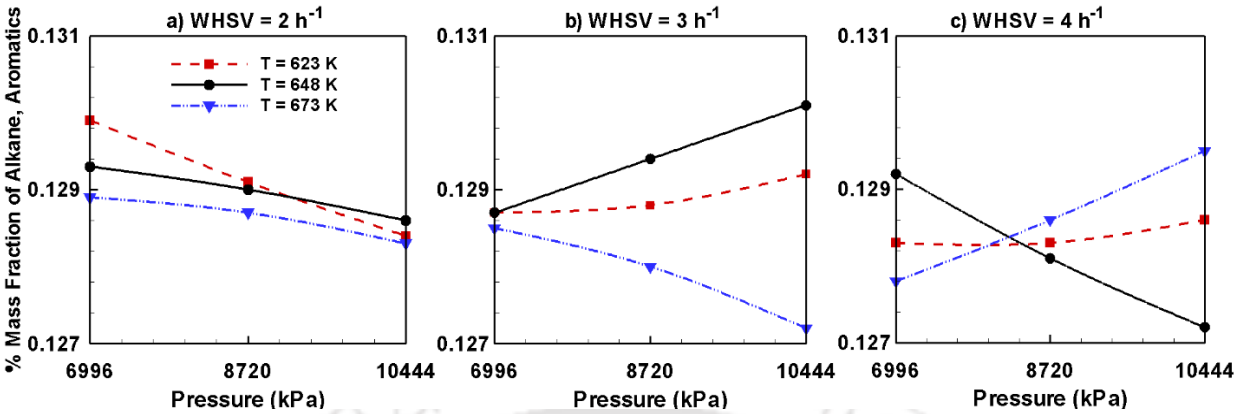

Figure 5.19: Mass fraction of alkane and aromatics obtained by upgrading pine oil in the presence of Pt/Al_2O_3 catalyst.

higher amount of alkane and aromatics while the yield is reduced significantly for the higher temperatures. There is no comparison of the alkane and aromatic product formation or remained after the hydrotreatment of bio-oil at higher pressures in comparison to Figure 5.19a. Finally at the shortest residence time 0.25 h (WHSV=4 h^{-1}) the mixed trend of alkane and aromatic product species formation with respect to temperature and pressure is continued and clearly seen in Figure 5.19c. The reduction in residence time resulted in the lower values of alkane and aromatics even at lower pressures (seen in Figure 5.19c) in comparison to Figure 5.19a, and Figure 5.19b. The moderate temperature reported higher yields of alkane and aromatics at lower pressures followed by lower and high temperature curves. The stable trend of the lower temperature curve tends to continue similar to that in Figure 5.19b shows that there is no effect of product formation at lower temperatures. However the reverse trend of moderate and higher temperature curves in comparison to Figure 5.19b is seen in Figure 5.19c i.e., the higher product values are seen at higher pressures in the case of higher temperature and lower values of products for moderate temperature.

These fluctuations in the product formation are majorly attributed due to the change in residence time. The increased residence time favors the reaction to complete and desired products are obtained; while the shorter residence times tend to incomplete reactions. Hence the suitability of the reaction conditions is very much important. For the specified reaction kinetics of the hydrotreatment of bio-oil in the presence of Pt/Al_2O_3 catalyst the lower temperature, lower pressure and longer residence time favors the higher yields of alkane and aromatics. This is due to the fact that as the pressure is increased the solubility is increased and also due to the higher residence time (lower WHSV=2 h^{-1}), the products (alkanes and aromatics) formed may undergo further reaction leads to the formation of secondary products. Similarly, with the increase in temperature the trend is similar in the declining mode and low values are reported at higher temperature due to the cracking of the formed products at higher temperatures i.e, at T=673 K.

5.4. Effect of Ni-Mo/Al_2O_3 catalyst on individual lumped species of bio-oil

5.4.1. Heavy Non-Volatile

Figure 5.20 illustrates the percentage mass fraction of the heavy non-volatile (HNV) residues with variable operating conditions in the presence of Ni-Mo/Al_2O_3 catalyst. The values of HNV reported in Table 5.5 gives an insight of conversion/left over residues (HNV) after the hydrotreatment of bio-oil. In other words, the amount of HNV converted by the hydrotreatment of bio-oil to the desired product species of alkane and aromatics according to the reaction mechanism specified in Figure 3.2. It is generally known that the heavy non-volatile (HNV) fractions are partially converted to various other fractions namely lighter fractions, phenols, alkanes and aromatics is due to the hydrotreatment process in the presence of a suitable catalyst. In the present study a gist on the hydrotreatment of bio-oil with a specified reaction mechanism

at specified operating conditions are presented in detail. Figure 5.20a portrays the conversion of heavy non-volatile fraction by the hydrotreatment of bio-oil at a very long residence time of 0.5 h i.e., (WHSV=2 h^{-1}). It is seen that the percentage mass fraction of HNV is higher at lower pressure, is higher in comparison to the higher pressures. The graph shows a linear change with respect to pressure in the case of T=623 K and T=673 K, but a mixed trend is observed in the case of T=648 K. The higher values of HNV with the increasing pressure and temperature is ascribed to the fact of coke formation with the temperature enhancement. The severity in the formation of coke by changing the temperature is as follows T=648 K > T=623 K > T=673 K. Shortening the residence time to 0.33 h (WHSV=3 h^{-1}), the similar trend of lower percentage of HNV are reported at lower pressures and tends to increase slightly with the increasing pressure. There are no major changes observed in the case of lower temperature curve T=623 K by changing the residence time; however, a significant increase in the values of HNV at higher temperature T=673 K and drastic downfall of HNV at moderate temperature T=648 K is clearly seen in Figure 5.20b in comparison to Figure 5.20a. Further shortening the residence time to 0.25 h (WHSV=4 h^{-1}), the reported mass fraction values of HNV are higher at lower pressures seen in Figure 5.20c and has no comparison with Figure 5.20a and Figure 5.20b. It is also noted that the conversion of HNV follows the similar patterns in the case of lower and moderate temperatures i.e., T=623 K, and T=648 K with a mixed trend and there is no change observed in the case of higher temperature T=673 K. The shortening of residence time forces the reactant to pass through the reactor quickly that implicates the shorter/incomplete reaction inside reaction inside the reactor resulting the higher values of HNV/lower conversion of heavy residues. As mentioned earlier that the lower values tends to higher conversion of HNV and higher values gives an insight of lower conversions.

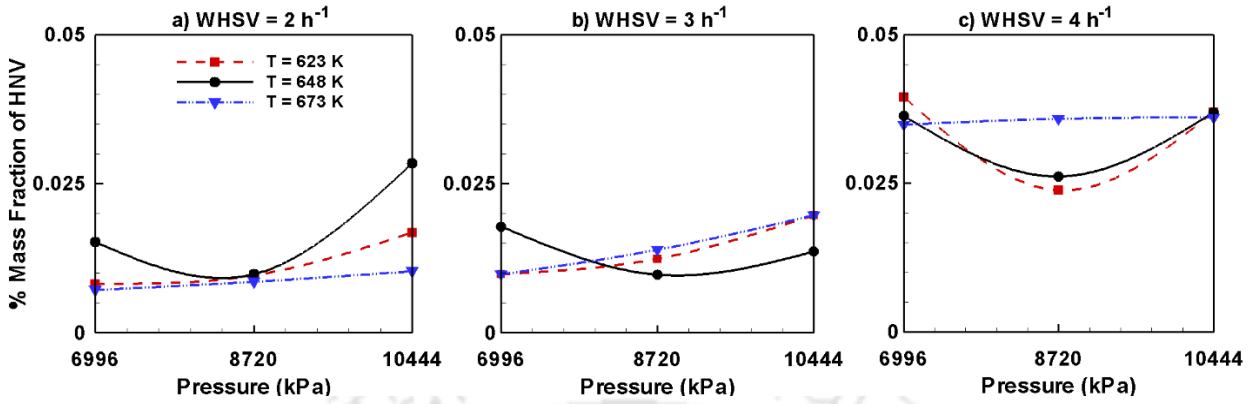

Figure 5.20: Mass fraction of HNV obtained by upgrading pine oil in the presence of Ni-Mo /Al_2O_3 catalyst.

Hence it is desired that the values should be as lower as possible in the case of non-volatile fractions in order to achieve higher mass fractions of desired product species. In summary, it is understood that lower residence times favors the higher conversions of heavy non-volatile fractions irrespective of the operating conditions in the presence of Ni-Mo/Al_2O_3 catalyst due to the higher activity of catalyst reported by Hart (2014).

5.4.2. Light Non-Volatile

Figure 5.21 presents a clear picture on the conversion of lighter residues/light non-volatiles with respect to residence time under trivial operating conditions of temperatures and pressures. This conversion of this category of non-volatile residues is also highly desirable for the higher yields of phenols which will be further reduced to alkane and aromatics. The change in the percentage mass fraction values of LNV at pertinent operating conditions are presented in Table 5.5. However, the changes are very marginal in the range of 10^{-2} with the change in temperature at low pressure. This trend seems to be increasing slightly where the conversion factor moves from 5×10^{-2} to 10^{-1} with the rise in

pressure and temperature. Hence lower values of percentage mass fraction of LNV denotes the higher conversion and higher values of LNV denote the lower conversion/unspent LNV reactant species. Initiating with higher residence time of 0.5 h (WHSV=2 h^{-1}), where the reactants are given sufficient time inside the reactor for contacting or the reaction to process the conversion seems to be the higher side at lower

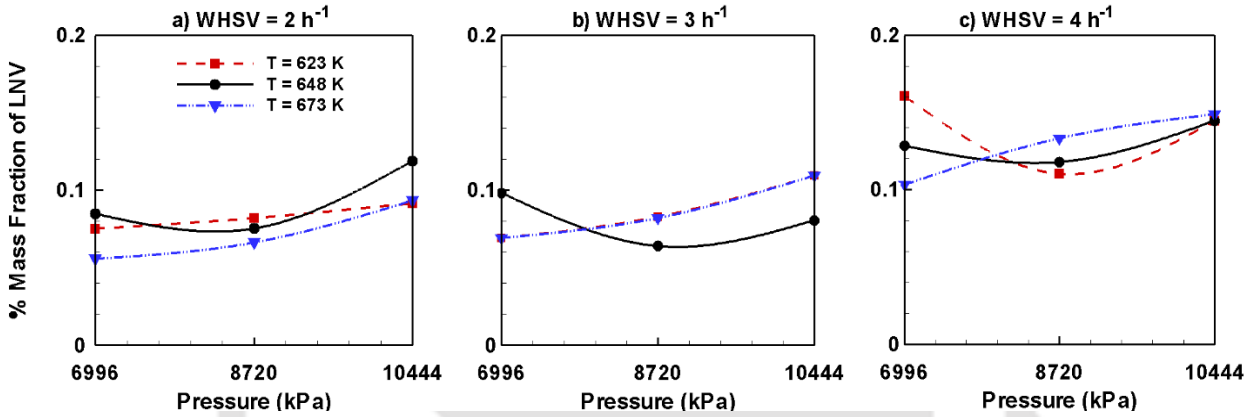

Figure 5.21: Mass fraction of LNV obtained by upgrading pine oil in the presence of Ni-Mo /Al_2O_3 catalyst.

pressures and higher temperatures from Figure 5.21a. These conversion rate tends to declining slowly with the increasing pressure represented an inclining temperature curves. This rising trends seems to be continued further deducting the residence time to 0.33 h in the case of lower and higher temperature curves seen in Figure 5.21b. The conversion tends to increase for the lower temperature T=623 K and WHSV=3 h^{-1} as in comparison with Figure 5.21a. Finally at higher WHSV values the conversion is very little and hence the values are very high in comparison to the Figure 5.21(a-b) seen from Figure 5.21c. From the comparative study it is noted that the conversion of lighter residues are favorable at lower WHSV, lower pressure and higher temperature.

5.4.3. Phenol

Figure 5.22 depicts the percentage mass fraction of the phenol species at various residence times in detail. Phenols are the major compounds used as a chemical solvent in the industries. The hindered oxygen in the phenol compound is having the greater resistance for the hydrotreatment process and hence the deoxygenation of the phenolic groups of bio-oil is very difficult. From Figure 5.22 it is clearly observed the variations in the mass fractions of phenols at different operating conditions are not highly influential. From Figure 5.22a it is clear that the mass fraction values of phenols are lower at lower pressures for all the operating temperatures. This can be presented in two ways that the conversion of phenols is higher at lower pressure and high residence time for the reaction or the amount of the phenol remaining after the conversion is low under the same operating conditions. It is also observed that the lower and moderate temperature

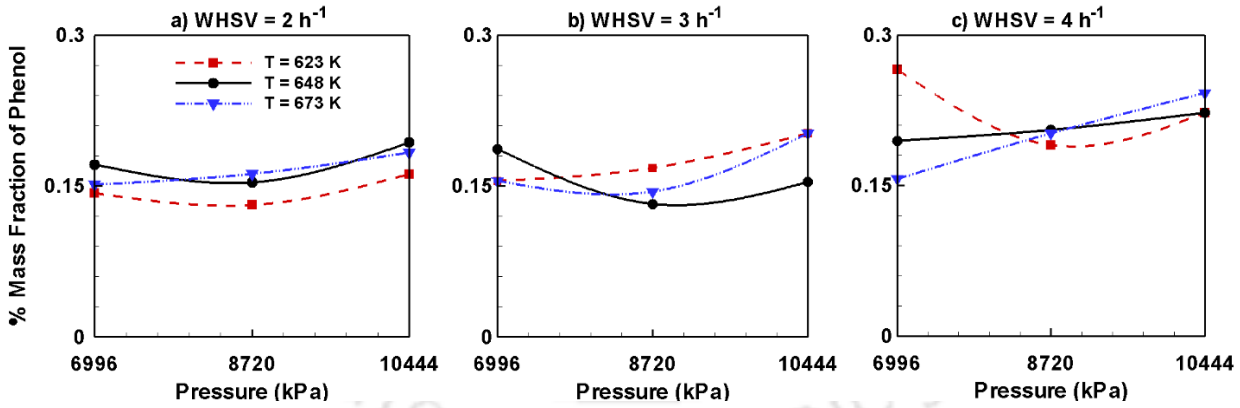

Figure 5.22: Mass fraction of phenols obtained by upgrading pine oil in the presence of Ni-Mo /Al_2O_3 catalyst.

curves shows a similar pattern of increasing trend while the higher temperature curve shows a stable incremental trend. The percentage mass fraction of the phenol at lower pressure is higher at moderate temperature followed by higher and lower temperatures. Reducing the residence time of the reaction the lower temperature curve shows a stable transformation with the pressure

(Figure 5.22b); while the moderate temperature curve still dominates the phenol formation at lower pressures and gradually decreases with increasing pressure and the higher temperature curve shows no deviation in comparison to Figure 5.22a. Finally at WHSV=4 h^{-1}, the attainment of stability is achieved by the moderate and higher temperature curves whereas the lower temperature curve reported the mixed trend of higher values initially and decreasing with respect to pressure. The mass fraction of the phenol is higher at higher temperature and higher pressure

Table 5.5: % Mass fractions of product species with respect to different operating conditions in the presence of (Ni-Mo/Al_2O_3) catalyst

Species	*WHSV=2h^{-1}*			*WHSV=3h^{-1}*			*WHSV=4h^{-1}*		
				P = 6996 kPa					
	T=623K	*T=648K*	*T=673K*	*T=623K*	*T=648K*	*T=673K*	*T=623K*	*T=648K*	*T=673K*
HNV	0.0082	0.0152	0.0714	0.0098	0.0178	0.0098	0.0395	0.0363	0.0348
LNV	0.0750	0.0847	0.0557	0.0691	0.0982	0.0691	0.1605	0.1282	0.1032
Phenol	0.1428	0.1713	0.1512	0.1549	0.1867	0.1550	0.1656	0.1944	0.1565
Alkane+ Aromatic	0.0543	0.0768	0.0555	0.0613	0.0815	0.0613	0.1228	0.0951	0.0768
				P = 8720 kPa					
HNV	0.0096	0.0098	0.0852	0.0124	0.0097	0.0139	0.0238	0.0261	0.0358
LNV	0.0819	0.0752	0.0662	0.0828	0.0638	0.0820	0.1102	0.1178	0.1332
Phenol	0.1310	0.1534	0.1619	0.1679	0.1320	0.1444	0.1902	0.2053	0.2020
Alkane+ Aromatic	0.0655	0.0663	0.0667	0.0706	0.05501	0.0723	0.0865	0.0929	0.0984
				P =10443 kPa					
HNV	0.0168	0.0284	0.1028	0.0197	0.0136	0.0197	0.0369	0.0369	0.0360
LNV	0.0915	0.1189	0.0933	0.1094	0.0806	0.1094	0.1446	0.1446	0.1487
Phenol	0.1617	0.1932	0.1831	0.2023	0.1539	0.2023	0.2224	0.2224	0.2422
Alkane+ Aromatic	0.0755	0.0907	0.0776	0.0892	0.0668	0.0892	0.1080	0.1081	0.1139

followed by moderate temperature curve and lower temperature curve seen in Figure 5.22c. The reasons ascribed for this changes in the mass fraction of phenols with respect to temperature, pressure, and residence time is due to the secondary reactions of HDO for phenol to form an intermediate range of boiling products. Here, residence times play a decisive role which determines the extent of the reactions. Higher residence times favors dealkylation and hydrogenation for the formation of aromatic products. So the mass fractions of phenols are reported to be at higher side in the case of Ni-Mo/Al_2O_3 catalyst and limiting the formation of alkane and aromatic products. The activity for the HDO of phenol is higher for the Ni-Mo/Al_2O_3 catalysts and hence the mass fraction of phenol formation is at higher end as compared to other catalysts.

5.4.4. Alkane and Aromatics

Figure 5.23 presents the percentage mass fraction of alkane and aromatics formed through the upgradation of bio-oil in the presence of Ni-Mo/Al_2O_3 catalyst at different operating conditions. The variable operating conditions along with the obtained values of mass fractions of alkane and aromatics are presented clearly in Table 5.5. The variations in the mass fraction values obtained are very marginal; however for a clear view the values are plotted in such a way that the minute variations are clearly projected. At constant WHSV=2 h^{-1}, the mass fraction values of alkane and aromatics are increasing in the case of lower (T=623 K) and higher (T=673 K) temperatures and mixed trend is observed in the case of intermediate temperature (T=648 K) depicted in Figure 5.23a. The lower values of alkane and aromatics are reported at lower pressures in the case of lower and higher temperatures while higher values are reported for moderate temperature curve. The formation of alkane and aromatics tends to increase with the

pressure and moderate temperature still dominate to produce more amount of alkane and aromatics as compared to the lower and higher temperatures. Progressing with the reduction of residence time to 0.3 h (WHSV=3 h^{-1}) the moderate temperature curves shows higher values of alkane and aromatics at lower pressure and tends to fall with the rising pressure. On the other hand the consistent increased formation of alkane and aromatic product species are seen in the case of lower and higher temperatures as shown in Figure 5.23b. Further decreasing the residence time to 0.25 h (WHSV=4 h^{-1}) the stable trend of higher temperature curve still continued while the moderate and lower temperature curves shows a slighter deviations; however irrespective of the temperature the alkane and aromatics formed at higher pressures are similar at higher WHSV values as seen in Figure 5.23c. The yield of alkane and aromatics is low at longer residence times (WHSV=2 h^{-1}) due to fragmentations of heavy non-volatiles via secondary and tertiary reactions resulting the formation of small fractions of liquids and gases. Further increasing the residence time enable the catalytic deactivation due to the formation of higher molecular weight compounds, and also the water formed during reaction also serve as a weak inhibitor of hydrodeoxygenation.

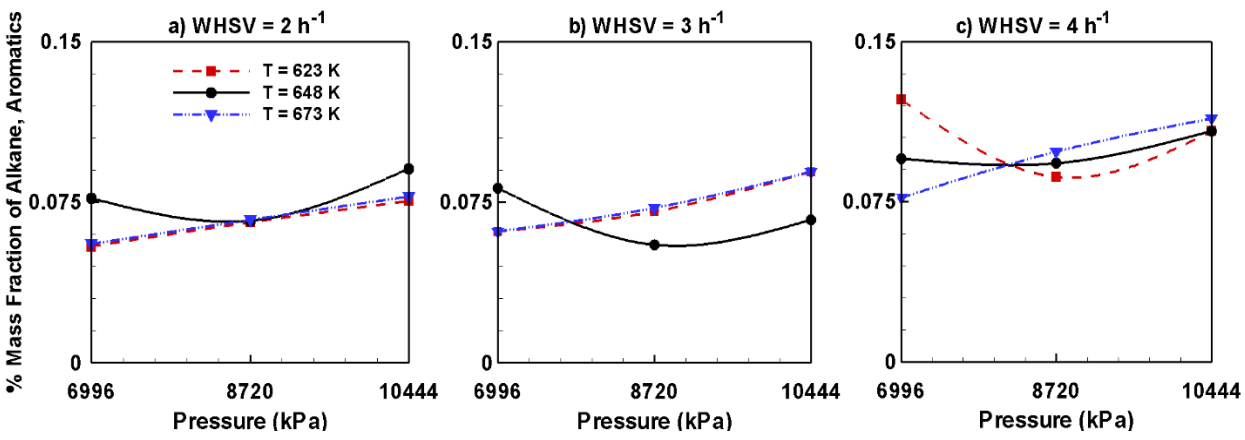

Figure 5.23: Mass fraction of alkane and aromatics obtained by upgrading pine oil in the presence of Ni-Mo /Al_2O_3 catalyst.

Hence shorter residence times (WHSV=4 h^{-1}) favor the higher yield of alkanes and aromatics for the specified catalyst for both lower and higher temperatures. Secondly, the stability in the case of moderate temperatures (T=648 K) is achieved due to partial loss of oxygen groups from aliphatic and aromatic oxygen containing compounds, reduces their ability to polymerize at higher temperatures. It is concluded that irrespective of the temperature, the increasing trend of alkane and aromatics formations continues with the pressure and higher yields are obtained for shorter residence times and higher pressures in the presence of Ni-Mo/Al_2O_3 catalyst for the reaction mechanism considered.

5.5. Effect of Co-Mo/Al_2O_3 catalyst on individual lumped species of bio-oil

5.5.1. Heavy non-volatiles

Figure 5.24 displays percentage of heavy non volatiles (remained or unconverted) via catalytic hydrodeoxygenation process in the presence of Co-Mo/Al_2O_3 catalyst at varying residence time, temperature, and pressure. From Figure 5.24a it is clearly seen that the mass percentage of the heavy non-volatile residue (HNV) is gradually declining with the increasing pressure. This attributes to the higher conversion of heavy residues in the presence of Co-Mo/Al_2O_3 at higher residence time 0.5 h and higher pressure P=10443 kPa, represents the higher catalytic activity at lower temperature and marginal deviations for moderate and higher temperature curves seen in Figure 5.24a. With the increase in WHSV to 3 h^{-1} the conversion of residues tends to increase with respect to increasing pressure and reported a maximum value at higher pressure and higher temperature as seen in Figure 5.24 b similar to that of Figure 5.24 a and the conversion tends to decrease with decreasing temperature. Further shortening the

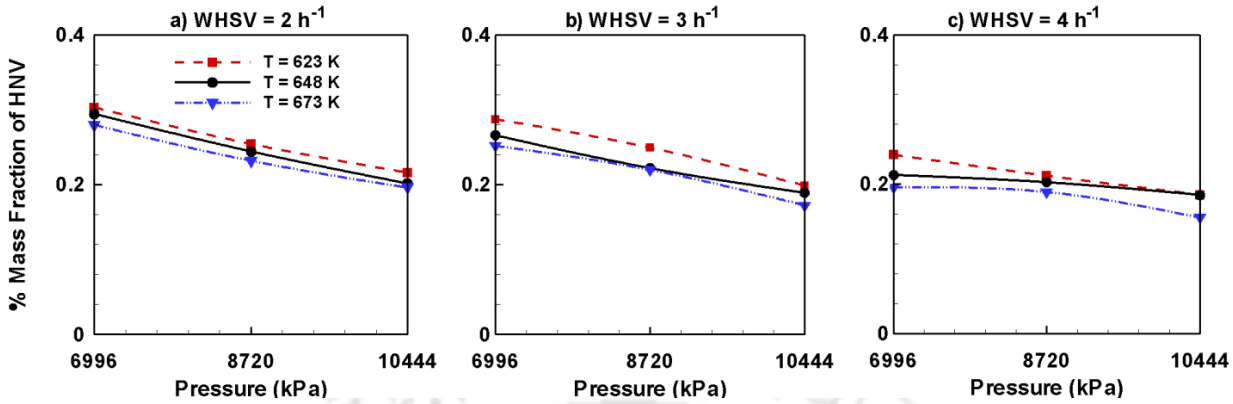

Figure 5.24: Mass fraction of HNV obtained by upgrading pine oil in the presence of Co-Mo /Al_2O_3 catalyst.

residence time to 0.25 h the reported mass fraction of heavy non-volatiles is continued to decline with the increasing pressure and lower temperatures at as seen in Figure 5.24 c. The higher conversion of the residues is seen at higher pressure and lower temperatures in line to that of Figure 5.24a and Figure 5.24b. The fact ascribed for the higher conversions at higher pressures is the increased solubility of the H_2 gas with the bio-oil on the catalyst surface is increased. Thus the vicinity of the gas on the catalyst particles is enhanced due to higher pressures shows higher conversion. Further, the higher activity of the catalyst is also prominent factor in higher product formation i.e., alkane and aromatic (by the conversion of HNV) leads to prevent the unwanted secondary reaction causing the coke formation. Furthermore, H_2 gas is effectively decreasing the carbon formation of the catalyst surface by converting carbon precursors into stable molecules by saturating adsorbed species like alkanes given by Richardson et al. (1995) and Furimsky (1999). Thus from the Figure 5.24 it is observed that the activity of the catalyst in converting heavy non-volatile residues is favorable at shorter residence times, higher pressures and higher temperatures.

5.5.2. Light non-volatiles

In the presence of Co-Mo/Al_2O_3 catalyst, the conversion of lighter non-volatile compounds after the upgradation of bio-oil is presented in details in Figure 5.25 at variable operating conditions. The conversion of lighter non-volatiles at longer residence time WHSV=2 h^{-1} with respect to temperature and pressure is seen in Figure 5.25 a. It is observed that the values tends to be reported at the higher side in the case of low pressure and decreases with the increasing pressure. The variation is significant such that solubility in terms of pressure is the major reason for the decreasing values of LNV. The higher values of conversion i.e., lower LNV is reported in the case of higher temperature and higher LNV values (low conversion comparatively) in the case of low temperature. Figure 5.25b shows the similar trends to higher values of LNV at low pressure and lower values of LNV at higher pressure. The temperature effects are similar with respect to Figure 5.25a. However, the values reported in Figure 5.25b are slightly lesser in comparison to Figure 5.25a. Finally from Figure 5.25c the same declining trend of LNV with respect to temperature is followed in line with Figures 5.25a, and 5.25b.

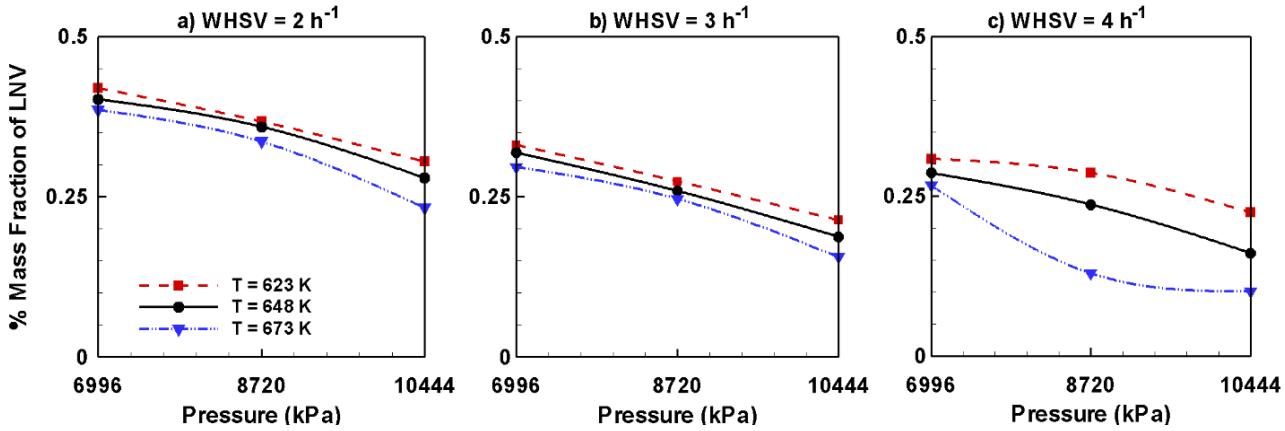

Figure 5.25: Mass fraction of LNV obtained by upgrading pine oil in the presence of Co-Mo/Al_2O_3 catalyst

products and the catalytic activity is maintained properly. In other words, the deposition of coke due to the secondary reactions is avoided for the shorter residence times and hence the activity is improved and maintained constantly. In conclusion, it is understood that higher values of WHSV at higher pressures and higher temperatures favors the higher conversion of lighter residues to desired products in the presence of Co-Mo/Al_2O_3.

5.5.3. Phenols

Figure 5.26 illustrates the formation of phenols through hydrodeoxygenation of LNV species of unprocessed bio-oil at different operating conditions. It is seen from the Figure 5.26 that the variations are very marginal with respect to the pertinent conditions. This means that the conversion percentage of the light non-volatiles (LNV) to phenols are very meager and the formed phenols which are turned into alkane and aromatics immediately; however the percentage conversion of alkane and aromatics product species through LNV is very less in comparison to the conversion from heavy non-volatiles (HNV). The incremental trend of the product mass fraction of phenol is the resultant of the percentage conversion of light non-volatiles or the amount of the phenol percentage present in the upgraded bio-oil during the catalytic hydrotreatment of bio-oil in the presence of Co-Mo/Al_2O_3 catalyst. The mass fraction of the phenol formation shows a consistent increasing trend with the increasing pressure for moderate and higher temperature zones; whereas, the lower temperature curve follows a steady rising trend at lower WHSV =2 h^{-1} seen in Figure 5.26 a. Augmenting the residence time to 0.33h, the elevated values of phenols with respect to temperature and pressures are clearly observed in Figure 5.26b. The values at lower pressure in this case is slightly lower in comparison to Figure 5.26a and reporting higher values as the pressure reaches the maximum value of

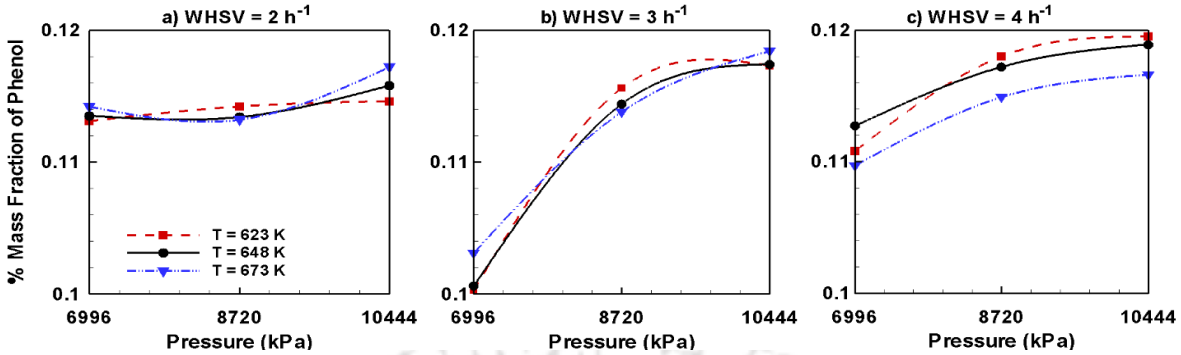

Figure 5.26: Mass fraction of phenols obtained by upgrading pine oil in the presence of Co-Mo/Al_2O_3 catalyst

P=10443 kPa. Finally, the marginal rising trends of phenol formation with respect to temperature and pressure are observed at higher values of WHSV=4 h^{-1} in Figure 5.26c in comparison to the mass fraction of phenols at lower WHSV values as reported in Figures 5.26a, and 5.26b. From the Figure 5.26 it is seen that the variations are very marginal denoting that the activity of the catalyst has a no role to play here. However, from the published literature it is fact that phenols are the most resistant compounds for the HDO reactions. This attributes to dealkylation and demethylation reactions that is dominant over the catalyst activity. Thus the bond strength between C-O in phenolic groups is very high, so that breakage of such bonds using the Co-Mo/Al_2O_3 catalyst with the specified reaction mechanism is a very critical step. Thus the present reaction kinetics used in the present simulation studies is showing a very little effect of the formation of phenol compounds or the conversion of LNV. The notable effect on the formation of phenols is higher at lower temperatures and higher pressures. The numerical values of the percentage change in the mass fraction of the phenols along with other lumped species at different operating conditions are presented in Table 5.6.

5.5.4. Alkane and aromatics

Figure 5.27 presents the percentage mass fraction of alkane and aromatics formed through the upgradation of bio-oil at various operating conditions in the presence of Co-Mo/Al_2O_3 catalyst. From the Figure it is observed that the mass fraction values tend to increase with respect to temperature, pressure, and WHSV values. Figure 5.27a, it is seen that the mass fraction of alkane and aromatics are continuously increasing and reported higher values at higher temperature (T=673 K) with respect to pressure. From Figure 5.27b it is noticed that the mass fraction values are higher even at lower pressures as compared to Figure 5.27a, and tends to incline with the operating pressure and temperature. Figure 3c reported similar trends with even higher values at lower pressures and tends to bounce rapidly with increasing temperature and pressure. The values are very much higher as compared to Figures 5.27a, and 5.27b. The increase in the alkane and aromatic formation is majorly attributed to the higher activity of catalyst which promotes the O-methyl bond breakage inhibited by ammonia but not by water or hydrogen sulfide (intermediate products) reported by Laurent and Delmon, (1994). The alumina support

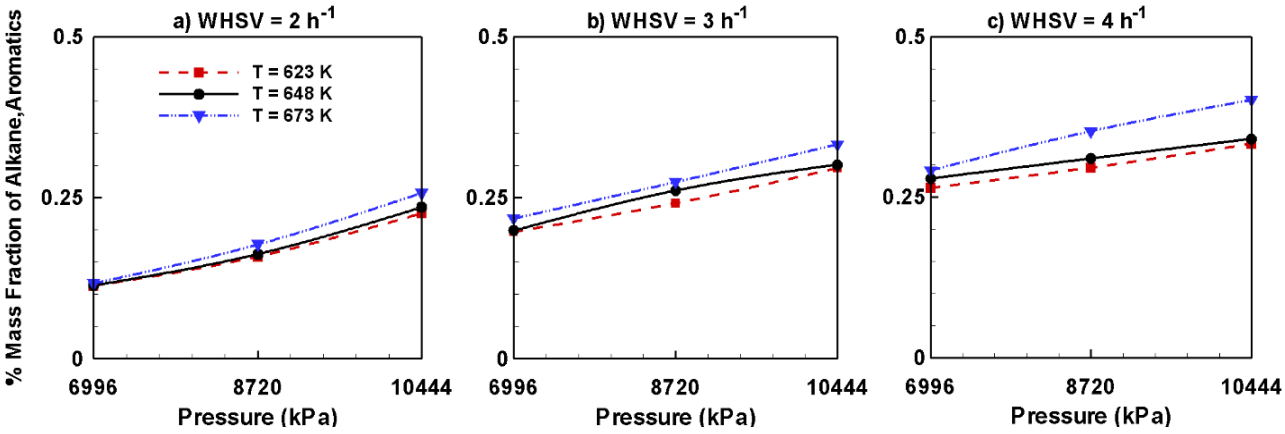

Figure 5.27: Mass fraction of alkane and aromatics obtained by upgrading pine oil in the presence of Co-Mo/Al_2O_3 catalyst

also has a role in the HDO process and is majorly depend on the acid sites available. However the sulfide phase also plays a major role in catalytic activity through the acidity of –SH groups. Co-Mo catalysts are capable of deoxygenating without hydrogenation of aromatic rings leads to higher hydrocarbon yields as compared to other catalysts due to the higher activity of the catalyst at higher pressures, and higher temperatures in the presence of hydrogen reported by Sharma and Bhakshi (1993) and Roy (2012). Also, the conversion of residues (non-volatiles) tends to decrease continuously with the increasing temperature and pressure and hence the higher compositions of alkane and aromatics are seen using Co-Mo/Al_2O_3 catalyst.

Table 5.6. % Mass fractions of product species with respect to different operating conditions in the presence of (Co-Mo/Al_2O_3) catalyst.

Species	*WHSV=2h^{-1}*			*WHSV=3h^{-1}*			*WHSV=4h^{-1}*		
				P = 6996kPa					
	T=623K	*T=648K*	*T=673K*	*T=623K*	*T=648K*	*T=673K*	*T=623K*	*T=648K*	*T=673K*
HNV	0.3029	0.2942	0.2795	0.2871	0.2656	0.2515	0.2391	0.2121	0.1958
LNV	0.4191	0.4017	0.3852	0.3306	0.3185	0.2963	0.3083	0.2862	0.2667
Phenol	0.1131	0.1135	0.1142	0.1003	0.1016	0.1031	0.1108	0.1127	0.1097
Alkane+ Aromatic	0.1129	0.1136	0.1167	0.1969	0.1987	0.2174	0.2642	0.2788	0.2915
				P = 8720kPa					
HNV	0.2541	0.2442	0.2316	0.2491	0.2218	0.2195	0.2111	0.2023	0.1892
LNV	0.3672	0.3589	0.3358	0.2739	0.2589	0.2465	0.2866	0.2369	0.1294
Phenol	0.1142	0.1134	0.1132	0.1156	0.1144	0.1138	0.1180	0.1172	0.1149
Alkane+ Aromatic	0.1585	0.1623	0.1772	0.2413	0.2610	0.2741	0.2958	0.3101	0.3526
				P =10443kPa					
HNV	0.2158	0.2013	0.1959	0.1985	0.1888	0.1722	0.1856	0.1854	0.1551
LNV	0.3045	0.2792	0.2325	0.2134	0.1876	0.1558	0.2245	0.1610	0.1005
Phenol	0.1146	0.1158	0.1172	0.1173	0.1174	0.1184	0.1195	0.1189	0.1166
Alkane+ Aromatic	0.2257	0.2351	0.2573	0.2958	0.3012	0.3325	0.3328	0.3407	0.4013

The detailed numerical values of the mass fraction changes with respect to variable operating conditions are presented in Table 5.6.

5.6. Yield of alkane and aromatics at different residence times

During the catalytic hydrotreatment process of upgradation of bio-oil the yield of aromatics are considered to be the prominent compound in order to improve/produce higher amounts of aromatic hydrocarbons. The presence of higher aromatic compounds improves the octane number, more compressing a fuel can withstand before igniting. The fuels with higher octane number are used in gasoline engines which requires higher compression ratio. The oxygen content of bio-oil is removed as water, CO, and CO_2 due to the presence of alkane aromatics and substantially reduces the weight percentage before hydrotreatment of bio-oil. Thus the aromatics have a higher heating value than the typical bio-oil because of their reduced oxygen content.

However the presence of aromatics increases the density and viscosity of the bio-oil; the strong interaction between C=C bonds and aromatic rings from oxy-compounds with active sites on the catalyst surface lead to the formation of carbon instead of hydrocarbon fuel and hence desired and optimal conditions are to be maintained to avoid ageing, coking effects of the bio-oil. Aromatic character of the upgraded bio-oils, unsaturated aromatics has a higher octane number value comparing with the saturated cyclic hydrocarbons (Elliott 2007). Therefore the presence of aliphatic and aromatic hydrocarbons enhances the quality of liquid bio-fuel (Aho et al., 2008; Antonakou et al., 2006; Triantafyllidis et al., 2007; Williams and Nugranad, 2000; Zhang et al., 2009). Figure 5.28 to Figure 5.30 denotes the yield of alkane and aromatics through the conversion of the heavy non-volatile residues and the phenolic fractions of the bio-oil as per the reaction mechanism of the present simulation studies reported in Chapter 3. The yield of alkane

$$Yield = \frac{Amount\ of\ alkane\ and\ aromatics\ formed}{initial\ input\ of\ (Mass\ of\ heavy\ non-volatiles + mass\ of\ phenols)}$$

and aromatics from the bio-oil is calculated by the following expression. The major contribution of alkane and aromatics production is through the conversion of heavy non-volatiles whereas phenols are converted very little to the desired alkane and aromatics as per the reaction mechanism considered in the present simulation study (See Figure 3.2).

Figure 5.28 compares the yield of alkane and aromatic from the heavy non-volatile residue and phenol fractions of bio-oil at longer residence time 2 h^{-1} at different operating temperatures, and pressures in the presence of three different catalysts namely (Pt/Al_2O_3, Ni-Mo/Al_2O_3, Co-Mo/Al_2O_3). At a fixed temperature of T=623 K and at higher pressures P=10443 kPa, the yield of alkane and aromatic with respect to catalyst activity is in the following order as Co-Mo/Al_2O_3 > Pt/Al_2O_3 > Ni-Mo/Al_2O_3; however, Pt/Al_2O_3 catalyst exhibit higher yields of alkane and aromatics at lower pressures for a fixed range of temperature. Similarly with the increasing temperature and constant low pressure (P=6996 kPa) Pt/Al_2O_3 yields higher values of alkane and aromatics as compared to other catalysts. It is also observed that the yields of alkane and aromatics in the presence of Ni-Mo/Al_2O_3 catalysts tends to increase gradually with the increasing pressure, but higher values are reported for the moderate range of temperatures T=648 K. In the case of Co-Mo/Al_2O_3 catalyst the values are consistently showing an increasing trend with respect to temperature, and pressure as compared to other two catalysts reporting the higher activity irrespective of the operating conditions. time WHSV=3h^{-1} in the presence of different catalysts at various operating conditions. It is observed from the figure that the formation of alkane and aromatic from the reactants (HNV, Phenol) is almost unchanged with respect to operating conditions in the case of Pt/Al_2O_3; however minute fluctuations are seen in the case of Ni-Mo/Al_2O_3 catalyst whereas Co-Mo/Al_2O_3 catalyst possess an increasing trend with the increasing pressure.

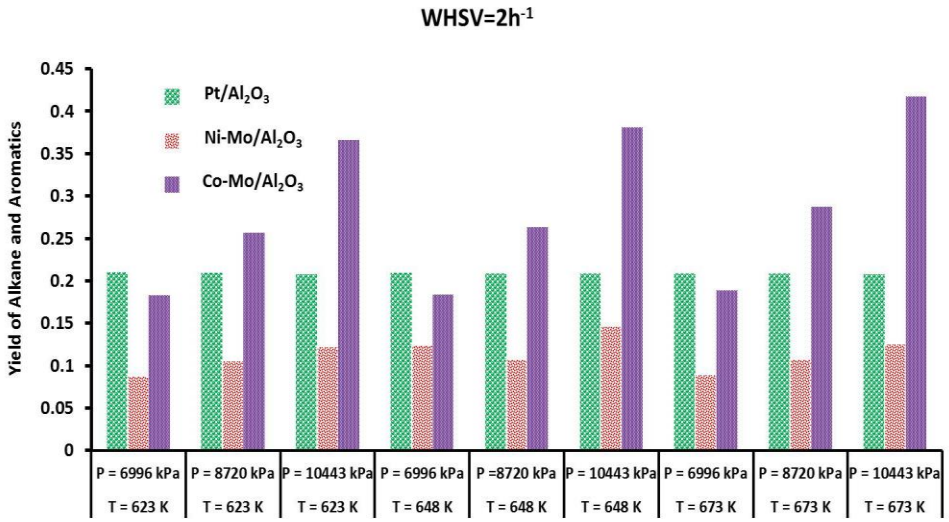

Figure 5.28: Yield of alkane and aromatic at WHSV=2 $h^{-1}$for different operating conditions

Figure 5.29 elucidate the yield of alkane and aromatic formation at moderate residence conditions in the case of Pt/Al_2O_3; however minute fluctuations are seen in the case of Ni-Mo/Al_2O_3 catalyst whereas Co-Mo/Al_2O_3 catalyst possess an increasing trend with the increasing pressure. As the residence time is reduced the formation of alkane and aromatics is significant in the case of Co-Mo/Al_2O_3 due to effect of the hydrogen pressure and higher temperatures reducing the coke formation tendency and converting the reactants to value added products. The overall yield of the alkane and aromatics has been increased from 45% to 50% with reducing residence time. Further shortening the residence time to 4 h^{-1} the product formation is still enhanced to 60% in the case of Co-Mo/Al_2O_3, followed by Pt/Al_2O_3 and Ni-Mo/Al_2O_3 catalysts.The lower residence times avoids the secondary reactions and also the formation of the secondary products. The secondary products are formed due to the prolonged reactions at such a high temperatures and pressures further leads to the blockage of acid sites of the catalysts or deactivations of the catalysts. On the other hand, Ni-Mo/Al_2O_3 catalyst tends to be more reactive at shorter residence times and hence the yield of alkane and aromatics is almost equal to the yield

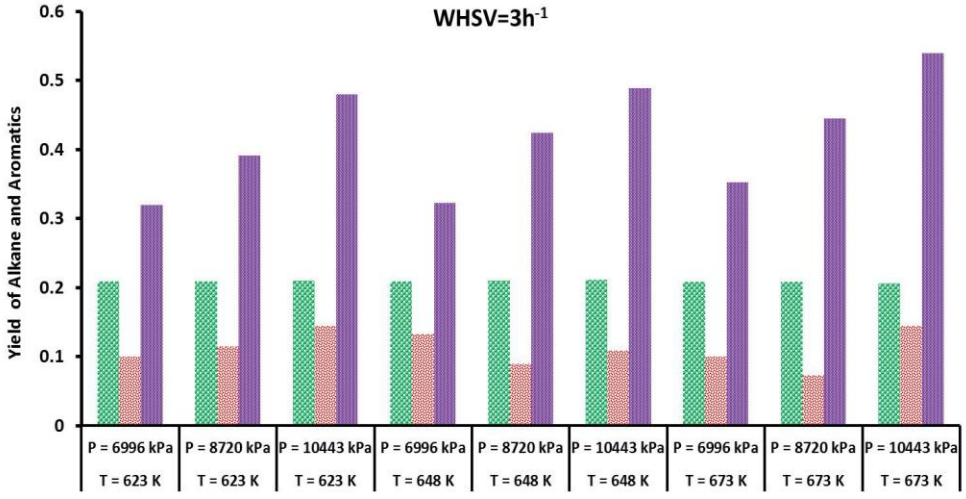

Figure 5.29: Yield of alkane and aromatic at WHSV=3 $h^{-1}$for different operating conditions

of alkane and aromatics through Pt/Al_2O_3 catalyst at P=6996 kPa and T=623 K as seen in Figure 5.30. Higher yields of alkane and aromatic via $Ni\text{-}Mo/Al_2O_3$ catalyst are possible with the lower pressures, lower temperatures and lower residence times. Pt/Al_2O_3 catalyst again follows the similar trend of constant yield of 20% alkane and aromatics at shorter residence time.

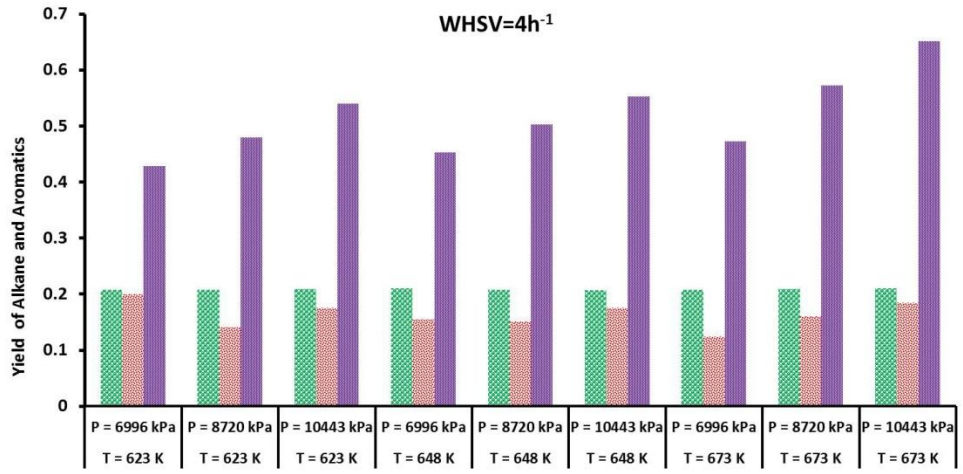

Figure 5.30: Yield of alkane and aromatic at WHSV=4 $h^{-1}$for different operating conditions

Conclusions Chapter-6

The effect of catalysts on the hydrodeoxygenation of bio-oil in an ebullated bed reactor is studied through CFD simulations. The aim was to identify the effects of temperature, pressure, and catalyst loading on the hydrodynamics of the process and to incorporate the chemical reaction kinetics in a numerical solver. Some of the key conclusions are given below.

6.1. Effect of catalyst load

The volume fraction contours of the three phases (bio-oil, H_2 gas and solid catalyst phases) varying with the catalyst load i.e., WHSV is presented in detail. The attainment of the steady state of catalyst bed is observed at t=80 sec for all the three catalysts namely Pt/Al_2O_3, Ni-Mo/Al_2O_3, and Co-Mo/Al_2O_3 catalysts.

For Pt/Al_2O_3, catalyst, it is observed that the increasing values of WHSV do not show any impact on the volume fraction of the catalyst phase irrespective of temperature and pressure. Similarly, the H_2 gas phase also reported the constant trend i.e., without much deviation with the increasing values of WHSV at all operating conditions. But, the fluctuations in the bio-oil phase is noted at the initial level i.e., at lower values of WHSV=2 h^{-1} and higher temperature and becomes linear for all the values of temperature and pressure; however the low and moderate temperature curves are not affected by the operating variables. In the case of Ni-Mo/Al_2O_3 catalyst, the catalyst and gas volume fractions doesn't deviate and follows a linear trend with the increasing values of WHSV at respective operating conditions of temperature and pressure. While, small deviations/fluctuations are seen in the case of oil volume fractions with the changing WHSV values. Finally for the Co-Mo/Al_2O_3 catalyst, the volume fraction of the gas phase is increasing continuously with the increasing WHSV. The reverse trend is clearly seen for the bio-oil phase, while the catalyst phase reported slighter reduction

in the values with the increasing WHSV. At higher values of WHSV all the three phases are stable with no deviations or changes further.

On the other hand the chemical reaction kinetics reported significant changes with the change in the WHSV values. As the value of the residence time is decreased the reaction is incomplete which reduces the formation of the desired product species. The effect of the residence time is also dependent on the reaction rates, catalyst activity, and reaction mechanisms i.e., some catalyst requires higher residence times for the completion of reaction to form desired products. While some catalyst possesses the catalytic inactivity due to the higher residence times due to the formation of secondary products which are cracked from the primary desired compounds. Hence, the optimized condition of WHSV is to be chosen for the higher quantity and quality of the desired products. It is observed that the non-volatile fractions of the bio-oil show minimal variations regardless of the WHSV values of Pt/Al_2O_3 catalysts. The phenols formation from the non-volatiles or the conversion of phenols to alkane and aromatics are almost constant at all WHSV values. The formation of the alkane and aromatics from the heavy non-volatile residues and the phenols tend to be higher at lower values of WHSV. In the case of $Ni-Mo/Al_2O_3$ catalyst the conversion of the non-volatile fractions to phenols are on higher note instead of forming alkane and aromatics. The major observation here is the phenol formation is higher at lower residence time as the activity of the catalyst tends to be very much higher at lower residence times. Similarly, the alkane and aromatics formation is also considerably higher at lower residence times. Further in the case of $Co-Mo/Al_2O_3$ catalyst as the values of the WHSV is increasing the conversion of the non-volatile fractions tends to increase and reported higher conversions at higher WHSV. The obtained results suggest that the decreasing trend of non-volatile fractions represents the higher conversions of non-volatiles to desired products. This

phenomena is observed majorly at the lower values of the WHSV i.e., higher residence times. Thus, the increase of space velocity shortens the reactants residence time in the catalyst bed, leading to decrease hydrodeoxygenation, cracking, gasification and other secondary processes such as removal of oxygenates from the unprocessed bio-oil.

6.2. Effect of temperature

The temperature has a major role to play in the hydrotreatment process of bio-oil. For Pt/Al_2O_3 catalyst the temperature has a marginal effect on the volume fraction and the mass fractions of lumped species of all three phases. The gas phase is predominant at all temperatures in the case of volume fraction; however the conversion of the heavy non-volatiles is also marginal at all temperatures. While the formation of alkane and aromatics favors the lower temperatures. Similarly, the gas phase volume fraction increases with respect to temperature, the non-volatile species conversions favors the lower temperatures and phenol formation favors the moderate temperature for $Ni\text{-}Mo/Al_2O_3$ catalyst. Finally, the gas phase volume fraction values increases with the increasing temperature followed by the conversion of the non-volatile species to the desired alkane and aromatics for $Co\text{-}Mo/Al_2O_3$ catalyst. Hence higher temperature favors the $Co\text{-}Mo/Al_2O_3$ catalyst while no significant effect of temperatures on Pt/Al_2O_3 and moderate temperatures favors $Ni\text{-}Mo/Al_2O_3$ catalysts.

6.3. Effect of pressure

Considering the case of Pt/Al_2O_3 catalyst the vicinity of the gas phase to the catalyst particles tends to increase continuously and hence higher conversion of non-volatile residue is achieved at higher pressures. Whereas the reverse trend is observed for $Ni\text{-}Mo/Al_2O_3$ catalyst i.e., higher conversion is achieved at lower pressures. For $Co\text{-}Mo/Al_2O_3$ catalyst, the similar

trend of the Pt/Al_2O_3 catalyst is observed i.e., higher conversion is observed at higher pressures. The higher conversion of non-volatile residues at the pertinent condition leads to the formation of products either phenol while using $Ni\text{-}Mo/Al_2O_3$ catalyst or alkane and aromatic in the case of $Co\text{-}Mo/Al_2O_3$ catalyst.

6.4. Yield of alkane and aromatics

The yields of alkanes and aromatics obtained from the hydroprocessing of lumped species of bio-oil in the presence of different catalysts at variable operating conditions are compared via histogram. The major observation is that the alkanes and aromatics are predominant in gaseous phase for all the three catalysts. The overall yield of alkane and aromatics increases with the WHSV for $Co\text{-}Mo/Al_2O_3$ catalyst while it is reverse for Pt/Al_2O_3 catalyst. Whereas, the yield of alkane and aromatics are considerably low for $Ni\text{-}Mo/Al_2O_3$ catalyst as compared to the other catalysts. The higher pressure values shows significant yields of alkane and aromatics for $Co\text{-}Mo/Al_2O_3$ catalyst; while the yield is unaffected for Pt/Al_2O_3 catalyst and mixed trends are seen for $Ni\text{-}Mo/Al_2O_3$ catalyst.

The overall conclusion of the present study states that the product formation in the form of gaseous phase is higher for Pt/Al_2O_3 catalysts followed by $Co\text{-}Mo/Al_2O_3$ and $Ni\text{-}Mo/Al_2O_3$ catalyst. On the other hand, the higher yield of alkane and aromatics are seen for $Co\text{-}MO/Al_2O_3$ catalyst followed by Pt/Al_2O_3 and $Ni\text{-}Mo/Al_2O_3$ catalyst. The phenol formation is dominant in $Ni\text{-}Mo/Al_2O_3$ catalyst followed by $Co\text{-}Mo/Al_2O_3$ and Pt/Al_2O_3 catalyst. It is also concluded that with the present reaction scheme and kinetics higher yields is possible at higher residence times for Pt/Al_2O_3 catalyst and lower residence times for $Co\text{-}Mo/Al_2O_3$ catalyst for the present reaction mechanism.

6.5. Future Scope

- Optimizing the type of catalyst for a specific feedstock based bio-oil upgradation.
- Optimizing the temperature conditions (higher/lower) for the high yield of alkane and aromatics using HDO of bio-oil
- Three-dimensional studies for the present simulations.
- Optimizing the catalytic characteristics for the high performance of HDO process
- Optimizing the solid catalyst load at lower values of WHSV enabling higher residence time for the reaction.

References

Adjaye, J.D., Bakhshi, N.N., Catalytic conversion of biomass-derived oil to fuels chemicals II: Chemical kinetics, parameter estimation model predictions, *Biomass Bioenergy,* **8**, 265 – 277 (1995).

Agarwal, R., Agarwal, M., Singh, N.R., Novel process for producing liquid hydrocarbon by pyrolysis of biomass in presence of hydrogen from a carbon-free energy source, *US Patent 2009/0082604 A1*, USA (2009).

Agblevor, F.A., Besler, S., Wiselogel, A.E., Production of oxygenated fuels from biomass: impact of storage conditions. *Fuel Sci. Technol. Int.,* **14**, 589–612 (1996).

Ahmad, M.M., Nordin, M.F., Azizan, M.T., Upgrading of bio-oil into high value hydrocarbons via hydrodeoxygenation, *Am. J. Appl. Sci.,* **7**, 746-755 (2010).

Aho, A., Kumar, N., Eranen, K., Salmi, T., Hupa, M., Murzin, D.Y., Catalytic pyrolysis of woody biomass in a fluidized bed reactor: Influence of the zeolite structure, *Fuel,* **87,** 2493-2501 (2008).

Aimaro, S., Vispute, T.P., Huber, G.W., Hydrodeoxygenation of the aqueous fraction of bio-oil with Ru/C and Pt/C catalysts, *Applied Catal. B, Environ.,* **165,** 446–456 (2015).

Alder, B.J., Wainright, T.E., Studies in Molecular Dynamics. II: Behavior of small number of spheres, *J. Chem. Phys.*, **33,** 1439-1451 (1960).

Ancheyta, J., Speight, J.G., *Hydroprocessing of Heavy Oils and Residua*; CRC Press, Boca Raton (2007).

Anderson, T.B., Jackson, R., A Fluid Mechanical Description of Fluidized Beds. *Ind. Eng. Chem. Fundam.,* **6**, 527-534 (1967).

Ansys Fluent 12.0 User's Guide , Ansys Fluent Inc (2009).

Antonakou, E., Lappas, A., Nilsen, M.H., Bouzga, A., Stöcker, M., Evaluation of various types of Al-MCM-41 materials as catalysts in biomass pyrolysis for the production of bio-fuels and chemicals, *Fuel*, **85,** 2202–2212 (2006).

Ardiyanti, A.R., Khromova, S.A., Venderbosch, R.H., Yakovlev, V.A., Heeres, H.J., Catalytic hydrotreatment of fast-pyrolysis oil using non-sulfided bimetallic Ni-Cu catalysts on a δ-Al_2O_3 Support, *Applied Catal. B, Environ.*, **117–118**, 105–117 (2012).

Ausavasukhi, A., Huang, Y., Anh T.T., Sooknoi T., Daniel E. Resasco., Hydrodeoxygenation of M-Cresol over gallium-modified beta zeolite catalysts, *J. Catal.*, **290,** 90–100 (2012).

Ayako Iino., Cho, A., Takagaki, A., Kikuchi, R., Ted Oyama, S., Kinetic Studies of Hydrodeoxygenation of 2-Methyltetrahydrofuran on a Ni_2P/SiO_2 catalyst at medium pressure, *J. Catal.*, **311**, 17–27 (2014).

Ayodele, O.B., Farouk, H.U., Mohammed, J., Uemura, Y., Daud, W.M.A.W., Hydrodeoxygenation of oleic acid into n- and iso paraffin biofuel using zeolite Supported fluoro-oxalate modified molybdenum catalyst : Kinetics study, *J. Taiwan Inst. Chem. Eng.*, **50**, 141–152 (2015).

Baker, E.G., Elliott, D.C., Catalytic upgrading of biomass pyrolysis oils, *Res. Thermo - Chem. Biomass. Conv.*, 883–895 (1988).

Balakrishna, A.R., David Pei, C.T., Heat transfer in Fixed beds, *Ind. Eng. Chem. Process Des. Dev.*, **13**, 441-446 (1974).

Baldauf, W., Balfanz, U., Rupp, M., Upgrading of flash pyrolysis oil and utilization in refineries, *Biomass Bioenergy*, **7**, 237–244 (1994).

Bhatti, H.N., Hanif, M.A., Faruq, U., Sheikh M.A., Acid and base catalyzed transesterification of animal fats to biodiesel, *Iran. J. Chem. Chem. Eng.*, **27,** 41-48 (2008).

Bird, M.I., Wurster, C.M., Paula Silva, P.H., Bass, A.M., Nys R., Algal biochar production and properties, *Bioresour. Technol.*, **102**, 1886-1891 (2010).

Blasi, C.D., Hernandez E.G., Santoro, A., Radiative pyrolysis of single moist wood particles. *Ind. Eng. Chem. Res*., **39**, 873-882 (2000).

Boonyawan, Y., Tumnantong, D., Prasassarakich, P., Unsupported MoS_2 and $CoMoS_2$ catalysts for hydrodeoxygenation of phenol, *Chem. Eng. Sci.*, **79,** 1–7 (2012).

Boucher, M.E., Chaala, A., Roy, C., Bio-oils obtained by vacuum pyrolysis of softwood bark as a liquid fuel for gas turbines. Part I: Properties of bio-oil and its blends with methanol and a pyrolytic aqueous phase, *Biomass Bioenergy*, **19,** 337-350 (2000).

Bowen, R.M., Theory of Mixtures. In *Continuum Physics*, Eringen, A.C., Waltham: Academic Press, 1-127(1976).

Bu, Q., Lei, H., Zacher, H.A.,Wang, L., Shoujie Ren., Liang, J., Yi Wei., Liu, Y., Tang, J., Zhang, Q., Ruan, R., A review of catalytic hydrodeoxygenation of lignin-derived phenols from biomass pyrolysis, *Bioresour. Technol.*, **124** ,470–477 (2012).

Bui, P., Cecilia, J.A., Oyama, T.D., Takagaki, A., Antonia, I.M., Zhao, H., Li, D., Enrique Rodriguez, C., Lopez, A.J., Studies of the synthesis of transition metal phosphides and their activity in the hydrodeoxygenation of a biofuel model compound, *J. Catal.,* **294,** 184-198 (2012).

Bui, V.N., Toussaint, G., Laurenti, T., Morodatos, C., Geantet, C., Co-processing of pyrolysis bio oils and gas oil for new generation of bio-fuels: Hydrodeoxygenation of guaiacol and SRGO mixed feed, *Catal. Today*, **143,** 172-178 (2009)**.**

Bui, V.N., Laurenti, D., Delichere, P., Geantet, C., Hydrodeoxygenation of guaiacol: Part II: Support of CoMoS catalysts on HDO activity and selectivity, *Applied Catal. B, Environ.*,**101,** 246-255 (2011).

Bykova, M.V., Yu Ermakov, D., Kaichev, V.V., Bulavchenko, O.A., Saraev, A.A., Yu Lebedev, M., Yakovlev, V., Ni-based sol-gel catalysts as promising systems for crude bio-oil upgrading: Guaiacol hydrodeoxygenation study, *Applied Catal. B, Environ.*, **113– 114,** 296–307 (2012).

Caballero, J.A., Conesa, J.A., Font, R., Marcilla, A., Pyrolysis kinetics of almond shells and olive stones considering their organic fractions, *J. Anal. Appl. Pyrolysis.*, **42**, 159-175 (1997a).

Centano, A., Laurent, E., Delmon, B., Influence of the support of Co-Mo sulfide catalysts and of the addition of potassium and platinum on the catalytic performances for the hydrodeoxygenation of carbonyl, carboxyl and guaiacol type molecules, *J. Catal.*, **154**, 288-298 (1995).

Chaiwat, W., Richard, G., Gholizadeh, M., Xiang, L., Lievens, C., Hu, X., Yi Wang., Mourant, D., Rossiter, A., Bromly, J., Zhu Li, C., Upgrading of bio-oil into advanced biofuels and chemicals. Part II. Importance of holdup of heavy species during the hydrotreatment of bio-oil in a continuous packed-bed catalytic reactor, *Fuel*, **112,** 302–310 (2013).

Chapman, S., Cowling, T.G., *The mathematical theory of non-uniform gases*, Cambridge university press, England (1990).

Chen Zhao., Kasakov, S., He, J., Lercher, J.A., Comparison of kinetics, activity and stability of Ni/HZSM-5 and Ni/Al_2O_3-HZSM-5 for phenol hydrodeoxygenation, *J. Catal.*, **296,** 12–23 (2012).

Chen, J., Zhu, D., Sun, C., Effect of heavy metals on the sorption of hydrophobic organic compound to wood charcoal, *Environ. Sci. Technol.*, **41**, 2536-2541 (2007).

Chen, L., Zhu, Y., Zheng, H., Zhang, C., Zhang, B., Yongwang, L., Aqueous-phase hydrodeoxygenation of carboxylic acids to alcohols or alkanes over supported Ru catalysts, *J. Mol. Catal. A: Chem.*, **351** 217–227 (2011).

Choudhary, T. V., Phillips, C.B., Renewable fuels via catalytic hydrodeoxygenation, *Appl. Catal., A*, **397**, 1-12 (2011).

Das, S., Frank, S., Single-Particle relaxation time versus scattering time in an impure electron gas, *Phy. Rev.*, **32,** 8442-8448 (1985).

De La Puente, G., Gil, A., Pis, J.J., Grange, P., Effects of support surface chemistry in hydrodeoxygenation reactions over CoMo/activated carbon sulfided catalysts, *Langmuir*, **15,** 5800–5806 (1999).

De Miguel Mercader, F., Groeneveld, M.J., Kersten, S.R.A., Way, N.W.J., Schaverien, C.J., Hogendoorn, J.A., Production of advanced biofuels: Co-processing of upgraded pyrolysis oil in standard refinery units, *Appl. Catal., B,* **96**, 57–66 (2010).

De, S., Basudeb, S., Luque, R., Bioresource technology hydrodeoxygenation processes : Advances on catalytic transformations of biomass-derived platform chemicals into hydrocarbon fuels, *Bioresour. Technol.*, **178,** 108–18 (2014).

Demirbas, A., Biomass resource facilities and biomass conversion processing for fuel and chemicals. *Energy Convers. Manage.*, **42**,1357–1378 (2001).

Demirbas, A., Effect of temperature on pyrolysis products from four nut shells. *J. Anal. Appl. Pyrolysis.*,**76**, 285-289 (2006).

Demirbas, A., Hydrogen production from biomass by the gasification process, *Energy Resour.*, **24**, 59-68 (2002).

Demirbas, A., Caglar, F.A., Conversion of Olive Husk to Liquid Fuel by Pyrolysis and Catalytic liquefaction, *Energy Sources*, **22**, 631–39 (2000).

Di Blasi, C., Gabriella, S., Carlo, D.R., Gennaro, R., Product distribution from pyrolysis of wood and agricultural residues. *Ind. Eng. Chem. Res.*, **38,** 2216–2224 (1999).

Dinesh, M., Pittman, C.U., Steele, P.H., Pyrolysis of wood / biomass for bio-oil : A critical review, *Energy Fuels*, **20**, 848–889 (2006).

Ding, J., Gidaspow. D., A bubbling fluidization model using kinetic theory of granular flow, *AIChE J.*, **36,** 523-528 (1990).

Domínguez, A., Fernández, Y., Fidalgo, B., Pis, J.J., Menéndez, J.A., Bio-syngas production with low concentrations of CO_2 and CH_4 from microwave-induced pyrolysis of wet and dried sewage sludge, *Chemosphere*, 70, 397-403 (2008).

Echeandia, S., Arias, P.L., Barrio, V.L., Pawelec, B., Fierro, J.L.G., Synergy effect in the HDO of phenol over Ni-W catalysts supported on active carbon: Effect of tungsten precursors, *Appl. Catal., B*, **101**, 1–12 (2010).

Elkasabi, Y., Mullen, C.A., Pighinelli, A.L.M.T., Boateng, A.A., Hydrodeoxygenation of fast-pyrolysis bio-oils from various feed stocks using carbon-supported catalysts, *Fuel Process. Technol.*, **123,** 11–18 (2014).

Elliott, D.C., Hart, T.R., Catalytic hydroprocessing of chemical models for bio-oil, *Energy Fuels*, **23**, 631–637 (2009).

Elliott, D.C., Historical Developments in Hydroprocessing Bio-Oils, *Energy Fuels*, **21**, 1792–1815 (2007).

Encinar, J.M., Beltrán, F.J., Bernalte, A., Ramiro, A., González, J.F., Pyrolysis of two agricultural residues: Olive and grape bagasse. Influence of particle size and temperature. *Biomass Bioenergy*,**11**, 397-409 (1996).

Ergun, S., Fluid Flow through Packed Columns, *Chem. Eng. Prog*., **48**, 89-94 (1952).

Fahmi, R., Bridgwater, A.V., Donnison, I., Yates, N., Jones, J.M. The effect of lignin and inorganic species of biomass on pyrolysis oil yields, quality and stability, *Fuel*, **87,** 1230-1240 (2008).

Furimsky, E., Catalytic Hydrodeoxygenation, *Appl. Catal., A*, **199,** 147–90 (2000).

Furimsky, E., Chemistry of Catalytic Hydrodeoxygenation, *Catal. Rev.: Sci. Eng.*, **25**, 421–458 (1983).

Furimsky, E., Massoth, F.E., Deactivation of hydroprocessing catalysts, *Catal. Today*, **52,** 381-495 (1999)**.**

Gidaspow, D., Bezburuah,R., Ding, J., Hydrodynamics of circulating fluidized beds, kinetic theory approach. Proceedings of the 7th Engineering Foundation Conference on Fluidization, Gold coast, Australia (1992).

Groeneveld, M.J., The change of fossil to solar and biofuels needs our energy. *Inaugural lecture*.University of Twente, Enchede (2008).

Guney, M.S., Utilization of hazelnut husk as biomass. *Sustainable energy technologies and assessments*, **4,** 72-77 (2013)

Gunn, D.J., Transfer of heat or mass to particles in fixed and fluidized beds, *Int. J. Heat Mass Transfer*, **21**, 467-476 (1978).

Gutierrez, A., Kaila, R.K., Honkela, M.L., Slioor, R., Krause, A.O.I., "Hydrodeoxygenation of guaiacol on noble metal catalysts, *Catal. Today*, **147,** 239–46 (2009).

Güvenatam, B., Osman, K., Heeres, E.H.J., Pidko, E.A., Hensen, E.J.M., Hydrodeoxygenation of mono- and dimeric lignin model compounds on noble metal catalysts, *Catal. Today*, **233,** 83–91 (2014).

Harris, E., Beglinger, E., Hajny, G., Sherrard, E., Hydrolysis of wood: Treatment with sulfuric acid in a stationary digester, *Ind. Eng. Chem. Res*., **37**, 12-23 (1945).

Hart, A., Advanced study on the upgrading of heavy oils. *Ph.D. Thesis*, University of Birmingham. United Kingdom (2014).

Hashem, A.M., Rashad, M.M., Production of ethanol by yeasts grown on hydrolyzate of Egyptian sweet potato, *Egypt . J. Food. Sci.*, **21,** 171-180 (1993).

He, Z., Wang, X., Hydrodeoxygenation of model compounds and catalytic systems for pyrolysis bio-oils upgrading. *Catal. Sustainable Energy*, **10**, 28-52 (2012).

Hellinger, M., Hudson, W.P., Carvalho, S.B., Wang, D., Wolfgang, K., Jan-dierk G., Catalytic Hydrodeoxygenation of Guaiacol over Platinum Supported on Metal Oxides and Zeolites, *Appl. Catal., A,* **490,** 181–192 (2015).

Hong, Y.K., Lee, D.W., Jun Eom, H., Young Lee, K., The Catalytic activity of Pd/WOx/γ-Al_2O_3 for hydrodeoxygenation of guaiacol, *Applied Catal. B, Environ.,* **150–151,** 438– 445 (2014).

Iino, A., Ara, C., Takagaki, A.,Kikuchi, R., Oyama, S.T., Kinetic Studies of hydrodeoxygenation of 2-methyltetrahydrofuran on a Ni_2P/SiO_2 catalyst at medium pressure, *J. Catal.*, **311,** 17–27 (2014).

Islam, M.R., Islam, M.N., Characterization of biomass solid waste for liquid fuel production, 4th International Conference on Mechanical Engineering, Dhaka (2001).

Jahirul, M., Rasul, M., Chowdhury, A., Ashwath, N., Biofuels production through biomass pyrolysis —A Technological review, *Energies,* **5,** 4952–5001 (2012).

Jęczmionek, L., Semczuk, K.P., Hydrodeoxygenation, decarboxylation and decarbonylation reactions while co-processing vegetable oils over a NiMo hydrotreatment catalyst. Part I: Thermal effects - theoretical considerations, *Fuel,* **131,** 1-5 (2014).

Jegers, H.E., Klein, M.T., Primary and secondary lignin pyrolysis reaction pathways, *Ind. Eng. Chem. Process Des. Dev.,* **24**, 173-183 (1985).

Jin, S., Xiao, Z., Li, C., Chen, X., Wang, L., Xing, J., Li, W., Liang, C., Catalytic hydrodeoxygenation of anisole as lignin model compound over supported nickel catalysts, *Catal. Today,* **234,** 125–132 (2014).

Jiraporn, P., Kangvansaichol, K., Reubroycharoen, P., Kuchonthara, P., Hinchiranan, N., Pt/Al_2O_3-catalytic deoxygenation for upgrading of leucaena leucocephala-pyrolysis oil, *Bioresour. Technol.,* **139,** 128–135 (2013).

Joshi, N., Lawal, A., Hydrodeoxygenation of pyrolysis oil in a micro-reactor, *Chem. Eng. Sci.*, **74,** 1–8 (2012).

Johnson, A., Lignin liquefaction in supercritical water, *Thermo. Chem. Biomass. Conv*., 485-496 (1988).

Khan, R., *Advances in clean hydrocarbon fuel processing science and technology*. Wood head publishing series in energy, Philadelphia (2011).

Kim, T.S., Oh, S., Kim, J.Y., Choi, G., Choi, J.W., Study on the hydrodeoxygenative upgrading of crude bio-oil produced from woody biomass by fast pyrolysis, *Energy*, **68**, 437–43 (2014).

Krishnamurthy, S., Panvelker, S., Shah, Y.T., Hydrodeoxygenation of dibenzofuran and related compounds, *AIChE J*., **27**, 994–1001 (1981).

Kyung, K.C., Mayfield, H., Marolla, T., Nichols, B., Mashburn, M., Catalytic deoxygenation of liquid biomass for hydrocarbon fuels, *Renewable Energy*, **36,** 907–15 (2011).

Larsson, S., Quintana-Sainz, A., Reimann, A., Nilvebrant, N.O., Jonsson, L.J., Influence of lignocellulose-derived aromatic compounds on oxygen-limited growth and ethanolic fermentation by Saccharomyces cerevisiae, *Appl. Biochem. Biotechnol*., **84**, 617-632 (2000).

Launder, B.E., Spalding, D.B., *Lectures in Mathematical Models of Turbulence*. Academic Press, London, (1972).

Laurent, E., Delmon, B., Study of the Hydrodeoxygenation of Carbonyl, Carboxylic and Guaiacyl Groups over Sulfided CoMo/ɣ-Al_2O_3 and NiMo/ɣ-Al_2O_3 Catalysts: I. Catalytic Reaction Schemes, *Appl. Catal., A,* **109**, 77–96 (1994).

Le, T.A., Hoang, V.L., Kim, J., Seung-Soo, K., Hyung Choi, J., Woo, H., Othman, M.R., Hydrodeoxygenation of 2-Furyl methyl ketone as a model compound in bio-oil from pyrolysis of saccharina japonica alga in fixed-bed reactor, *Chem. Eng. J.*, **250,** 157–**163** (2014).

Lebowitz, J.L., Exact solution of generalized percus-yevick equation for a mixture of hard spheres. *The Phy. Rev.*,**133,** 895-899.

Leng, S., Wang, X., He, X., Liu, L., Liu, Y., Zhong, X., Zhuang, G., Wang, J.G., NiFe/γ- Al_2O_3: A universal catalyst for the hydrodeoxygenation of bio-oil and its model compounds, *Catal. Commun.*, **41**, 34–37 (2013).

Lin, S.C., Hydrocarbons via catalytic hydrogen treatment of wood pyrolytic oil, Texas A & M University, Texas (1981).

Lippitz, A., Hubert, T.H., XPS investigations of chromium nitride thin films, *Surf. Coat. Technol.*, **200**, 250–253 (2005).

Liu, C., Shao, Z., Xiao, Z., Liang, C., Hydrodeoxygenation of benzofuran over activated carbon supported Pt, Pd, and Pt-Pd catalysts, *React. Kinet., Mech. Catal.*, **107,** 393–404 (2012).

Lucie, A.P., Mario, D.B., Emma, C.C., Vitaly, B., James, H.C., Food waste biomass: a resource for high-value chemicals, *Green Chem.*, **15**, 271-282. (2013).

Lun, C.K.K., Savage, S.B., Jeffrey, D.J., Chepurniy, N., Kinetic theory of granular flow: Inelastic particles in coutte flow and slightly inelastic particles in a general flow field, *J. Fluid. Mech.*, **140,** 223-256 (1984).

Ma, D., Ahmadi, G., A Thermodynamic formulation for dispersed multiphase turbulent flows, *Int. J. Multiphase Flow*, **16,** 323-351 (1990)**.**

Madsen, A.T., Ahmed, E.H., Christensen, C.H., Fehrmann, R., Riisager, A., Hydrodeoxygenation of waste fat for diesel production: Study on model feed with Pt/alumina catalyst, *Fuel*, **90**, 3433–3438 (2011).

Maggi, R., Delmon, B., A Review of Catalytic Hydrotreating Processes for the Upgrading of Liquids Produced by Flash Pyrolysis, *Hydrotreatment and Hydrocracking of Oil Fractions Proceedings of the 1st International Symposium/6th European Workshop*, **106**, 99–113 (1997).

Mahfud, F.H., Exploratory Studies on Fast Pyrolysis Oil Upgrading, Doctoral thesis, University of Gronigen, The Netherlands (2007).

Majhi, A., Sharma, Y.K., Rajaram, B., Babita, B., Kumar, J., Upgrading of Bio-oils over PdO/Al_2O_3 catalyst and fractionation, *Fuel*, **107,** 131–37 (2013).

Massoth, F. E., Politzer, P., Concha, M.C., Murray, J.S., Jakowski, J., Simons, J., Catalytic hydrodeoxygenation of methyl-substituted phenols: Correlations of kinetic parameters with molecular properties, *J. Phys. Chem. B,* **110,** 14283–14291 (2006).

McKendry, P., Energy production from biomass (part 2): conversion technologies, *Bioresour. Technol.*, **83,** 47-54 (2002).

Mortensen, P.M., Grunwaldt, J.D., Jensen, P.A., Knudsen, K.G., Jensen, A.D., A review of catalytic upgrading of bio-oil to engine fuels, *Appl. Catal., A,* **407**, 1–19 (2011).

Muhlbauer, A., David Raal, J., *Phase Equilibria: Measurement & Computation*. Taylor and Francis, USA, (1997).

Mullen, C.A., Boateng, A.A., Goldberg, N.M., Lima, I.M., Laird, D.A., Hicks, K.B., Bio-Oil and bio-char production from corn cobs and stover by fast pyrolysis, *Biomass Bioenergy*, **34**, 67–74 (2010).

Nava, R., Pawelec, B., Castaño, P., Álvarez-Galván, M.C., Loricera, C.V., Fierro, J.L.G., Upgrading of bio-liquids on different mesoporous silica-supported CoMo catalysts, *Applied Catal. B, Environ.* **92**, 154–**167** (2009).

Nie, L., Resasco, D.E., Kinetics and mechanism of m-Cresol hydrodeoxygenation on a Pt/SiO_2 catalyst, *J. Catal.*, 317, 22–29 (2014).

Oasmaa, A., Boocock, D.G.B., The catalytic hydrotreatment of peat pyrolysate oils, *Can. J. Chem. Eng.*, **70**, 294-300 (1992).

Oasmaa, A., Czernik, S., Fuel oil quality of biomass pyrolysis oils-state of the art for the end users. *Energy Fuels*, **13**, 914-921 (1999).

Oasmaa, A., Czernik, S., Fuel oil quality of biomass pyrolysis oils. In *Biomass. A growth opportunity in green energy and value-added products*, Kidlington: Elsevier Science. 1247–1252 (1999).

Odebunmi , E.O., Ollis, D.F., Catalytic Hydrodeoxygenation I: conversion of o-p-and m-Cresols, *J. Catal.*, **80**, 56–64 (1983).

Ogawa, S., Umermura, A., Oshima, A., On the equation of fully fluidized granular materials, *J. Appl. Math. Phys.* 31, 483-490 (1980).

Oh, S., Hwang, H., Choi, H.S., Choi, J.W., Investigation of chemical modifications of micro- and macromolecules in bio-oil during hydrodeoxygenation with Pd/C catalyst in supercritical ethanol, *Chemosphere*, **117**, 806–814 (2014).

Olah, G.A., Molnar, A., *Hydrocarbon Chemistry;* John Wiley & Sons, Hoboken, New Jersey (2003).

Olcese, R.N., Bettahar, M., Petitjean, D., Malaman, B., Giovanella, F., Dufour, A., Gas- Phase hydrodeoxygenation of guaiacol over Fe/SiO_2 catalyst, *Applied Catal. B, Environ.*, **115–16**, 63–73 (2012).

Othman, N., Basri, N.E.A., Yunus, N.M., Sidek, L.M., (2008) Determination of physical and chemical characteristics of electronic plastic waste (Ep-Waste) resin using proximate and ultimate analysis method. *Int. conf. constr. Build. Technol.*, **16**, 169–180 (2008).

Oyama, S.T., Introduction to the Chemistry of Transition Metal Carbides Nitrides, In *The Chemistry of Transition Metal Carbides and Nitrides*, Oyama, S.T., Glasgow: Blackie Academic& Professional, 1–27 (1996).

Pham, T.T., Lobban, L.L., Resasco, D.E., Mallinson, R.G., Hydrogenation and Hydrodeoxygenation of 2-Methyl-2-Pentenal on supported metal catalysts, *J. Catal.*,**266**, 9–14 (2009).

Popov, A., Elena, K., Gilson, J.P., Mariey, L., Travert, A., Mauge, F., IR Study of the Interaction of phenol with oxides and sulfided Co Mo catalysts for bio-fuel hydrodeoxygenation, *Catal. Today*, **172**, 132–135 (2011).

Popov, A., Elena, K., Mariey, L., Goupil, J.M., Jaffar, E.F., Gilson, J.P., Travert, A., Mauge, F., Bio-oil hydrodeoxygenation: Adsorption of phenolic compounds on sulfided (Co) Mo catalysts, *J. Catal.*, **297**, 176–186 (2013).

Pütün, A.E., Ozcan, A., gercel, H.F., Putun, E., Production of biocrudes from biomass in a fixed-bed tubular reactor: Product yields and compositions, *Fuel*, **80,** 1371–1378 (2001).

Qader, S.A., Wiser, W.H., Hill, G.R., Kinetics of the hydroremoval of sulfur, oxygen and nitrogen from a low-temperature coal tar, *Ind. Eng. Chem. Process Des. Dev.*, **10,** 390-397 (1968).

Ramadhas, A.S., Jayaraj, S., Muraleedharan, C., Characterization and effect of using rubber seed oil as fuel in the compression ignition engines. *Renewable Energy*, **30**, 795–803 (2005).

Ramanathan, S., Oyama, S.T., New Catalysts for Hydroprocessing: Transition Metal Carbides and Nitrides, *J. Phys. Chem.*, **99**, 16365–16372 (1995).

Ranz, W.E., Marshall, W.R., Evaporation from Drops, Part I. *Chem. Eng. Prog.* **48,** 141-146 (1952).

Raymundo, A., Gouveia, L., Batista, A.P., Empis, J., Sousa, I., Fat mimetic capacity of chlorella vulgaris biomass in oil-in-water food emulsions stabilized by pea protein, *Food Res. Int.*, **38**, 961-965 (2005).

Reina, J., Velo, E., Puigjaner, L., Kinetic study of the pyrolysis of waste wood, *Ind. Eng. Chem. Res*., **37,** 4290-4295 (1998).

Richardson, S.M., Nagaishi, H., Gray, M.R., Initial car-bon deposition on a NiMo/γ -Al_2O_3 bitumen hydrocracking catalyst-the effect of reaction time and hydrogen pressure,

Proceedings of the 210th National Meeting of the American Chemical Society, Chicago (1995).

Rocha, J.D., Luengo, C.A., Snape, C.E., Hydrodeoxygenation of oils from cellulose in single and two-stage hydropyrolysis, *Renewable Energy*, **9**, 950–953 (1996).

Rollmann, L.D., Catalytic hydrogenation of model nitrogen, sulfur, and oxygen compounds, *J. Catal.*, **46**, 243-252 (1979).

Romero, Y., Richard, F., Brunet, S., Hydrodeoxygenation of 2-ethylphenol as a model compound of bio-crude over sulfided Mo-based catalysts: Promoting effect and reaction mechanism, *Applied Catal. B, Environ.*, **98**, 213–223 (2010).

Roy, M.J., Hydrodeoxygenation of Lignin Model Compounds via Thermal Catalytic Reactions, *Post-graduation Thesis*, Georgia Institute of Technology, Atlanta (2012).

Ryymin, E.M., Honkela, M.L., Viljava, T.R., Krause, A.O.I., Competitive reactions and mechanisms in the simultaneous HDO of phenol and methyl heptanoate over sulphided NiMo/ɣ-Al_2O_3, *Appl. Catal., A*, **389**, 114–121 (2010).

Saidi, M., Samimi, F., Karimipourfard, D., Nimmanwudipong, T., Gates, B.C., Rahimpour, M.R., Upgrading of Lignin-Derived Bio-Oils by Catalytic Hydrodeoxygenation, *Energy Environ. Sci.*, **7,** 103-129 (2014).

Sankaranarayanan, T.M., Berenguer, A., Ochoa-hernández, C., Moreno, I., Jana, P., Coronado, J.M., Serrano, D.P., Patricia Pizarro., Hydrodeoxygenation of anisole as bio-oil model compound over supported Ni and Co catalysts : Effect of metal and support properties, *Catal. Today*, 243, 163–172 (2015).

Sanna, A., Vispute, T.P., Huber, G.W., Hydrodeoxygenation of the aqueous fraction of bio-oil with Ru/C and Pt/C catalysts, *Applied Catal. B, Environ.*,**165,** 446-456 (2015).

Sathish, T.K., Steele, P.H., Pretreating bio-oil to increase yield and reduce char during hydrodeoxygenation to produce hydrocarbons, *Fuel*, **133,** 326–**331** (2014).

Scheirs, J., Kaminsky, W., *Feedstock Recycling and Pyrolysis of Waste Plastics: Converting Waste Plastics into Diesel and Other Fuels*, John Wiley & Sons, UK, (2006).

Schiller, L., Naumann, A., A drag correlation, *Z. Ver. Deutsch. Ing*. 77, 318 (1935).

Schneider, A., Hollstein, E.J., Janoski, E.J., Scheibel, E.G., Research and development of an advanced process for the conversion of coal to synthetic gasoline and other distillate fuels. TID-28447, U.S. Department of Energy, Washington (1979).

Scott, D., Piskorz, J., The flash pyrolysis of aspen-poplar wood, *Can. J. Chem. Eng.*, **60**, 666-674 (1982).

Sepúlveda, C., Leiva, K., García, R., Radovic, L.R., Ghampson, I.T., Desisto, W.J., García Fierro, J.L., Escalona, N., Hydrodeoxygenation of 2-Methoxyphenol over Mo_2N catalysts supported on activated carbons, *Catal. Today*, **172**, 232–239 (2011).

Sharma, R.K., Bakhshi, N.N., Catalytic upgrading of pyrolysis oil, *Energy Fuels*, **7**, 306–314 (1993).

Shan, I., Zhang, D., Low temperature pyrolysis of sewage sludge and putrescible garbage for fuel oil production, *Fuel*, **84**, 809–815 (2005).

Shen, L., Zhang, D., Low temperature pyrolysis of sewage sludge and putrescible garbage for fuel oil production, *Fuel*, **84,** 809–815 (2005).

Sheu, Y.H.E., Rayford G.A., Soltes, J., Kinetic Studies of Upgrading Pine Pyrolytic Oil by Hydrotreatment, *Fuel Process. Technol.*, **19**, 31–50 (1988).

Shi, H., Chen, J., Yang, Y., Tian, S., Catalytic deoxygenation of methyl laurate as a model compound to hydrocarbons on nickel phosphide catalysts: Remarkable support effect, *Fuel Process. Technol.*, ***118,*** 161-170 (2014).

Šimáček, P., Kubička, D., Šebor, G., Pospíšil, M., Fuel properties of hydroprocessed rapeseed oil, *Fuel*, **89** 611–615 (2010).

Sipila, K., Kuoppala, E., Fagernas, L., Oasmaa, A., Characterization of biomass based flash pyrolysis oil. *Biomass Bioenergy*, **14**, 103-113 (1998).

Soltes, E.J., Lin, S.C.K., Sheu, Y.H.E., 1977, Catalyst specificities in high pressure hydroprocessing of pyrolysis and Gasification tars, *Prepr. Pap. Am. Chem. Soc., Div. Fuel Chem.,* **32**, 229-239 (1987).

Song, C., Green oil production by hydroprocessing. Int. J. Clean Coal Energy. **1,** 43-55 (2012).

Stowe, L.R., Method of conversion of heavy hydrocarbon feed stocks, *US Patent 5547563 A*, USA (1996).

Taher, Z., Karimi., Enzyme based ethanol, *Bio Resour*., **2**, 707-738 (2007).

Taherzadeh, M.J., Ethanol from Lignocellulose: Physiological Effects of Inhibitors and Fermentation Strategies, *Ph.D. Thesis*, Chalmers University of Technology, Sweden (1999).

Tang, Y., Miao, S., Mo, L., Zheng, X., Shanks, B.H., One-step hydrogenation/esterification activity enhancement over bifunctional mesoporous organic-Inorganic hybrid silicas, *Top. Catal.*, **56,** 1804-1813 (2013).

Tchobanoglous, G., Theisen, H., Eliassen, R., *Solid wastes: Engineering Principles and Management issues*, Mc-Graw Hill Publications, New York (1977).

Ternan, M., Brown, J.R., Hydrotreating a distillate liquid derived from subbituminous coal using a sulphided CoO-MoO_3-Al_2O_3 Catalyst, *Fuel*, **61,** 1110–1118 (1982).

Train, P.M., Klein, M.T., Chemical and Stochastic Modeling of Lignin Hydrodeoxygenation, *Prepr. Pap. – Am. Chem. Soc., Div. Fuel Chem.,* **32,** 240–248 (1987).

Venderbosch, R. H., Ardiyanti, A.R., Wildschut, J., Oasmaa, A., Heeres, H.J., Stabilization of Biomass-Derived Pyrolysis Oils, *J. Chem. Technol. Biotechnol.,* **85**, 674–686 (2010).

Triantafylidis, K.S., Iliopoulou, E.F., Antonakou, E.V., Lappas, A.A., Wang, H., Pinnavaia, T.J., Hydrothermally stable mesoporous alumino silicates (MSU-S) assembled from zeolite

seeds as catalysts for biomass pyrolysis, *Microporous and Mesoporous Mater.*, **99**, 132–139 (2007).

Verardi, A., Bari, I., De, R.E., Calabrò, V., Hydrolysis of lignocellulosic biomass: Current status of processes and technologies and future perspectives, *Tech, Rep. Intech. Open.*, (2011).

Wan, H., Vitter, A., Chaudhari, R.V., Subramaniam, B., Kinetic investigations of unusual solvent effects during Ru/C catalyzed hydrogenation of model oxygenates, *J. Catal.*, **309**, 174–184 (2014).

Wandas, R., Surygała, J., Ewa Śliwka., Conversion of Cresols and naphthalene in the hydroprocessing of three-component model mixtures simulating fast pyrolysis tars, *Fuel*, **75**, 687–694 (1996).

Wang, W. Y., Yang, Y.Q., Guo Bao, J., Luo, H., Characterization and catalytic properties of Ni-Mo-B amorphous catalysts for phenol hydrodeoxygenation, *Catal. Commun.*, **11**, 100 – 105 (2009).

Wang, W., Yang, Y., Luo, H., Hu, T., Liu, W., Amorphous Co-Mo-B catalyst with high activity for the hydrodeoxygenation of bio-oil, *Catal. Commun.*,**12**, 436–440 (2011).

Wang, W., Zhang, K., Liu, H., Qiao, Z., Yang, Y., Ren, K., Hydrodeoxygenation of P-Cresol on unsupported Ni-P catalysts prepared by thermal decomposition method, *Catal. Commun.*, **41**, 41–46 (2013).

Wang, X., Biomass Fast Pyrolysis in a Fluidized Bed. Ph.D. Thesis, University of Twente, Enscheda, The Netherlands, (2006).

Wang, Y., Fang, Y., He, T., Hu, H., Wu, J., Hydrodeoxygenation of dibenzofuran over noble metal supported on mesoporous zeolite, *Catal. Commun.*, 12, 1201-1205 (2011).

Wang, Y., He, T., Liu, K., Wu, J., Fang, Y., From biomass to advanced bio-fuel by catalytic pyrolysis/hydro-processing: Hydrodeoxygenation of bio-oil derived from biomass catalytic pyrolysis." *Bioresour. Technol.*, **108,** 280–**184** (2012).

Wen, C.Y., Yu. Y.H., Mechanics of Fluidization. *Chem. Eng. Prog. Symp. Series*, **62**, 100-111 (1966).

Wess, J.A., Olsen, L.D., Sweeney, M.H., Asphalt (Bitumen), *Concise Int. Chem.Assess. Doc.*, **59,** 1-50 (2004).

White, P.J., Jones, J.F., Eddinger, R.T., Treat and track oil from coal, *Hydrocarbon Process*, 47, 97 (1968).

Wildschut, J., Mahfud, F.H., Venderbosch, R.H., Heeres, H.J., Hydrotreatment of fast pyrolysis oil using heterogeneous noble-metal catalysts, *Ind. Eng. Chem. Res*., **48**, 10324–10334 (2009).

Williams, P.T., Horne, P.A., The influence of catalyst type on the composition of upgraded biomass pyrolysis oils, *J. Anal. Appl. Pyrolysis.*, **31,** 39–61 (1995).

Williams, P.T., Nugranad, N., Comparison of products from the pyrolysis and catalytic pyrolysis of rice husks, *Energy*, **25,** 493–513 (2000).

Xu, Y., Wang, T., Longlong, M., Zhang, Q., Liang, W., Upgrading of the liquid fuel from fast pyrolysis of biomass over MoNi/ɣ-Al_2O_3 Catalysts, *Appl. Energy*, 87, 2886–2891 (2010).

Xiangyu, L., Zhang, H., Li, J., Su, L., Zuo, J., Sridhar, K., Wang, Y., Improving the Aromatic production in catalytic fast pyrolysis of cellulose by co-feeding low density polyethylene, *Appl. Catal., A,* **455**. 114-121 (2013).

Xu, X., Zhang, C., Liu, Y., Zhai, Y., Zhang, R., Two-step catalytic hydrodeoxygenation of fast pyrolysis oil to hydrocarbon liquid fuels, *Chemosphere*, **93**, 652–660 (2013).

Yakovlev, V.A., Khromova, S.A., Sherstyuk, O.V., Dundich, V.O., Ermakov, D.Y., Novopashina, V.M., Lebedev, M.Y., Bulavchenko, O., Parmon, V.N., Development of new catalytic systems for upgraded bio-oil production from bio-crude-oil and biodiesel, *Catal. Today*, **144,** 362–366 (2009).

Yang, Y., Gilbert, A., Xu, C., Hydrodeoxygenation of bio-crude in supercritical hexane with sulfided CoMo and CoMoP catalysts supported on MgO: a model compound study using phenol. *Appl. Catal.* , **360**, 242–249 (2009).

Yunquan, Y., Luo, H., Tong, G., Smith, K.J., Thian Tye, C., Hydrodeoxygenation of phenolic model compounds over MoS_2 catalysts with different structures, *Chin. J. Chem. Eng.*, 16, 733–739 (2008).

Yang, Y., Ochoa-Hernández, C., O'Shea, V., Pizarro, P., Coronado, J.M., Serrano, D.P., Effect of metal-support interaction on the selective hydrodeoxygenation of anisole to aromatics over Ni-based catalysts, *Applied Catal. B, Environ.*,**145,** 91–100 (2014).

Ying, X., Wang, T., Longlong, M., Chen, G., Upgrading of fast pyrolysis liquid fuel from biomass over Ru/ɣ-Al_2O_3 catalyst, *Energy Convers. Manage.*, **55**, 172–177 (2012).

Zanzi, R., Sjostrom, K., Bjornbom, E., Rapid high-temperature pyrolysis of biomass in a free fall reactor, *Fuel* ,**75**, 545-550 (1996).

Zhang, C., Xing, J., Song, L., Xin, H., Lin, S., Xing, L., Li, X., Aqueous-Phase Hydrodeoxygenation of lignin monomer Eugenol: Influence of Si/Al ratio of HZSM-5 on catalytic performances, *Catal. Today*, **234,** 145–152 (2014).

Zhang, S., Yan, Y., Li, T., Ren, Z., Lumping kinetic model for hydrotreating of bio-oil from the fast pyrolysis of biomass. *Energy Sources, Part A,* **31**, 639–**645** (2009).

Zhang, S.P., Study of hydrodeoxygenation of bio-oil from the fast pyrolysis of biomass, *Energy Sources*, 25, 37–41 (2010).

Zhang, X., Zhang, Q., Wang, T., Longlong, M., Yu, Y., Chen, L., Hydrodeoxygenation of lignin-derived phenolic compounds to hydrocarbons over Ni/SiO_2-ZrO_2 catalysts, *Bioresour. Technol.*, **134**, 73–80 (2013).

Zhao, C., Kasakov, S., He, J., Lercher, J.A., Comparison of kinetics, activity and stability of Ni/HZSM-5 and Ni/Al_2O_3-HZSM-5 for phenol hydrodeoxygenation, *J. Catal.*,**296,** 12–23 (2012).

Zhao, H.Y., Li, D., Bui, P., Oyama, S.T., Hydrodeoxygenation of guaiacol as model compound for pyrolysis oil on transition metal phosphide hydroprocessing catalysts, *Appl. Catal., A* **391,** 305–310 (2011).

Zheng, J., Bio-Oil from fast pyrolysis of rice husk: Yields and related properties and improvement of the pyrolysis system, *J. Anal. Appl. Pyrolysis.*, **80,** 30–35 (2007).

Zhong, H., Wang, X., Hydrodeoxygenation of model compounds and catalytic systems for pyrolysis bio-oils upgrading, *Catal. Sustainable Energy*, **1**, 28–52 (2012).

Zhu, J.F., Wang, J.C., Li, Q.X., Transformation of bio-oil into BTX by bio-oil catalytic cracking, *Chin. J. Chem. Phys.*, **26**, 477-483 (2013).

Zoccola, M., Aluigi, A., Tonin, C., Characterization of keratin biomass from butchery and wool industry wastes, *J. Mol. Struct.*, **938**, 35–40 (2009).